



Division of Biomedical Engineering
Department of Human Biology
Faculty of Health Sciences
University of Cape Town

Minor Dissertation

Design and Development of a Lower Limb Rehabilitation Device for Spinal Cord Injury Patients

In partial fulfilment of the requirements for the degree:
MSc. Biomedical Engineering by Coursework and Dissertation

Author: Matthew Trusler (TRSMAT005)

Supervised by: Assoc. Prof. Sudesh Sivarasu & Dr Juliette Stander

The copyright of this thesis vests in the author. No quotation from it or information derived from it is to be published without full acknowledgement of the source. The thesis is to be used for private study or non-commercial research purposes only.

Published by the University of Cape Town (UCT) in terms of the non-exclusive license granted to UCT by the author.

Declaration

I, **Matthew Trusler**, hereby declare that the work on which this dissertation is based is my original work (except where acknowledgements indicate otherwise) and that neither the whole work nor any part of it has been, is being, or is to be submitted for another degree in this or any other university.

I empower the university to reproduce for the purpose of research either the whole or any portion of the contents in any manner whatsoever.

Signature:

Signed by candidate

Date: 2021/10/06

Abstract

Introduction: Spinal cord injuries (SCI) are seen commonly in Southern Africa and can completely change the course of the affected's life. Lower limb disability is a common complication from this injury, but a patient can be rehabilitated in some cases. Research and clinical observations suggest that early mobilisation and rehabilitation leads to shorter hospital stays and better clinical outcomes. Relieving the time dedication placed onto the rehabilitation team could mean that patients receive a higher standard of care.

Methods: A cyclic movement device has been designed to mimic the gait cycle that a patient is attempting to recover. The device was intended towards providing a ground reaction force simulation at the correct points of the gait cycle. The device was tested *in-silico* with validated skeletal models to determine joint torques and angles. *In-silico* testing was also utilised to determine the loads placed onto the patient by the device through its use. The force data could then be used to predict possible ground reaction forces.

Results: The device allows for a gait similar trace path of the ankle, comparable to that found in the literature. The ankle has a range of motion of 31° as the device completes a full cycle in which the crank rotates 360° . The hip has a range of motion of 28° and the knee 35° in this same movement. The shape of the displacements of the joints of the lower limb is comparable to that seen in researched gait patterns. However, the timing of the knee and hip joints' movements are not synchronous with that of the gait patterns. The device is validated to be sufficiently stable to use, and the motor and power components can provide the 7259N.mm of torque needed to move the model.

Conclusion: The results suggest that the device has potential as an adjunct to rehabilitation schemes. *In-silico* testing showed that the device is able to simulate some of the kinetic and kinematic parameters seen in normal gait. Further work is needed to prototype the device to physically and clinically validate the device.

Dedication

I would like to dedicate this thesis and the work collected herein to all of my educators to this point. Thank you for pushing me and for helping me on this journey.

Contents

Chapter	Page
List of Figures	v
List of Tables	ix
Acknowledgements	x
List of Abbreviations	xi
1. Introduction and Problem Identification	1
1.1 Background to Study	1
1.2 Clinical Problem Description	2
1.3 Research Approach.....	3
1.4 Hypothesis	4
1.5 Study Aim.....	4
1.6 Research Objectives	4
1.7 Project Parameters	5
1.7.1 Design Constraints	5
1.7.2 System Parameter Definitions.....	5
1.8 Study Scope	5
1.9 Dissertation Overview	6
2. Literature Review	8
2.1 The Spinal Cord.....	8
2.1.1 Anatomy of the Spinal Cord	8
2.1.2 Neurons	9
2.1.3 Reflex Arc.....	10
2.2 Injury to the Spinal Cord	11
2.2.1 Pathophysiology.....	11
2.2.2 Clinical Presentation of Impairment	11
2.2.3 Stroke Comparability.....	13
2.2.4 CNS Plasticity Post-Injury	13
2.3 Lower Limb Rehabilitation	15
2.3.1 Path to Rehabilitation	15
2.3.2 Conventional Rehabilitation and Recovery	16
2.3.3 Evidence Of Technology-Assisted Therapies	17
2.3.4 Current Devices	18
2.3.5 Limitations.....	24
3. Design	25
3.1 Design Methodology	25
3.1.1 Design of Lower Limb Rehabilitation Device	25
3.1.2 Leg Drive Mechanism Design	28
3.1.3 Patient Attachment Design	33

3.1.4 Clinician Interface Design.....	35
3.2 Resultant Design.....	36
3.2.1 Anthropomorphic Considerations	36
3.2.2 Working Principle	37
3.2.3 Leg Drive Mechanism Design	37
3.2.4 Patient Attachment Design	48
3.2.5 Clinician Interface Design.....	49
3.2.6 Design Validation	54
3.2.7 Failure Modes and Effects Analysis	59
4. Methodology and Results	61
4.1 Purpose of <i>In-silico</i> Study	61
4.2 OpenSim to SolidWorks Cross-over	62
4.2.1 Lower Limb Model 2010	62
4.2.2 Solid-Body Modelling	65
4.2.3 <i>In-silico</i> Study Design	67
4.3 Experimental Results	71
4.3.1 Change of Angle	72
4.3.2 Rate of Change of Angle.....	76
4.3.3 Trace Paths	80
4.3.4 Ground Reaction Forces.....	82
4.3.5 Forces Experienced in the Joints.....	84
4.3.1 Device Validation	85
5. Discussion	86
5.1 Design.....	86
5.2 Experimentation	87
6. Conclusion and Recommendations	89
6.1 Conclusion.....	89
6.1.1 Rehabilitation Device Design	89
6.1.2 Device Usability	90
6.1.3 Recommendations, Inferences and Future Work.....	90
7. References	92
Appendix A ISNCSCI Impairment Exam	98
Appendix B Dempster’s Parameters	100
Appendix C ICF Components	102

List of Figures

Figure	Page
Figure 2-1	The entirety of the spinal cord, displaying the regions and innervations of cervical (pink), thoracic (yellow) lumbar (green) and sacral (grey) zones. Adapted from (Ahuja et al., 2017) 9
Figure 2-2	Neuron structure(Matthew, 2018)10
Figure 2-3	Reflex arc displaying the stimulus to action loop (P. McGurrin, 2016) 11
Figure 2-4	Sympathetic nervous systems affected by an SCI seen in the cervical region (Ahuja et al., 2017)14
Figure 2-5	A typical mobilization and stretch movement for the hip, knee and ankle applied by a therapist. (Physio.co.uk, 2020)15
Figure 2-6	Robotic system classifications for lower-limb rehabilitation: (a) treadmill gait-trainers, (b) foot-plate gait trainers, (c) overground trainers, (d) stationary gait trainers, and (e) active foot orthosis trainers. (Díaz, Gil, & Sánchez, 2011)18
Figure 2-7	Current devices, a.) Erigo Tilt Table, b.) Silverfit Intensive Care, c.) Ergys, d.) MotionMaker20
Figure 3-1	Detail of design methodology with regards to the subsystems of the rehabilitative device.....26
Figure 3-2	Flow of Design Methodology.....27
Figure 3-3	Gait pattern trajectory of the ankle with relevant horizontal and vertical positions adapted from (Mendoza-Crespo et al., 2019).....28
Figure 3-4	The gait cycle with included loading states from (Cheung et al., 2016)28
Figure 3-5	Elliptical machines left to right, they are made by Life Fitness, Precor, Matrix, and ProForm. (a) Photos (courtesy of their websites). (b) Sketches of their linkages with the foot position shown in pink (c) Approximate pedal trajectory from the design. Adapted from (DeJong, 2007)30
Figure 3-6	Concept design, shown with the patient supine on a hospital bed, with their feet attached to the ends of the arms of the device31
Figure 3-7	Gait pattern achieved (shown in orange), through the trunnion (green point) as the end is driven by the rotary arm (whose radius is traced in blue)31
Figure 3-8	Patient mock-up for illustrative purposes of the concept.....32
Figure 3-9	Patient force control strategy to ensure rehabilitation exercise and continual stimulation.34
Figure 3-10	SilverFit device with lower limb support to stop unwanted rotation.35
Figure 3-11	Design of the lower limb exercise device with 1) The crank and bearing subassembly, 2) The mechanical arms, 3) Foot attachment points, 4) The frame body, 5) The motor tension and adjustment mechanisms, 6) The motor and housing 7) The joint between crank and arms of the device.....36

Figure 3-12	Frame body render with critical areas of note	38
Figure 3-13	Roller with dimensions (Interoll, 2020)	39
Figure 3-14	Crankset with the attached gear or chainring. The spindle is shown in red and is the hub that is welded to the frame body. (Meriam & Kraige, 2011)	39
Figure 3-15	Hub bracket and related components in a salvaged bike frame (Smith, 2019).....	40
Figure 3-16	Radius added to the top of the frame body to allow for location during welding.....	40
Figure 3-17	Von Mises Stresses seen in the frame body during loading.	41
Figure 3-18	Displacement simulation during loading.	42
Figure 3-19	Symmetrical metal arms for the movement of the feet. 1) the proximal end to the cranks, 2) the slot within which the rollers are located, 3) the distal end for foot attachment	43
Figure 3-20	NEMA 23, 112mm stepper motor with 2.94Nm rated torque (3D-Printing-Store, 2020).....	44
Figure 3-21	Designed gearbox and motor housing 1) Sun gear (8 teeth), 2) Motor housing, 3) Annulus (32 teeth), 4) Planet gear (12 teeth), 5) Carrier connection to the output shaft, 6) Pinion.....	45
Figure 3-22	Cross-section of the gearbox, showing inner details. 1) The NEMA 23 motor and its shaft, 2) The pins that connect the planetary gears to the carrier, 3) Pins for torque transmission between shaft and attachments, 4) Locating bearing, 5) bearing for smooth rotation of the carrier.	46
Figure 3-23	Motor housing and frame attachment system is shown interfacing with the frame body.....	47
Figure 3-24	Isolated view of the clamps used to hold the motor housing to the frame body.....	48
Figure 3-25	Foot attachment design with adjustable heel position	49
Figure 3-26	TB6600 V1.1 Motor driver (DIYElectronics.co.za, 2020).....	50
Figure 3-27	TB6600 Wiring scheme for connection to the power supply and the stepper motor.	51
Figure 3-28	Arduino Mega Board (Arduino, 2020).....	51
Figure 3-29	Mean Well 24V Power Supply.....	53
Figure 3-30	3D printed housing for the Arduino and Motor Driver with computer linking cable and PSU positioned to the side	54
Figure 3-31	Design validation process methodology for each subsystem	54
Figure 3-32	Prototyped patient interface made of rubber and a slot fixture mechanism to adapt to foot size.	55
Figure 3-33	Traced path of the lowest point of the arms	57
Figure 3-34	Life cycles under the stresses of operation of the frame body.....	58
Figure 4-1	Visual representation of the location of the joints coordinate systems (Delp et al., 1990).....	64
Figure 4-2	Fully Extended Lower Limb Model 2010 (E. M. Arnold et al., 2010) imported to SolidWorks	66

Figure 4-3	Fully Flexed Lower Limb Model 2010 (E. M. Arnold et al., 2010) imported to SolidWorks	66
Figure 4-4	The foot placement of the patient onto the device, with the foot attachments hidden to show the foot and the arm	68
Figure 4-5	Motor direction and application zone, indicated by the red arrow	69
Figure 4-6	Simulation environment with constraints checked and the initial starting position of the legs.....	69
Figure 4-7	Angles measured during simulation results plotting (Richards, Chohan, & Erande, 2017)	70
Figure 4-8	Snapshots of the movement of the simulated legs in quarterly rotations.....	71
Figure 4-9	The joint angle changes of the ankle during the gait cycle (Richards et al., 2017)	72
Figure 4-10	Angular displacement of the left foot with respect to the tibia.....	73
Figure 4-11	The knee joint angle during the gait cycle (Richards et al., 2017)	74
Figure 4-12	Angular displacement of the left knee joint during device movement.....	74
Figure 4-13	The extension and flexion of the hip during the gait cycle (Richards et al., 2017)	75
Figure 4-14	The angular displacement of the left hip during device movement from the initial position.	76
Figure 4-15	The ankle velocity profile of normal patients shown as the dotted line (Granata, Abel, & Damiano, 2000).....	77
Figure 4-16	Velocity profile of the left simulated ankle during movement.	77
Figure 4-17	The knee velocity profile of normal patients shown as the dotted line (Granata et al., 2000)	78
Figure 4-18	Angular velocity of the left knee during device movement.	79
Figure 4-19	The hip velocity profile of normal patients shown as the dotted line (Granata et al., 2000)	80
Figure 4-20	Angular velocity of the left hip during device movement.	80
Figure 4-21	Trace paths, bottom to the top: the tip of the device's arms, the talus bone, the centre of the tibial plateau, and the centre of the femoral condyles. Displayed on the left with the reference bodies and on the right without solid bodies.....	81
Figure 4-22	Normal step trajectory with reference person travelling left to right (Vallery et al., 2008).....	82
Figure 4-23	Ground reaction forces experienced by the foot during device use	82
Figure 4-24	Typical vertical ground reaction forces during gait in healthy adults (Haddas & Ju, 2018).	83
Figure 4-25	Magnitude of force experienced in the left hip during device use	84

Figure 4-26	Magnitude of force experienced in the left knee during device use	84
Figure 4-27	Magnitude of force experienced in the left ankle during use.....	85
Figure 4-28	Torque requirement of the motor used to drive the device	85
Figure 6-1	Possible implementation of a knee brace to reduce rotational movement of the legs.....	91

List of Tables

Table		Page
Table 2-1	Gait training systems and reciprocal rehabilitation stage	19
Table 2-2.	Current Devices and their listed attributes	20
Table 2-3.	Gait Rehabilitation Devices with passive-active exercise modalities and their control and speed methods.	23
Table 3-1.	Anthropomorphic measurements.....	37
Table 3-2	Technical Specifications of TB6600 V1.1 as per DIYElectronics.co.za (2020).....	50
Table 3-3	Technical Specifications of the Arduino Mega	52
Table 3-4	Power consumptions of system components.....	53
Table 3-5	Usability assessment of patient interface system	55
Table 3-6	FMEA model of device and subsystems.....	60
Table 4-1.	Bones with their mass and inertial properties	63

Acknowledgements

I want to thank the following people:

Kristin Miller, for her unwavering support and love.

My colleagues, Catherine de Beer, Jannes Le Roux, Lara Timm, Tertius Devilliers, Edmund Wessels and Catherine Bradshaw, for their advice, laughs and fiercely critical minds.

My family, Jessica, Graham and Ryan Trusler for their dedication to my cause and for always having my back. They push me every day to be better than I previously was, and I cannot thank them enough for what they have done.

Dr Juliette Stander, for her keen enthusiasm and helpfulness and critical assessments of my work.

Assoc. Prof Sudesh Sivarsu, for all of the resources, trust and opportunities offered to me. I have gained so much experience because of you.

To all of the staff in the background of UCT keeping the lights on and the floors clean. You make the university a pleasure to study at, and I wouldn't have been able to come to campus every day if it wasn't for you

List of Abbreviations

AC	Alternating Current
ALEX	Active Leg Exoskeleton
ASCI	Acute Spinal Cord Injury
ASIA	American Spinal Injury Association
BWS	Bodyweight Stimulation
CNS	Central Nervous System
CPG	Central Pattern Generator
DC	Direct Current
DIY	Do It Yourself
DVT	Deep vein thrombosis
EMG	Electromyography
FEM	Finite Element Methods
GRF	Ground Reaction Forces
GSH	Groote Schuur Hospital
GT	Gait Trainer
ICU	Intensive Care Unit
ICF	
KB	Kilobyte
LOPES	Lower Extremity Powered Exoskeleton
MH	MegaHertz
NEMA	National Electrical Manufacturers Association
PD	Partial Discharge
PID	proportional integral derivative
PNS	Peripheral Nervous System
PSU	Power Supply Unit
PWM	Pulse Width Modulation
ROM	Range of Movement
RPM	Revolutions Per Minute
SCI	Spinal Cord Injury

SN	Stress and Number of Cycles
STL	Stereolithography
SUS	System Usability Scale
UCT	University of Cape Town

1. Introduction and Problem Identification

1.1 Background to Study

Spinal cord injuries (SCI) are an incapacitating and costly condition that often stops many of the affected patients from returning to work or engaging in various social settings. In South Africa, SCI has an annual incidence rate of 75.6 per million (Joseph, 2016; Khorasanizadeh et al., 2019). 60% of all injuries come from assaults in South Africa, which is the leading cause of SCI in the country (Joseph et al., 2015). The knock-on economic impact that burdens survivors of SCI is \$1.5 million over the span of their life, for incomplete paraplegia. For complete tetraplegia as reported by Krueger, Noonan, Trenaman, Joshi, and Rivers (2013) this figure rises to \$3 million. SCI involves the damage to the spinal cord that extends between the foramen magnum and the cauda equina. Affected patients tend to spend extended periods in SCI facilities. The length of time can range between 2-9 weeks, according to research by Bloch and Basbaum (1986). This period's length is often longer due to Spinal Cord Injury related complications, e.g. lung collapse, pneumonia, respiratory failure (requiring intubation, ventilation and subsequent weaning off of the ventilator), and pressure ulcers. Many patients are mechanically and physiologically stable during the prolonged weaning off of ventilation and may start with lower limb rehabilitative exercises during this time. The rehabilitative movement aims to reduce the risks of heart conditions, blood pressure problems, contractures, and reductions of joint range of movement (Nas, Yazmalar, Sah, Aydin, & Ones, 2015). The movements involved in exercising aid with the reduction of muscle atrophy and strengthens the bodies cardiovascular system, which leads to shorter rehabilitation times. If not appropriately rehabilitated, the complications that arise from SCI can lead to expensive and drawn-out hospital stays.

SCI patients' rehabilitation often depends on their remaining motor and sensory function, assessed upon their admission to a clinical facility. A physical assessment is done upon the patient, evaluating two main areas of the central nervous system and the peripheral nervous systems, the motor functioning and the sensory functioning (Curt, Keck, & Dietz, 1998). Two variants of SCI patients exist, namely complete,

and incomplete, which are then further classified with the injury level along the spine. This assessment is graded on the American Spinal Injury Association (ASIA) scale. The treatment of the patients is grouped into three categories, the acute, post-acute and rehabilitation stages. There is considerable relation between the ASIA scale rating that is initially graded and the patient's conversion to a different level of neurological deficit. Those patients graded at ASIA scale D saw the worst conversion rates (Spiess, Müller, Rupp, Schuld, & van Hedel, 2009).

The acute stage's focus is to stabilise the patient and ensure that no further damage occurs (Bloch & Basbaum, 1986). This stage may involve surgical procedures and teams of medical professionals working towards ensuring the patients' safety. The rehabilitation stage begins as soon as the patient is in a stable state. Rehabilitation involves both the injuries sustained and that of the possible neural functioning losses. The progress and rate at which the rehabilitation proceeds is at the discretion of the clinicians involved (Dijkers & Zanca, 2013). Gait retraining and limb loading/unloading are particularly useful in helping patients recover walking ability and motor control of their limbs (Sargsyan, Arakelian, & Briot, 2012).

1.2 Clinical Problem Description

Regrettably, training protocols often rely on bulky and expensive equipment, operated by a large team. This standard of care is far from ideal for the South African public health sector, whose nursing, physiotherapist, and occupational therapist care system is heavily overburdened.

The problem to be solved is to develop a device that provides aid in the exercise, mobilisation, and rehabilitation of spinal cord injury patients' lower limbs. This device would potentially fulfil the need of reducing the burden on the current nursing and physiotherapy assistants while providing independence in rehabilitation programs of those afflicted by a spinal cord injury. There is a need for an affordable device that can be used in the South African public healthcare system to rehabilitate SCI members to allow afflicted members of society to return to the workforce and maintain their lifestyles. This device should reduce the burden of disability on society and allow the

early resumption of exercise in ICUs associated with a decrease in Hospital Stay Days and therefore reduces overall healthcare delivery expenditure.

Problem Significance

The research within this paper is focussed primarily on the early mobilisation and rehabilitation of individuals with spinal cord injuries. Clinicians at the Acute Spinal Cord Injury Unit (ASCI) with Groote Schuur Hospital (GSH), have found that many of their patients do not proceed in recovery as quickly as they could, due to the lack of access to technology. This could be due to a lack of exercise of patients' lower limbs in the ASCI intensive care unit (ICU) and post-acute wards during critical stages of recovery. Physiotherapy students from the University of Cape Town (UCT) do aid in the exercise management of spinal cord injury patients' however, due to time constraints and the number of admitted patients, this is not sufficient to for optimal rehabilitation.

Patients that are unable to play an active role in their recovery programmes have expressed frustration. Included in this is the patient's satisfaction with treatment and rehabilitation in the public healthcare system within South Africa. Community satisfaction research conducted by Maart and Jelsma (2014) communicates the portion of the unmet needs for services is as follows: 34.5% for assistive devices used in hospitals; 28.9% for medical rehabilitation services offered to them. Joseph et al. (2015) showed that 75.6 per million in the population were affected by traumatic spinal cord injuries. This statistic, coupled with the average of 185 spinal cord injury patients seen annually by the Groote Schuur ASCI ward (Sothmann, Stander, Kruger, & Dunn, 2015), means that the rehabilitation services have to be spread to those patients who need them most and have the highest chance of success (Joseph, Scriba, Wilson, Mothabeng, & Theron, 2017). Having the burden of tetraplegia or paraplegia reduced is evident through a return to functional independence and social reintegration and as such, should be prioritised (Joseph et al., 2013; Key & Hurford, 1982).

1.3 Research Approach

The first step of the process is the scoping of the problem. The issues that are found from the literature are assessed for significance and possibility for a feasible

solution. Following this is the frugal contextual design of the device and all the components. The design is followed by design validation, then *in-silico* testing of the subsystems after assembly with a validated anatomical bone model. Validation of the parameters is the precursor to the pre-clinical validation, which involves the device's *in-silico* testing. The test results can then be correlated to how the device might affect the found problem.

1.4 Hypothesis

The hypothesis proposed is that the device, which allows for repetitive practice of the lower limbs, will replicate early mobility movements that are prescribed by physiotherapists and when compared to literature will simulate conditions that enable earlier recovery and faster, focused rehabilitation.

1.5 Study Aim

This proposed research aims to design and validate *in-silico*, an appropriate lower limb exercise device that aids in the early mobilisation and rehabilitation of SCI patients, assisting with motor and sensory functioning recovery.

1.6 Research Objectives

The following objectives must be met to achieve the aim, as mentioned above. The objectives can be classified into the design, assembly, and testing phases:

- i. Design and develop a patient safe gait-similar exercise device for use on a hospital bed that includes:
 - a) A novel movement pattern system,
 - b) A clinician interface to control the rehabilitation.
- ii. Perform experimental pilot verification *in-silico* tests to determine and to validate clinically:
 - a) The perceived usability of the device,
 - b) The kinematic and kinetic interactions of lower limb movement during use.

1.7 Project Parameters

The design process focuses on developing the core working mechanisms: the leg drive mechanism, patient interface, and clinician interface to create an integrated device that can mobilise a patient into ranges of movement similar to standard walking. Emphasis is also placed on the stimuli that the feet and leg receive from the ground during walking.

1.7.1 Design Constraints

The following are the constraining factors in designing a device for use in a hospital ward with SCI patients. These constraints were gathered during observation of the Groote Schuur ASCI ward and are the assumed conditions of a standard patient in the ward.

- The patient is limited to a supine position on top of a hospital bed
- Compatible with hospital bed sizing
- Average patient body mass of 75kg
- Average patient height of 1.7m

1.7.2 System Parameter Definitions

The system parameters identified are generated from reviewed literature, lower limb anatomy, and the patient's safety. These system parameters are also based on the insights into the sector shared by the clinician. The parameters identified as critical are:

- Range of motion of the major joints of the lower limb,
- Adjustability to patient morphology,
- Ability to simulate ground reaction forces,
- Safety of patient

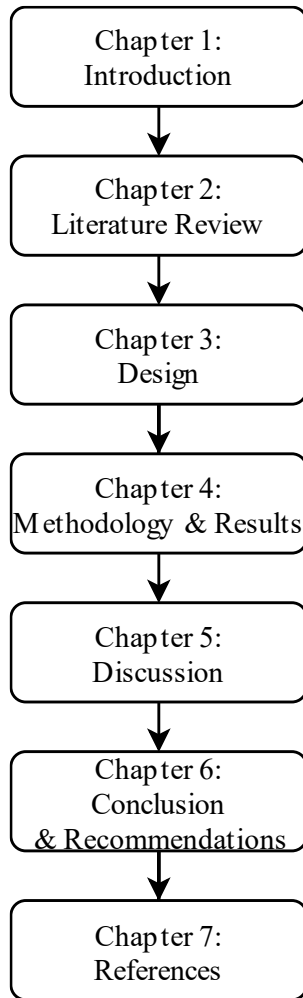
1.8 Study Scope

The study was focused on developing a theoretical rehabilitative exercise device that could be used by patients suffering from SCI that were still bed-bound. This study investigates whether the device would be considered to fulfil a role in a rehabilitation

program. During the COVID-19 Pandemic, stress was placed onto the prototyping stages of the project, and delays were incurred. These delays would have a knock-on effect onto the approval of ethics and a meaningful human trial. The project pivoted after the design stage towards *in-silico* testing, as a way to reduce the burden on time and monetary resources and in light of the minor dissertation requirements.. The testing method provides a number of advantages over original patient testing methods, and different parameters could be assessed. It was decided that the *in-silico* testing would replace conventional testing, in an effort to evaluate plausibility of the device.

1.9 Dissertation Overview

Chapter 1 presents the introduction and the research motivation, while also discussing the research problem, scope and limitations, and objectives,. In Chapter 2, a review of the literature surrounding the rehabilitation of spinal cord injuries of the lower limbs was conducted, including an anatomical overview of the injury. Chapter 2 also discusses the devices currently available to the market and their purposes. The device design methodology is outlined in Chapter 3 for the research, with the then presented outcome of this design process and the device's prototyping stages with the intermediary validation steps. Chapter 4 presents the methodology for the *in-silico* trial and testing of the device, wherein some clinician thoughts and comments are also captured. Chapter 4 also discusses the data analysis methods followed by the trials' results and data being presented and analysed. The data is then followed in Chapter 5, discussing the device's results and overall design. In Chapter 6, the conclusions of the research and results are presented, and future research is discussed with recommendations being made. A complete list of references that were used in the direction of this research is provided in Chapter 7. In the appendices, all of the raw data and calculations collected and performed respectively in this study are presented in the appendices.



2. Literature Review

This chapter focusses on detailing the current motor and sensory rehabilitation methods and includes a brief overview of the anatomy involved. The current market landscape for rehabilitation devices and procedures is analysed and efficacies compared. This chapter culminates in a list of criteria for a successful rehabilitation device and placement of the study in the research sphere.

2.1 The Spinal Cord

To understand a spinal cord injury and how neurorehabilitation might occur, the underlying mechanisms must be understood. There is little consensus about SCI rehabilitation's best practices because much of SCI rehabilitation is new, and many rehabilitation schemes only became established within the last two decades (Dietz & Fouad, 2013). The nervous system is widely researched, and new findings are published regularly. The investment globally into the spinal cord, and SCI research, is promising. In the developing world, region-specific techniques are being developed to deal with the burdens of injury to the spinal cord. Methods to augment the nervous systems' natural abilities are also a topic of interest in markets worldwide.

2.1.1 Anatomy of the Spinal Cord

The spinal cord is separated into sections for ease of identification by the vertebrae, and with the inclusion of the brain, the central nervous system (CNS) is made up. These sections are separated into the cervical, thoracic, lumbar and sacral segments. The spinal cord comprises both grey and white matter, containing neuronal cell bodies and myelinated axons, respectively. The white matter described is divided into bundles of axons that make up tracts connecting areas of the brain to the peripheral systems. These tracts convey essential sensory and motor functioning tasks. The spinal cord has 31 pairs of spinal nerves extending to the trunk and limbs. As the spinal cord progresses down through the vertebrae, nerves leave the cord to sections of skin, organs or muscle tissue through the peripheral nervous system (PNS).

Figure 2-2 indicates spinal cord housing within the protective vertebrae and its' basic innervations of the body. Noted from this is the spinal cords overall functionality

and divided control system. The spinal cord acts as a carrier passage for networking to the brain from these regions. This passageway is made up of a bundle of neurons. The brain is not used in isolation for information and control of the regions; local control does occur.

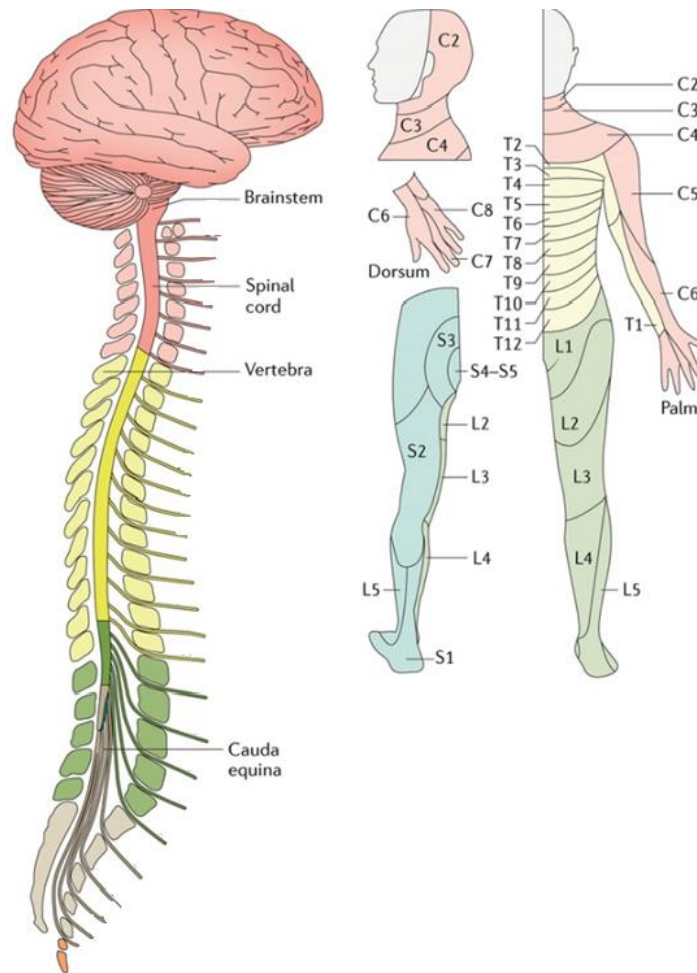


Figure 2-1 The entirety of the spinal cord, displaying the regions and innervations of cervical (pink), thoracic (yellow) lumbar (green) and sacral (grey) zones. Adapted from (Ahuja et al., 2017)

2.1.2 Neurons

The nervous system comprises of two main cell types, neurons and supporting cells. The neuron is the basic structural and functional unit of the nervous system. They are specialised to respond to physical and chemical stimuli, through their synapse integration between units. The synapses conduct electrochemical impulses and

release chemical regulators. Through these mechanisms, neurons can provide sensory perception, learning, memory, and muscles and glands' control. While they can be broken up into different groups, they have a similar basal structure to that shown in

Figure 2-2. The neurons are the mechanism by which nerve impulses are transmitted through the body.

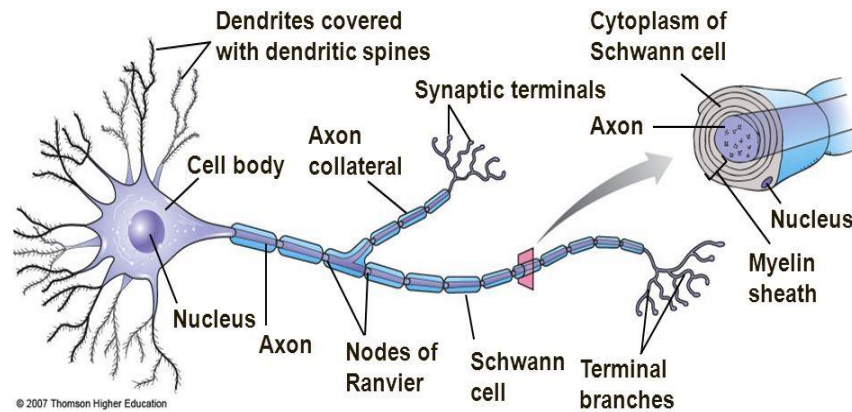


Figure 2-2 Neuron structure(Matthew, 2018)

2.1.3 Reflex Arc

The PNS can be divided into the autonomic nervous system and the somatic nervous system. The autonomic nervous system controls unconscious actions and its' functioning and is critical to survival. Meanwhile, the somatic nervous system functioning plays a larger role in the body's coordination and reflex reactions. The reflex arc is the unit that allows for the rapid dissemination of stimulus to the body. This reflex arc contains three neurons: a sensory neuron, a relay neuron (part of the spinal cord) and the motor neurons. These neurons are illustrated in Figure 2-3, as a stimulus is received by the afferent neuron, transmitting the potential to the relay neuron, across the spinal cord, to the efferent neuron.

This process occurs due to membrane potential changes resulting from depolarization leading to a graded potential within the neurons—this graded potential, with accompanying neurotransmitters, relays information across the body.

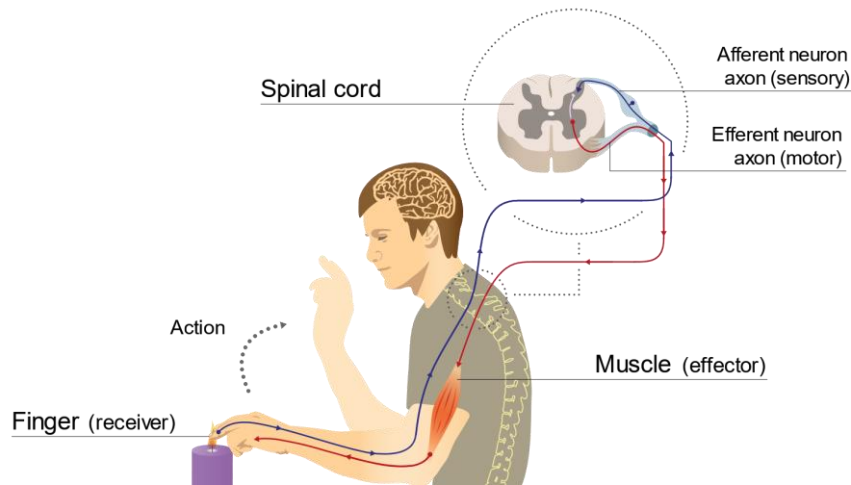


Figure 2-3 Reflex arc displaying the stimulus to action loop (P. McGurrin, 2016)

2.2 Injury to the Spinal Cord

2.2.1 Pathophysiology

Following a spinal cord injury, loss of motor and sensory functioning occurs due to the interruption of the axonal channels caused by the mass death of the neurons (Ruff, McKerracher, & Selzer, 2008). This death occurs, primarily due to the compressive, tensile, or shearing forces, that occur during the injury. The damage can be split into two injury types: primary and secondary. Primary damage occurs with the mechanical forces upon the spinal cord, thereafter in the secondary stage, acute pathophysiologic processes occur which can include vascular abnormalities, free radical and lipid peroxidation, excitotoxicity (the lethal effects on a cellular level of excess glutamate stimulation) and electrolyte imbalances, and concluded with large scale necrotic and apoptotic cell death. These can be further divided into the acute, the sub-acute, the intermediate and the chronic phases of injury for a patient (Ahuja et al., 2017). These events cause widespread sensorimotor losses and need to be managed rapidly to mitigate the effects.

2.2.2 Clinical Presentation of Impairment

Following the initial mechanical disruption to the working mechanisms, the sensorimotor losses can be evaluated and assessed. The assessment determines the injury level and is performed according to the ASIA examination (Appendix A). There is a

correlation between the patient's functional abilities and prognosis. These two classifications can be defined as loss of motor and sensory function at the distal levels of injury, or partial preservation of sensorimotor function below the neurological levels respectively (Nas et al., 2015). It should be noted that, in the acute stages of injury, spinal shock often occurs, masking the lesion's full status (Somers, 2001).

The losses sustained from this form of injury are not only limiting in physical and independence capacities, but also carry the risk of, orthostatic hypotension, urinary tract infections, fractures, spasticity, deep vein thrombosis (DVT), heterotrophic ossification, pressure ulcers, contractures, autonomic dysreflexia, pulmonary & cardiovascular problems, neurogenic bladder and bowel and depressive disorders (Bloch & Basbaum, 1986; Nas et al., 2015; Ruff et al., 2008). In addition to the sensorimotor losses sustained and the secondary complications, sympathetic innervation can also be reduced, resulting in basal vascular tone below the injury.

The injuries sustained that lead to SCI are often severe and could require surgical intervention. The stabilisation of the patient is crucial, and these injuries could determine the recovery methods employed by a multidisciplinary team of therapists and nurses. Rehabilitation tasks change most in scenarios where the respiratory system is compromised. The linking of bodily functions to the injury level can be seen in Figure 2-4. The image also displays an example of injury and how this would affect the patient. Figure 2-4 shows how loss occurs throughout the nervous system below the lesion level and its subsequent effect on functioning.

In addition to the immobilised state an SCI patient finds themselves in from motor functioning losses, secondary complications may arise. The complications may include muscle atrophy, characterised by a loss of strength and range of movement, and respiratory degradation from sympathetic nerve injury (Colombo, Schreier, Mayr, Plewa, & Rupp, 2005). Included are other side effects, such as sensory deprivation, depression and anxiety, due to possible isolation from society and the confinements of the housing or hospital (Dijkers & Zanca, 2013; Williams & Murray, 2015).

2.2.3 Stroke Comparability

There are comparable attributes between incomplete tetraplegia patients and those affected by hemiplegia after a stroke event. The incomplete tetraplegic patients often have altered sensorimotor inputs, similar to those presented in patients with hemiplegia. For these reasons, much of the rehabilitation research and data that applies to hemiplegia can be correlated with incomplete SCI rehabilitation (Backus, 2010). The degree of functionality according to the WHO's International Classification of Functioning (ICF) of the patient can also be cross correlated between etiologies and will play an important role in the indication of treatment methods (See Appendix C).

2.2.4 CNS Plasticity Post-Injury

After injury to the spinal cord, plastic changes are observed to the cord's physical structure. The plastic change occurs with a cortical reorganisation, both in Complete or Incomplete cases (Backus, 2010). This cortical reordering occurs with or without surgical intervention and is a crucial part of neural plasticity and the brains' attempt to regain function (Beekhuizen & Field-Fote, 2005; Cramer, Lastra, Lacourse, & Cohen, 2005; Green, Sora, Bialy, Ricamoto, & Thatcher, 1998). Neural plasticity is seen during motor learning of specialised tasks and skills and plays a large role in adolescent and infant development. Neural plasticity within the realm of spinal cord injuries should be instead considered as function improvement excluding strength improvements (Curt, Van Hedel, Klaus, & Dietz, 2008)

Age has shown to play a role in the amount of plasticity that occurs in an individual. Older individuals observe less neuroplasticity after an injury than their younger counterparts (Jakob, Wirz, van Hedel, & Dietz, 2009). This fact should be recognised in the analysis of future results and studies.

Research has shown that a central pattern generator (CPG) in the spinal cord allows for the production of rhythmic stepping movements after rehabilitative training and task orientated practice (V. R. Edgerton et al., 1997; Harkema, 2008; Pearson & Misiaszek, 2000). The motor training gains are realised from a successful scheme (primarily functional training) involving sufficient proprioceptive feedback. When

achieved, this feedback results in cortical reorganisation and normalisation of reflex activity (Luft, Bastian, & Dietz, 2012).

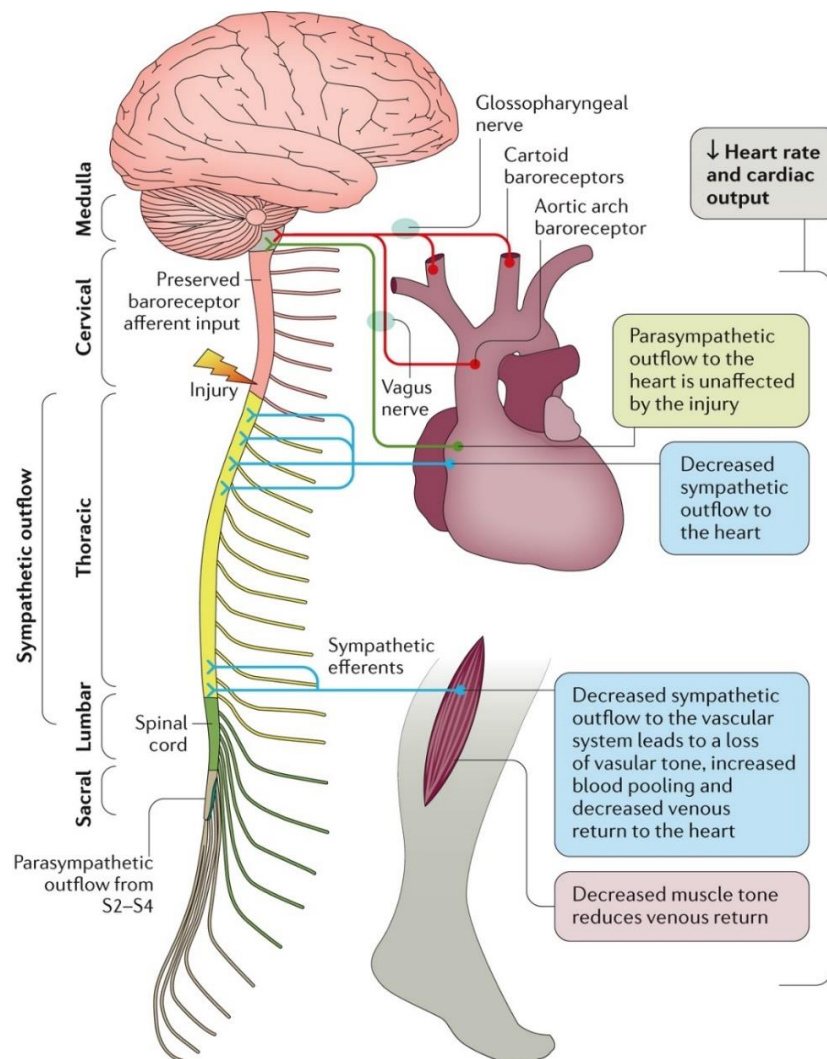


Figure 2-4 Sympathetic nervous systems affected by an SCI seen in the cervical region (Ahuja et al., 2017)

Pattern and motor recovery is amplified with the simulated effects of ground reaction forces to the feet (Nas et al., 2015). The benefits of this ground reaction force simulation have been shown repeatedly in cats and other vertebrates. There is evidence that training effects persist after spinal cord transection (Ward, Brown, Thompson, & Frackowiak, 2003). While not explicitly shown in research, this could suggest learning that occurs within individual neuronal circuits. The premise of neuronal learning can be shown within limb motor responses when pairing stimuli with a different, more

significant stimulus (Luft et al., 2012). However, it should be noted that the research performed on vertebrates has limited parallels to that of humans (Cote, Murray, & Lemay, 2017).

2.3 Lower Limb Rehabilitation

2.3.1 Path to Rehabilitation

Rehabilitation begins as soon as the patient's injury is stabilised. Physiotherapists assess the patient's condition before stabilisation to enable planning for prompt rehabilitation commencement. However, mobility and range of movement (ROM) exercises can only begin once the patient is no longer at risk of causing more damage to the lesion (Bloch & Basbaum, 1986). An example of such exercise can be seen in Figure 2-5. Rehabilitation procedures aim to regain normal bodily functions and promote independence in daily living activities while enhancing the limbs' remaining sensorimotor functions. This section focusses on nonsurgical rehabilitation procedures used in alignment with the spinal cord's neural plasticity.



Figure 2-5 A typical mobilization and stretch movement for the hip, knee and ankle applied by a therapist. (Physio.co.uk, 2020)

2.3.2 Conventional Rehabilitation and Recovery

Research available in the literature suggests that patients exposed to exercise and rehabilitative movement closer to the date of injury present with greater neuroplasticity and faster functional regeneration (Behrman, Bowden, & Nair, 2006; Santos, Zahner, & McKiernan, 2006). For this reason, it is also essential to look at current rehabilitation techniques used by clinicians in an acute ward setting.

While there is some evidence discussing the paucity of conclusive research for conventional rehabilitation methods, the quality of these sources is low, and not conclusive towards the reduction of traditional conventional recovery methods (McGlinchey, James, McKevitt, Douiri, & Sackley, 2020; Prabhu, Swaminathan, & Harvey, 2013). Passive exercises should be completed to resolve muscle atrophy, contractures, and possible pain, during hospitalisation in patients with a complete SCI. ROM exercises are completed to maintain a degree of functional capacity. It has been recommended that the optimal frequency of these ROM exercises is between 2 and 3 times a day if the patient is without observable muscle tone (Nas et al., 2015).

Functional training is thought to be the most effective way to enhance neural plasticity and recover motor function. The task of functional training is defined as a task-specific training towards a motor function which includes the actions: grasping, walking, and balancing exercises. Research has shown that since the findings on CPG, this functional training promotes preferential recovery modes and has a higher success rate even without supraspinal stimulation (Dietz & Fouad, 2013). Research also shows the benefits of massed practice (high repetitions) exercises during rehabilitation, especially when coupled with sensory stimulation (Beekhuizen & Field-Fote, 2005).

Locomotor training benefits carry considerable weight for patients with SCI. Motor training alone has been shown to reduce inflammatory responses, strengthen residual functionality and guide cortical and spinal reorganisation (Cote et al., 2017). In locomotor training, unloading of the body, coupled with the gait and stance training, significantly promotes significantly meaningful amounts of neuroplasticity (Behrman & Harkema, 2000). A trial investigating the effects of weight supported locomotor training compared to similar physical rehabilitation did not find any significant outcome difference. Both investigated groups did show locomotion improvement at six

months (Dobkin et al., 2006). These findings point towards a rehabilitation protocol that includes increased intensity, massed practice, and an approach that simulates a gait cycle's ground interaction forces without a patient weight-bearing requirement.

As discussed previously, with the discovery of the spinal cord being capable of walking patterns even when wholly transected, there is an immense promise to return to functional activities (Ashrafiun, Grosh, Burke, & Bommer, 2010). While this research has been primarily proven in mammals, correlation is drawn to human gait retraining regarding the similarities in the anatomies' neural pathways.

Critical sensory cues accompany the limbs' loading and unloading (Ashrafiun et al., 2010). Passive patterns allow for the stimulation of the Golgi tendons and the muscle spindles. This stimulation produces measurable EMG signals in the surrounding muscle tissue. It is particularly effective at reducing spasticity; however, many motor training protocols that emphasise active movements have a more significant effect in producing plasticity in spinal circuits and thereafter have a noted increase in locomotor performance compared to passive movements. Thus, to maximise locomotor recovery and cortical reorganisation, rehabilitation for adults after stroke and SCI events should emphasise repetitive, active, task-specific practices.

The benefits of rehabilitation are clear in the reduction of the impairments and consequences of SCI and are the most important aspect of the acute phase recovery.

2.3.3 Evidence Of Technology-Assisted Therapies

Globally, therapists require a large portion of their rehabilitation efforts to focus on the physical labour of moving a patient and their limbs. Robotic technologies have been developed to help automate some of these labours to reduce these healthcare workers' strain. Automated devices have a clear advantage as they can be designed to provide sensory input in both kinematic and kinetic manipulation of the lower limbs for extended periods. For example, a manually manipulated treadmill session may occur for 20 minutes, where an equivalent robotic manipulation task could be performed for up to 60 minutes (Colombo, Wirz, & Dietz, 2001). The ability to note patient performance is one of the critical benefits of an automated rehabilitation protocol and allows the therapist to quantify therapy effects and patient progress.

Functional gains received from robotic orthoses and gait training devices are contested. A study containing 63 stroke patients receiving locomotor rehabilitation showed more remarkable functional outcomes having received conventional therapies when compared to those who had been trained on the robotic orthosis, Lokomat (Mehrholtz et al., 2017). For the Lokomat gait training robot, motor power output was placed at 50 % of that compared to when physical therapist-assisted SCI patients with gait motion. This result was measured by the total of energy expenditure that was gauged by the patient oxygen draw. This decrease in motor output could play a role in explaining why motor gains with a robotic gait training protocol that did not contain feedback reinforcement were about fifty percent less than with therapist-assisted gait training (Israel, Campbell, Kahn, & Hornby, 2006).

However, when a study of 155 patients included conventional therapy, there was a significantly greater result when compared to exclusive conventional therapy (Pohl et al., 2007). These results were corroborated when studied in SCI patients (Swinnen, Duerinck, Baeyens, Meeusen, & Kerckhofs, 2010). These outcomes are contradictory and do not show either method as having a distinct advantage in functional outcome performance. However, the studies show that locomotor devices can be used to help alleviate physical therapist burdens.

2.3.4 Current Devices

There are two categories of devices available: stationary and connected to a stable base, and those that move with a patient. A breakdown of the subcategories can be seen in Figure 2-6.

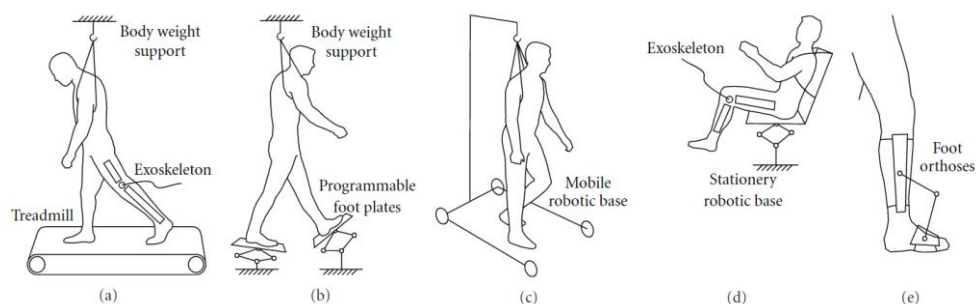


Figure 2-6 Robotic system classifications for lower-limb rehabilitation: (a) treadmill gait-trainers, (b) foot-plate gait trainers, (c) overground trainers, (d) stationary gait trainers, and (e) active foot orthosis trainers. (Díaz, Gil, & Sánchez, 2011)

The latter is more for individuals who are stable enough to allow for physical movement and are already on their way to making gait recovery. This subsection of devices is less relevant to this study and its design criteria, as with the study parameter of bed-bound patients.

Rehabilitation systems are often chosen with both the surgeon and the physical and occupational therapists involved in the rehabilitation process. This protocol depends on the patient’s rehabilitation stage. Some examples of gait rehabilitation methods and their reciprocating rehabilitation stage can be seen in Table 2-1

*Table 2-1
Gait training systems and reciprocal rehabilitation stage*

Stage	Acute - non-ambulatory patients	Subacute - assisted walking	Chronic -proprioception and balance assistance
Technologies implemented	Functional Electrical Stimulation	Lokomat	ZeroG overground
	MotionMaker	ZeroG	Treadmill
	Lokomat	Walk Trainer	HAL
		Rewalk	Overground training with BWS

The most relevant devices found in the literature (seen in Figure 2-7) are the Erigo Tilt Table, the Ergys Rehabilitation system, the MotionMaker, and the intensive care SilverFit (which is the only device that is aimed towards rehabilitation while on a hospital bed). These devices are all devices used in partially supine or seated positions.



Figure 2-7 Current devices, a.) Erigo Tilt Table, b.) Silverfit Intensive Care, c.) Ergys, d.) MotionMaker

Table 2-2 contains a summary of the advantages and disadvantages of the mentioned devices for ease of reference.

Table 2-2. Current Devices and their listed attributes

Device	Advantages	Disadvantages
Erigo	<ul style="list-style-type: none"> Allows for BWS through the tables tilting mechanism Is well researched Proven design principles 	<ul style="list-style-type: none"> High Cost Requires mobilisation of the patient No inherent passive motion capabilities No patient stimulation
Ergys	<ul style="list-style-type: none"> Continuous passive motion design Patient variability design choices 	<ul style="list-style-type: none"> No BWS Only a cyclical movement pattern Little similarity and transferability to gait Requires transport of patient into the device

Device	Advantages	Disadvantages
Motion Maker	Intensive monitoring of imposed gait pattern Patient-specific training Passive motion opportunities	Mobility of patient required Increased patient set up time due to the number of components
SilverFit	Interactive patient design Hospital bed compatible design Passive and driven operation	Pure cyclical movement No patient variability other than fit No BWS

The **Erigo Tilt Table** benefits from extensive background research and significant clinical backing. However, it is limited to those patients who have recovered from the spinal shock and severe orthostatic hypertension and can tilt their bodies. This tilting motion allows for partial weight-bearing to be experienced in the lower limbs. Patients would need to be placed into the machine, which would involve the transferral from a hospital bed and as such, it is not ideal for an acute ward setting with patients with possibly unstable injuries from which they are recovering.

The **Ergys Rehabilitation** system utilises a cycling device connected to functional electrical stimulation which fulfils the sensorimotor aspect of neuroplastic recovery. This device is again limited to those patients that can be moved onto the device safely.

The **MotionMaker** utilises a full leg exoskeleton that is actuated into a gait pattern. This motion helps to retrain a patient to restore motor function. This device is limited to the size of the patient by the dimensions of the device and exoskeleton. This device's costliness is detrimental to its feasibility within the healthcare environment that it is intended to impact.

The **SilverFit Intensive Care** falls into a range of products that utilise graphical interfaces to stimulate the program's engagement. These may be a video of a hike or walk. The patient is attached to the exercise device to appear synchronous with the exercise with the stimulation. This device plays heavily into the research of stimulated, engaged rehabilitation and how it is beneficial to recovery.

Devices found in the literature for rehabilitation programmes follow different exercise strategies and control methods. These can be classified into passive, passive-active, and active devices. The purpose of utilising devices within a rehabilitation scheme is to create a repetitive, progressive training programme. When multiple joints are actuated and exercised, better functional outcomes result. The multiple degrees of freedom (DoF) allows for a greater muscle set activation. Several actuation and control mechanisms exist for the gait trainers that are designed. A list of all would be too extensive for this literature review. A condensed version can be found in Table 2-3

Table 2-3.

Gait Rehabilitation Devices with passive-active exercise modalities and their control and speed methods.

Rehabilitation Device	Application	Control Strategy	Control Technique	DoF	Technical notes	Therapeutic gait speeds (km/h)
Lower Extremity Powered Exoskeleton (LOPES)	Leg Joints	Position and force/ moment measurement and EMG signalling	Impedance control	6	Servomotor: maximum speed 8000 rpm to 567 W, continuous torque 0.87 Nm, and peak torque: 2.73 Nm. Sideways motion: maximum speed 6000 rpm to 690 W. Linear motor: peak force 204 N to 250 W	2.7
Lokomat	Gait cycle	Position and force, computer- control	Impedance control and conventional PD controller	7	Average torque: 30- 50 Nm to 150 W, maximum peak torques are 120 and 200 Nm	3.2
G-EO Systems (end-effector robot)	Gait trajectory	Position and force control	Task-specific repetitive	6	Programmable trajectories generated in moving footplates, suitable for patients in wheelchairs	2.3
Gait Trainer (GT)	Restoration of gait	Position	Center of Mass (CoM) Control	7	McKibben pneumatic actuators	4.032
Active Leg Exoskeleton (ALEX)	Moving legs	Force-field controller	Force-field and PID controller	7	Rotary motors geared 1:50 and 1:60 gearboxes in hip and knee joints	-
Walk Trainer	Leg trajectory	Muscle stimulation, position control	PD controller and a compliance algorithm	6	Average torque @ joints: hip: 30 Nm, knee: 20 Nm, ankle: 10 Nm	4

Devices with passive-active exercise modalities and their control and speed methods. Adapted from (Chaparro-Cárdenas, Lozano-Guzmán, Ramirez-Bautista, & Hernández-Zavala, 2018)

2.3.5 Limitations

In most of the devices described, when utilised, there is a notable reduction in the hip joints' phasic shifts, which would facilitate the beginning swing phase of the gait cycle. The kinematic patterns of the hip, knee, and ankle joints are often not realised in synchrony with the patient's normal gait cycle (V. Reggie Edgerton & Roy, 2009). Fixed trajectories are also synonymous with passive movement of the limbs and an inactive and unengaged training regimen. Patient participation is crucial to the rehabilitation of the lower limb's motor functions, and as such, all entirely passive movement should be avoided.

Many of the systems that are created create a large amount of complexity. This complexity is similar to that complexity exhibited by the neural networks and their innovations. Previously, the recording and computation of such large data sets presented a problem. However, with the progression of software optimisations and the reduction of size in many computer components, higher-order calculations can be run in real-time.

Patient engagement with the task and training is often put in second place to the kinematics and kinetics of human gait replication and physical assistance. The lack of engagement should be avoided to reduce the onset of 'learned disuse', or when the spinal circuitry gradually becomes non-responsive to a fixed, imposed kinematics pattern. Active engagement and progression protocols must be implemented to avoid this.

The costliness of the devices brings about a lack of access to their services. In an already financially strained public health care system, South African SCI patients would not have access to these costly technologies.

Many technologies developed implement very complex mechanisms to enable a gait-similar trajectory of the limbs. However, there is still room to improve in this field as each patient is different with different joint ranges of motion and individual section lengths.

3. Design

3.1 Design Methodology

This chapter describes the design methodology followed during the design and development of the rehabilitation system. The chapter describes the parameters that were considered and each subsystem that resulted in the final design. It was shown in the researched literature that rehabilitation devices are in their infancy, and there is much research being undertaken to ascertain optimal methods. However, the lack of definite requirements does not mean that the challenges seen by devices are insurmountable. Much complexity is placed on designing tools for spinal cord patients, especially those trying to regain locomotor control. However, the fundamentals of patient recovery begin from relatively simple mobilisation and strengthening of the lower limbs. The early recovery stage is where the massed limb movement practice occurs, and much strain is placed onto the physical therapy staff.

After the design of the device and partial prototyping work the study pivoted away from the possibilities of human testing and validation towards *in-silico* testing. The resulting validation of the design is done *in-silico* and the testing of the device derived from the *in-silico* testing capabilities. The resulting design from the initial stages however is presented below.

The proposed design considers the flaws of complexity in design and addresses the need for an applicable device in the South African public health care system.

3.1.1 Design of Lower Limb Rehabilitation Device

Design Constraints and Specifications

The following are the constraining factors in the design of a device for use in a hospital ward with SCI patients:

1. The patient is limited to a supine position on top of a hospital bed
2. Compatible with hospital bed sizing
3. The manoeuvrability of the device. Must be able to place a patient's lower limbs into the device safely
4. Average patient body mass of 75kg

5. Average patient height of 1.7m
6. Use standard body segment parameters and standard deviation of masses as baselines for force and weight calculations

It should also be noted that frugality is of high importance in the design process. Many of the design decisions made hereafter were made with this in mind. Frugality was pursued; however, the integrity of the structure, and safety of the user, was of higher importance.

Subsystem Identification

The subsystems identified in the preliminary design process play an essential role in ensuring the device's efficacy. These subsystems can be seen in Figure 3-1 with their corresponding critical criteria for success. It is also understood that the integration of the components is crucial to the design and is considered.

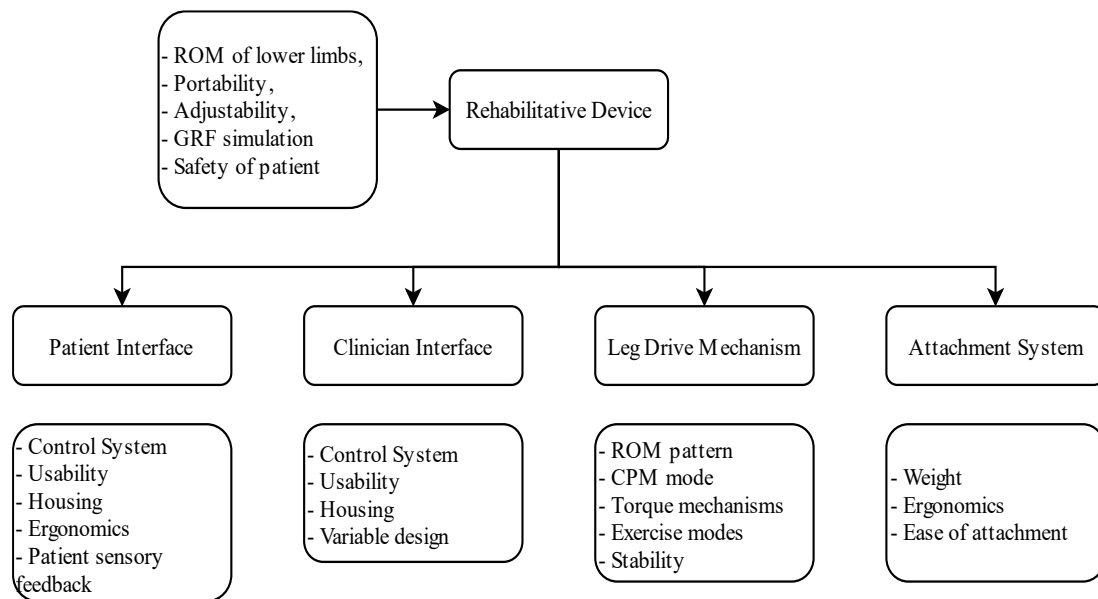


Figure 3-1 Detail of design methodology with regards to the subsystems of the rehabilitative device

The design process is focussed on developing the core working mechanisms. The mechanisms are the leg drive mechanism, patient interface, and clinician interface to create an integrated device for a standard hospital ward bed. The design methodology that is followed hereafter is laid out in Figure 3-2.

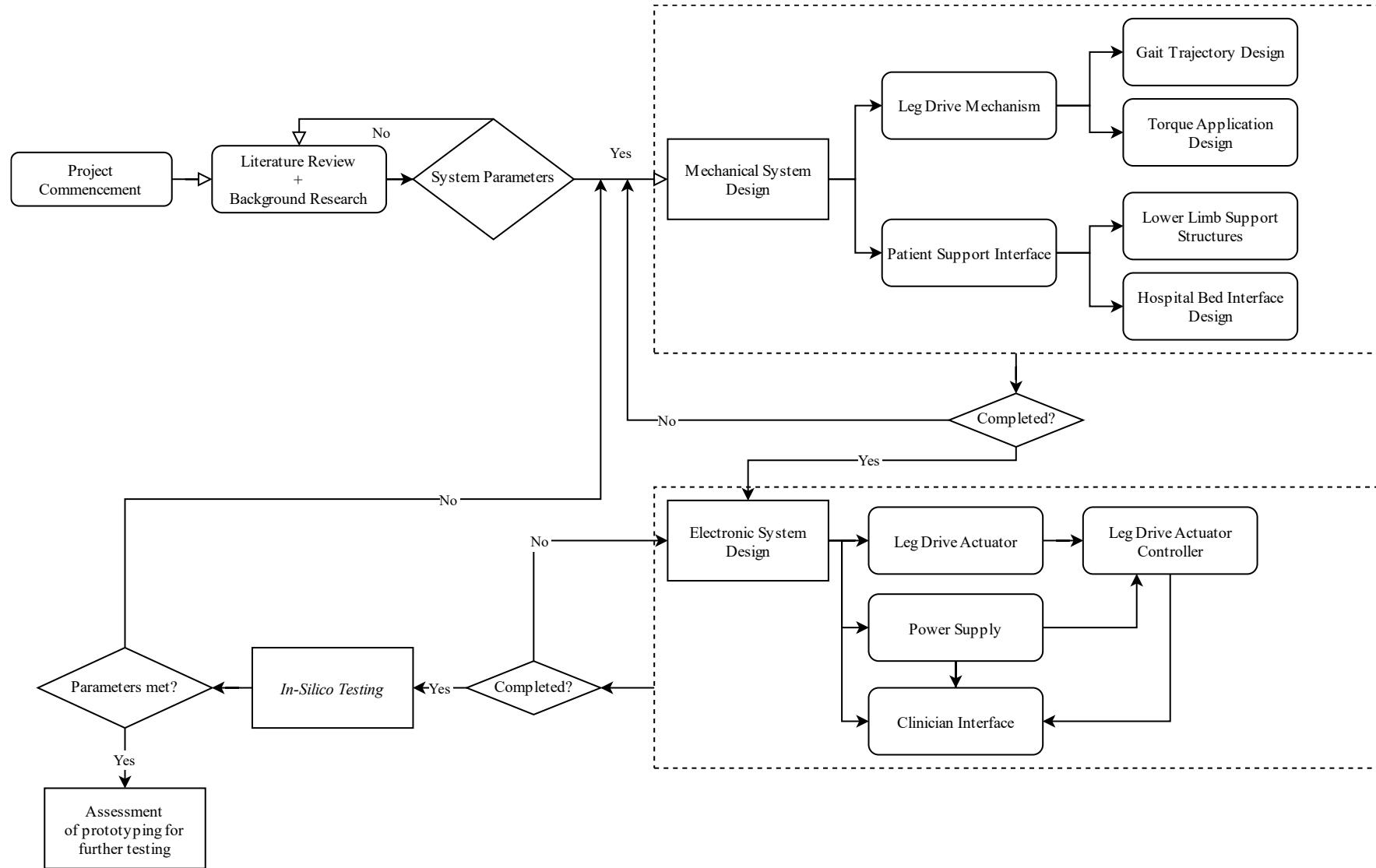


Figure 3-2 Flow of Design Methodology

3.1.2 Leg Drive Mechanism Design

The leg drive mechanism was designed according to researched principles, in which the device attempts to recreate portions of the gait cycle. Simulating the gait cycle is limited by the position of the bed. Therefore, the portions of the gait cycle, which include hip extension, are excluded. The patient completes the exercise of a targeted functional exercise, attempting a full translation of the exercise into motor function recovery (Lederman, 2010). The pattern that is implemented and repositioned in front of the patient can be seen in

Figure 3-3.

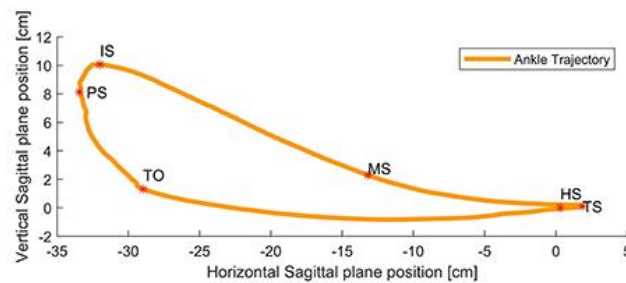


Figure 3-3 Gait pattern trajectory of the ankle with relevant horizontal and vertical positions adapted from (Mendoza-Crespo et al., 2019)

The requirements of the design are then focussed on the maintenance of a gait similar shape. Movement through this shape should be at a constant rate due to the symmetry of the gait pattern. The gait cycle and stance phases can be seen below in Figure 3-4.

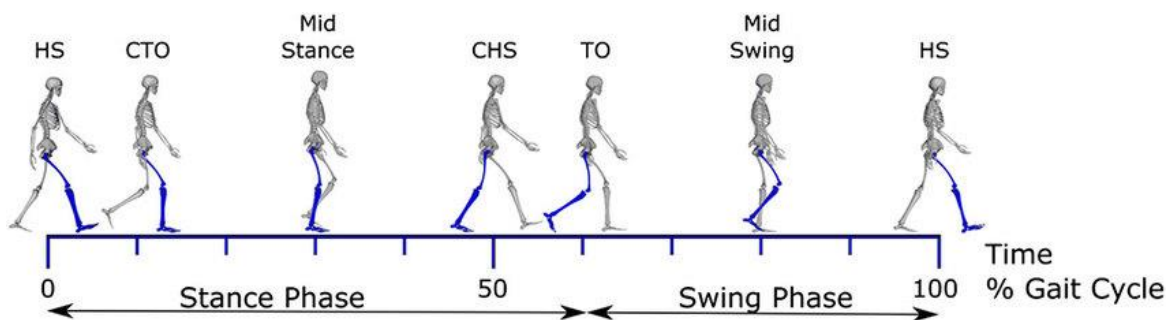


Figure 3-4 The gait cycle with included loading states from (Cheung et al., 2016)

After the gait cycle's primary motion and timings, forces that are generated in the leg should be imitated. These would be the reaction forces that are seen by the soles of the feet and in the joints of the leg during normal walking.

The primary requirements are summarised as follows:

- Maintenance of gait symmetry
- Allow for continuous movement even when there is no output exertion from the patient
- Should allow for the patient's strength capabilities to be taken into account.
- Lead the legs in a gait similar pattern, minus all portions that include hip extension, as this is limited by the hospital beds position posterior to the patient.
- Impart a force onto the legs similar to that of ground reaction forces.
- According to the gait cycle's inflection points, the movement achieved must mobilise the Ankle, Knee, and Hip joints according to the gait cycle's inflection points.
- The device must be of a weight suitable to be placed and mobilised by hospital staff. This would allow for the device to be transferred between different hospital beds.
- The patient's positioning into the device should not require the mass displacement of the patient's entire body. Should require only minimal leg lifting and placement.

There are several methods of achieving cyclic movements of the lower limbs, all with substantial differences. The industry utilises ellipticals as walking devices for exercise for upright individuals. Shown in Figure 3-5 are a few such machines and their expected pedal trajectories. All of the elliptical concepts described portray various solutions to the ankle trajectories desired; however, they require several linkages to achieve this.

When considering that the number of linkages then to be doubled to account for both legs, the number of mechanical parts to control becomes too great. While increased complexity allows for more degrees of freedom, it also means higher mechanical maintenance and electronic control.

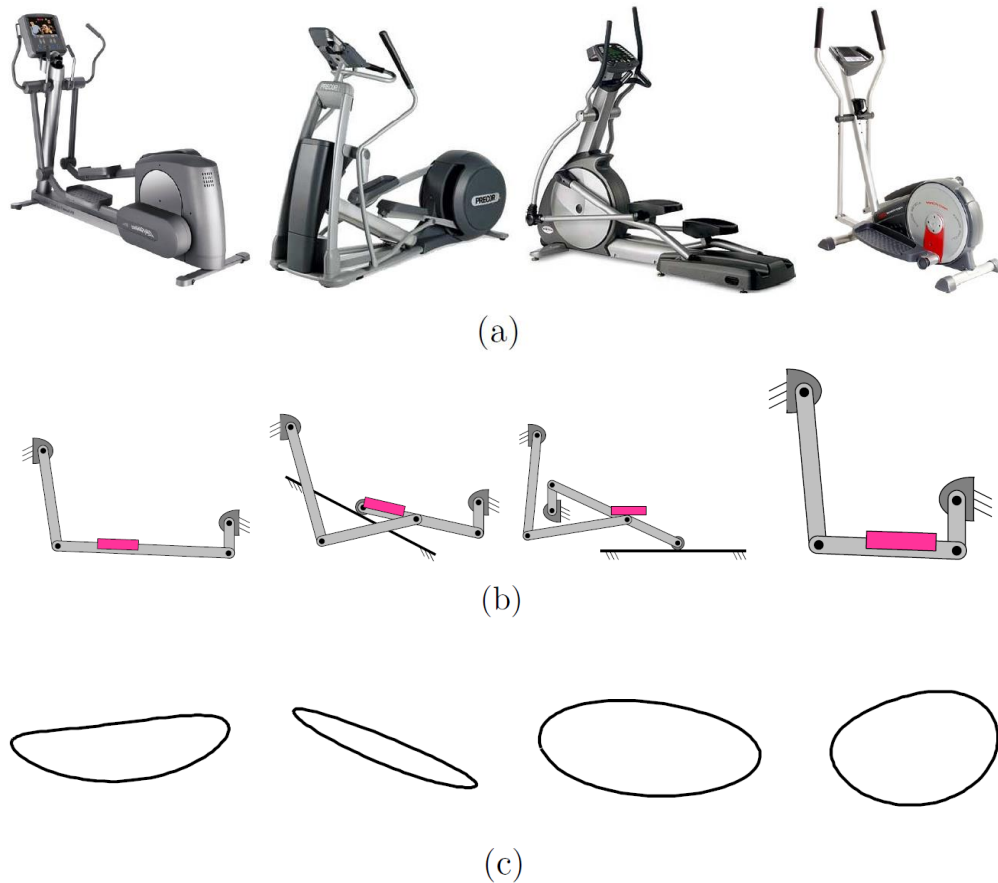


Figure 3-5 Elliptical machines left to right, they are made by Life Fitness, Precor, Matrix, and ProForm. (a) Photos (courtesy of their websites). (b) Sketches of their linkages with the foot position shown in pink (c) Approximate pedal trajectory from the design. Adapted from (DeJong, 2007)

An alternative concept of leg movement is seen in Figure 3-6 which focuses on bilateral leg stimulation with knee extension and flexion, attempting to mimic the ankle flexion and extension, gait pattern, and ground reaction force stimulation. This concept also uses the idea of an elliptical gait pattern. It is achieved through a fixed trunnion with sliding arms. The end of this arm is attached to the patient's feet and traces the desired pattern.

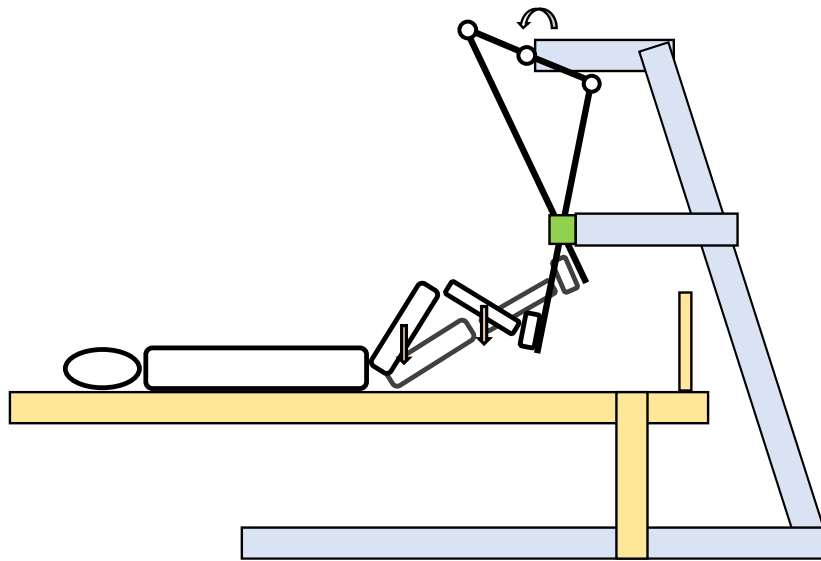


Figure 3-6 Concept design, shown with the patient supine on a hospital bed, with their feet attached to the ends of the arms of the device

The device uses two arms that are in turn attached to two cranks, reflected from one another. As the rotors are driven counterclockwise, the arms are forced through and pulled back from the trunnion, causing the foot attachments to move. The movement of the feet (attached to the device as seen in Figure 3-8) follows the pattern shown in Figure 3-7 below. The achieved trajectory is a partial gait pattern in the sagittal plane. The gait pattern is limited by the patient's bed, which stops the hip joint from reaching extension. The design is limited by how high a patient's ankle may be displaced vertically without disturbing their trunk placement. However, this can be controlled by the length of the cranks.

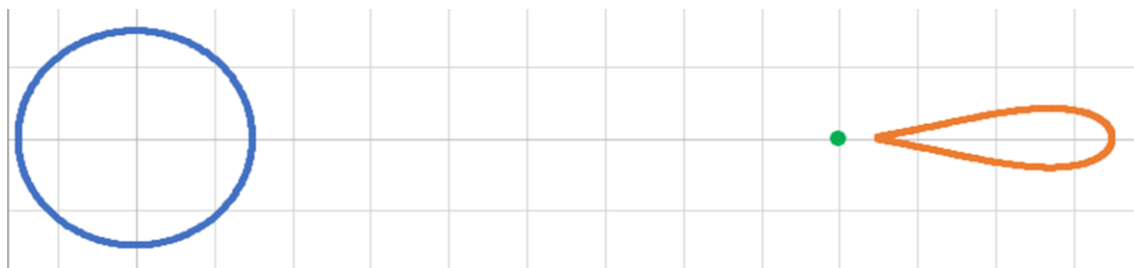


Figure 3-7 Gait pattern achieved (shown in orange), through the trunnion (green point) as the end is driven by the rotary arm (whose radius is traced in blue)

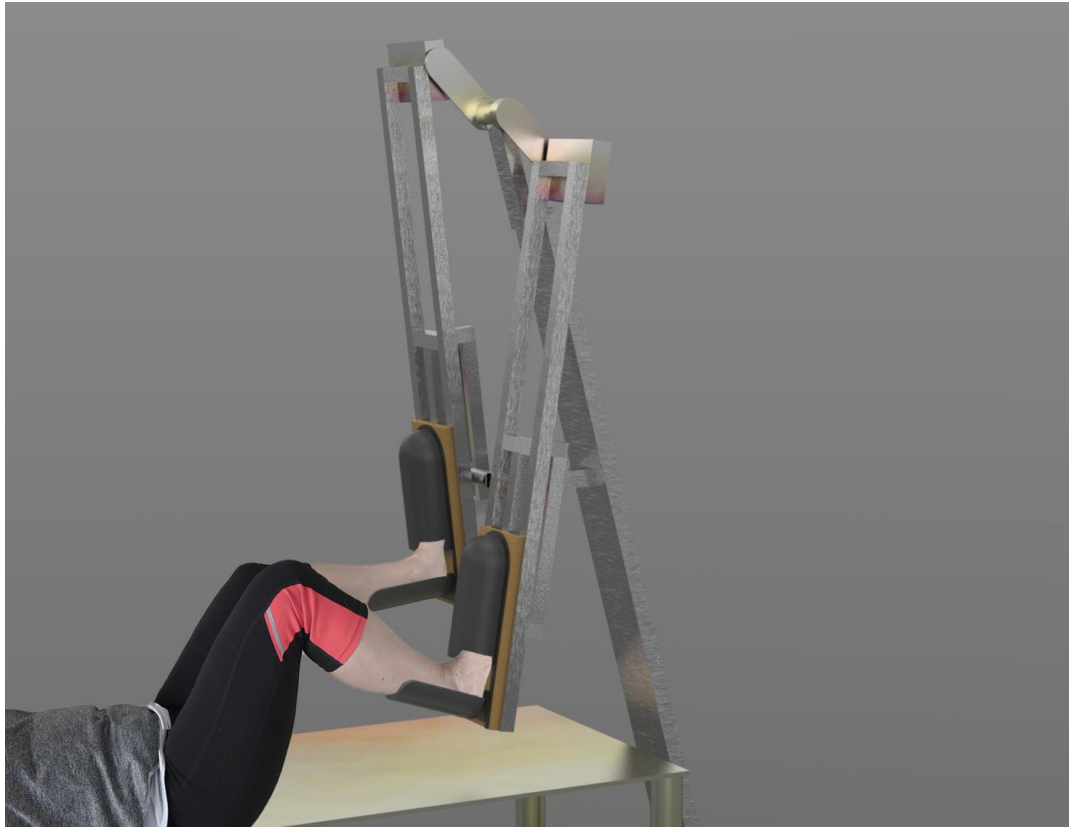


Figure 3-8 Patient mock-up for illustrative purposes of the concept

The concept design means that the ankle angle is closely related to how the shank is angled about the arm. The angle this creates simulates that of the toe-off and heel grounding positions that the ankle would achieve in a normal gait cycle.

The concept was modelled and then simulated in SolidWorks to evaluate the design constraints that this design would place on the rest of the system. Utilising the body segment parameter calculations for the idealised subject; a simulated patient was modelled, and their interactions with the design noted. The calculations of the body segment parameters can be seen in Appendix B.

Actuator

The device requires an actuator to move the arms in a cyclic pattern. Several types of actuators could be used for this project. Due to the symmetrical loading conditions and the continued application of power to the device, there is no need for ultimate precision in the movement. However, torque holding capabilities and design for close control must be considered. An actuator is chosen according to the following requirements:

- Apply torque necessary to move both patients limbs (peak torque 8N/m)
- High torque, low speed
- Attains a 30 steps/minute requirement speed
- The motor can alter the speed and torque profile

The final requirement is for the eventual control scheme that would allow for the inclusion of a master-slave driving control mechanism for the device. This control method allows for the continued training progression as the motor adapts to the patient's input stimulation. Transforming patient effort to a change in motor output allows for engaging training.

Power Supply

The requirements of the power supply are determined based on the chosen actuator and controller. The chosen power supply should be sufficient to power both components to their full specified capacities.

3.1.3 Patient Attachment Design

The safety of the patient in their interaction with the device is of critical importance. This factor is placed above all else when considering the design of the patient interfacing. The following other requirements were identified:

- The patient's physical rehabilitation with the device is designed to allow for the continued progression of exercise. It is thought that an active feedback mechanism could be beneficial in the eventual implementation of this device. The control mechanism for this can be seen in Figure 3-9.
- The insertion of the legs into the device should also be safe and comfortable to accomplish so that there is no risk of further injury to the patient. All attachment points must also avoid any skin irritation.

- There is a requirement for lower limb support, which is to be designed such that it stops the medial and lateral rotation of the lower limbs when they are suspended on the device. This rotation occurs due to the individual's lack of muscle control and could lead to unsatisfactory kinematics and possibly injury to the patient given altered proprioception, spasticity, increased or decreased muscle tone and the inability of tetra- and paraplegic patients to control joint position
- The patient interaction is done through the attachment of the patient to the leg drive mechanism. The leg drive mechanism must interface with the patient to support the ankle to allow dorsiflexion and plantarflexion. An example of this can be seen in Figure 3-10.

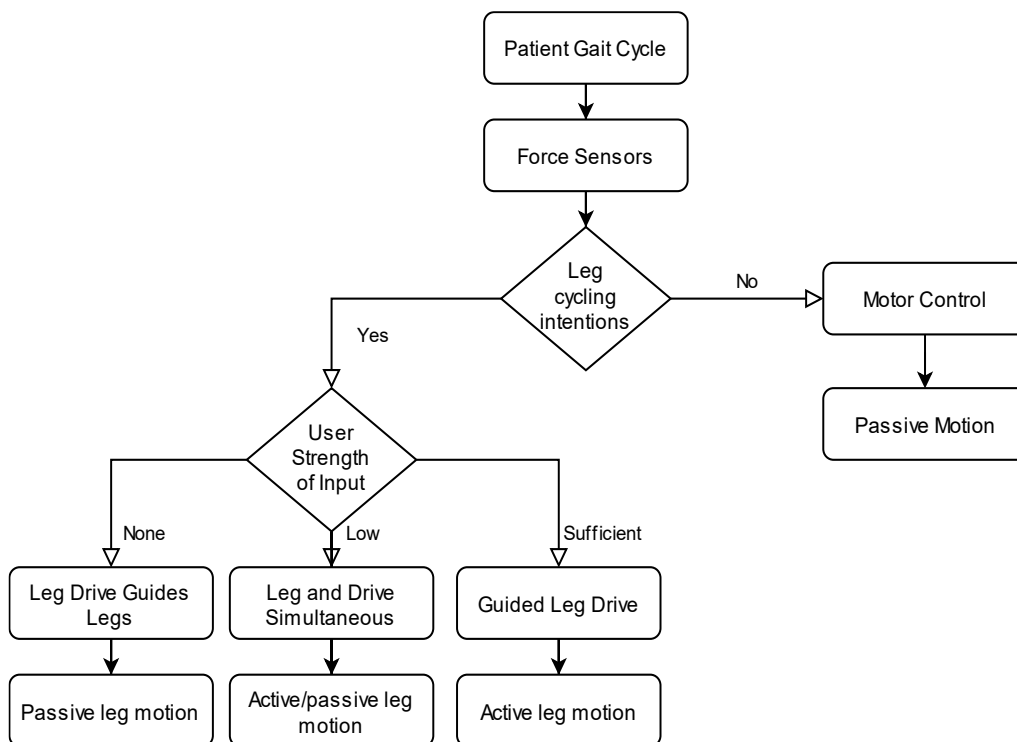


Figure 3-9 Patient force control strategy to ensure rehabilitation exercise and continual stimulation.



Figure 3-10 SilverFit device with lower limb support to stop unwanted rotation.

3.1.4 Clinician Interface Design

The **clinician interface** is designed so that exercise modes can be adjusted and programmed for a rehabilitation session. The interface allows for the adjustment of the velocities and the time profiles. The settings for a rehabilitation programme is inputted into the device before the session. The settings to be inputted to the device from the clinician are:

- Cadence (steps/min)
- Rest periods
- Exercise duration (minutes)

The control of the master-slave relationship is to be evaluated. An expected power input level can be programmed as a targeted goal for a patient to achieve. A similar input is seen with various rehabilitation machines, including the Biodex. The working principle of the Biodex device is to provide Isokinetic exercise to the patient in which the effort put in is matched in resistance by the machine.

This mode of exercise means that muscle loading occurs throughout the movement if angular displacement is to occur. In this exercise method, the device's angular velocity dictates the amount of torque generated. The slower the speed, the larger the torques that the user can generate.

3.2 Resultant Design

The following chapter describes the design process's outcomes and provides detail into the design's mechanisms. The design takes into consideration the parameters listed previously. The concept that was proceeded with for *in-silico* testing is shown in Figure 3-11 and lists the major components.

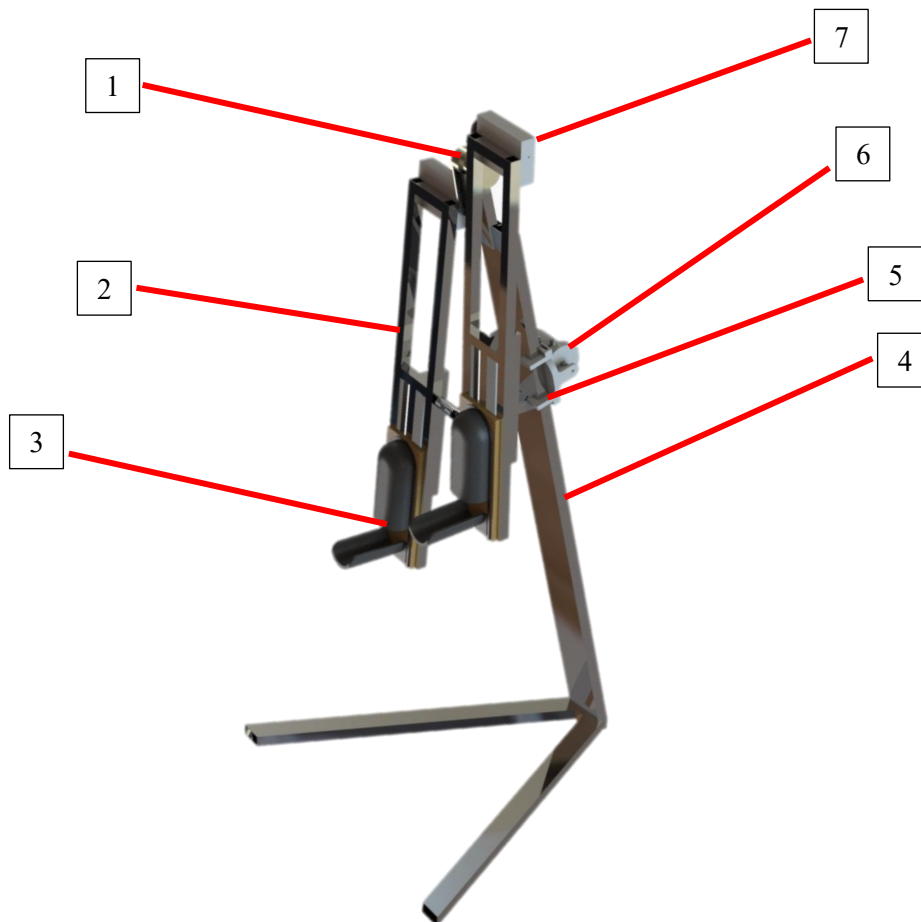


Figure 3-11 Design of the lower limb exercise device with 1) The crank and bearing subassembly, 2) The mechanical arms, 3) Foot attachment points, 4) The frame body, 5) The motor tension and adjustment mechanisms, 6) The motor and housing 7) The joint between crank and arms of the device

3.2.1 Anthropomorphic Considerations

The following dimensions were used as base considerations for the exercise device's design as per the MakeHuman open-source software for anatomically correct three-dimensional human models imported into SolidWorks. These measurements were

then used as a starting point for calculations surrounding human interaction with the device.

*Table 3-1.
Anthropomorphic measurements*

Variable	Measurement
Height	1.7m
Mass	75kg
Waist	88cm
Femur Length	42cm
Tibia Length	38cm
Foot Length	22cm

3.2.2 Working Principle

The device was designed to allow for an elliptical gait shape. The motor, with attached gearbox, turns a pinion, connected to a chain. This gear train causes the devices cranks to rotate. As the cranks rotate, the device's arms' proximal ends are moved in a circular motion. Towards the distal ends of the arms, the slots limit the motion. This limiting effect causes the elliptical shape. The patient's feet and lower legs are secured into the foot attachments to reduce unwanted joint movement due to the paralysis and lack of control and are thus forced to follow the motion of the arms' distal ends when active. The clinician can choose how fast and how long, the patient's legs should be mobilised.

3.2.3 Leg Drive Mechanism Design

Mechanical Design

During the design process, frugality was heavily considered, and with an end prototype in mind, design choices were made accordingly. To prototype, components were used from a bicycle. These components were namely the pedals, the crank, the crank axle, and the hub.

Frame Body

The frame of the device (seen in Figure 3-12) was designed to hold both articulating arms. The frame interfaces the arms with the motor as well as the crank. It provides a 'pin' for the slotted section of the arms that replaces the previously mentioned trunnion's function. The bicycle hub component is welded on the top of the frame to provide housing for the crank axle. The centre to centre distance between the pin and the crank axle is 800mm, this with the crank length of 150mm, creates a step distance of 300mm length. The frame is designed for a clearance of 100mm above the supine patient's bed to avoid interference. The legs of the frame were designed to stabilise the movement of the device and avoid unnecessary tipping.

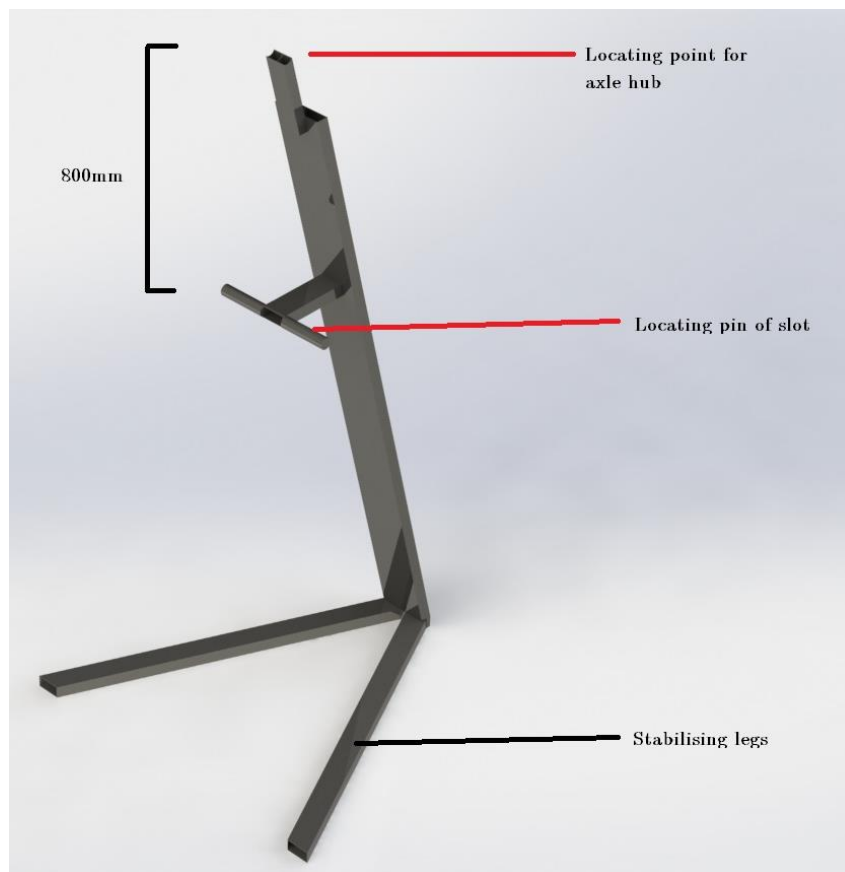


Figure 3-12 Frame body render with critical areas of note

The locating pin has two rollers placed on either end. The roller is a plastic body containing two bearings and is commonly used in conveyor systems. The roller that was chosen was the Interroll Polyamide Round Flanged Conveyor Roller 50mm x

51.3mm. This roller allows for a dynamic load capacity of 30kg. The loading capabilities of the roller made them suitable for the application with an included safety factor.

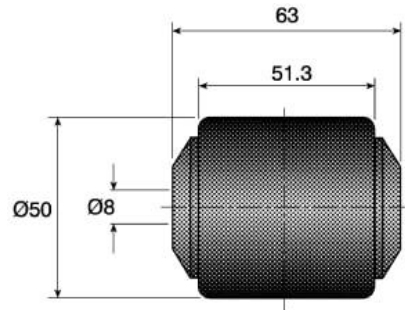


Figure 3-13 Roller with dimensions (Interroll, 2020)

The axle hub's locating point was welded to the axle hub's outer bracket (Figure 3-14). This hub component was chosen as it included many of the smaller, precision manufactured components necessary for the device's smooth operation, which can be seen in Figure 3-15. The sub-assembly would allow for smooth power transmission to the cranks with the attached gear.

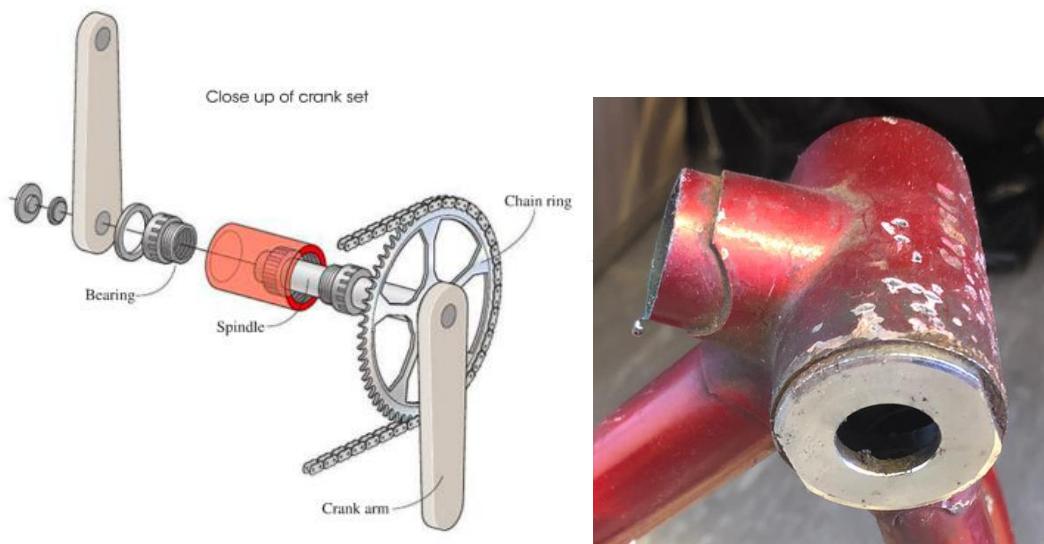


Figure 3-14 Crankset with the attached gear or chainring. The spindle is shown in red and is the hub that is welded to the frame body. (Meriam & Kraige, 2011)

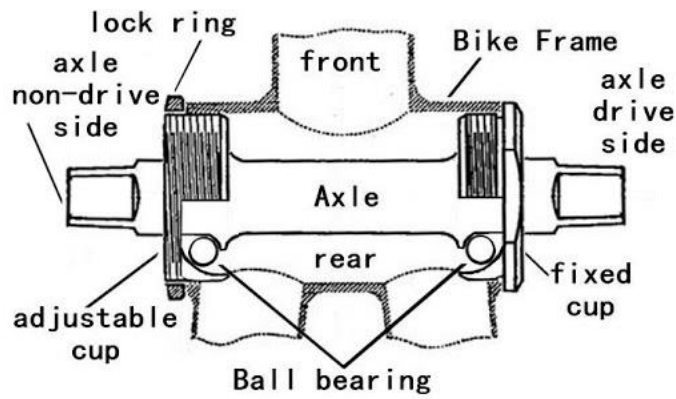


Figure 3-15 Hub bracket and related components in a salvaged bike frame (Smith, 2019)

The radius that is matched to the hub of the parts of the bracket is seen in Figure 3-16; the measurement is purely to allow for better location of the hub during the welding process and the width is matched to that of the hub width, allowing for the chain, and cranks to run true without interference.

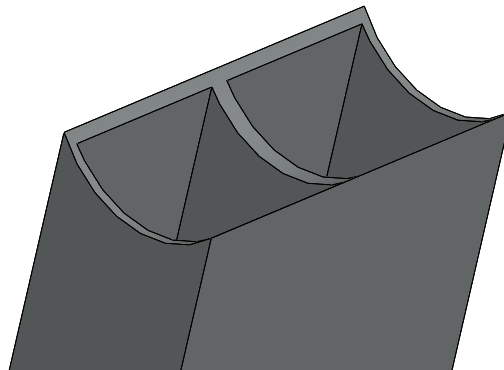


Figure 3-16 Radius added to the top of the frame body to allow for location during welding

Fabrication of the frame would utilize standard mild steel tubing. The bicycle hub and common bicycle hubs are made from mild steel. Higher cost bicycles can increase the complexity of material choices used as different alloys are used. However, mild steel is most commonly used in lower-end bicycles and ageing bicycles. The choice of material would allow the bicycle hub bracket to be successfully welded onto the frame and access to various hubs from other bicycles. The frame design is considerate of manufacturing processes; each piece can be cut to length before being welded together. There is no need for intensive machining processes other than basic

chamfering and drilling. The top of the frame requires a hub-specific radius to be bored so that welding can occur.

A SolidWorks static simulation was run to determine whether the frame design was acceptable, which determined the frames reaction to static loading of both a patient. The loading condition was a static load, placed onto the face of the radius cut into the frame body as previously seen in Figure 3-16. The weight of the patients legs were 24.1kg. The weight simulated included an added 20.9kg to allow for a range of patient weights. The addition of this weight saw a loading of 45kg onto the frame. We see the Von Mises stress distribution in Figure 3-17.

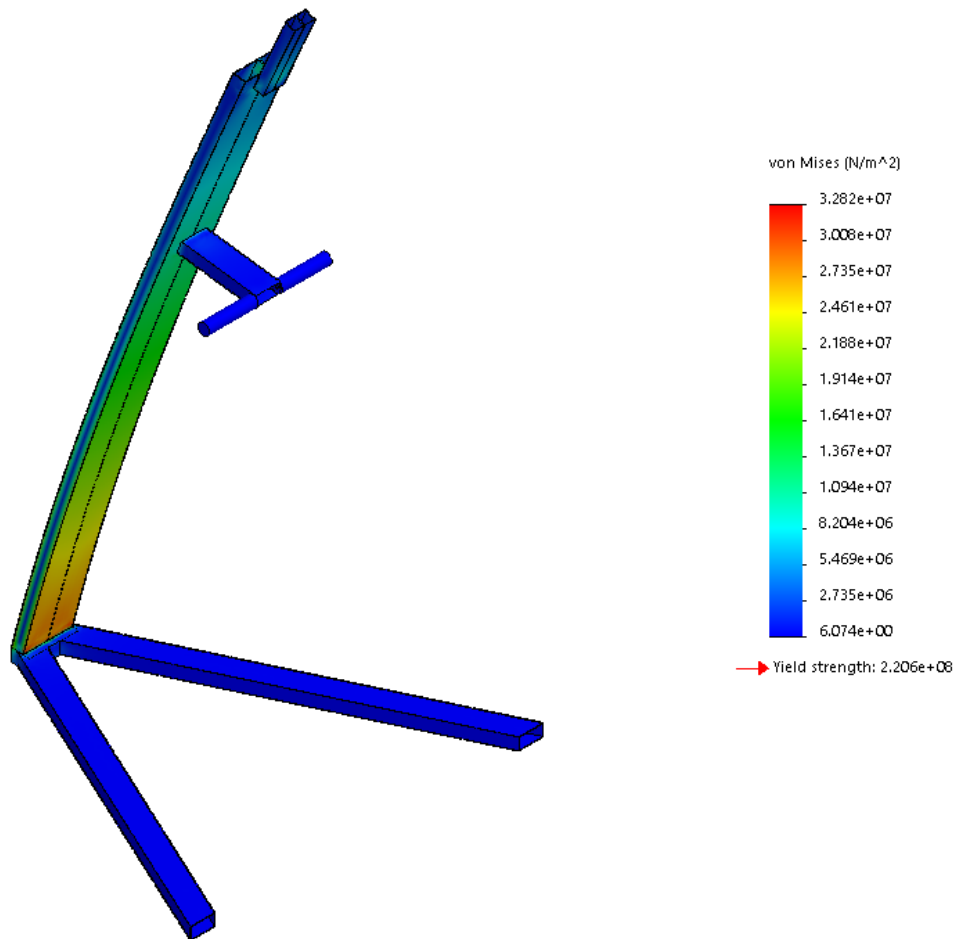


Figure 3-17 Von Mises Stresses seen in the frame body during loading.

The simulation result shows that the highest distribution of stress is realised in the lower portion of the frame, which is expected. The frame made out of mild steel

has a minimum safety factor of 6.17, which is more than sufficient for the device's safety and shows that the frame would be able to withstand loading of 277.65kg before reaching failure. This result is satisfactory, as it confirms that the device does not need ribbing or further support from the frame's legs. The shape can thus be inserted under a hospital bed without hindrance or clearance issues.

Similarly, as seen in Figure 3-18, the maximum displacement of the frame body's tip is just over 10mm, under maximum load, which is a satisfactory amount of displacement and does not impact the device's functioning. The displacement incurred will also not hinder the clearances with the hospital bed.

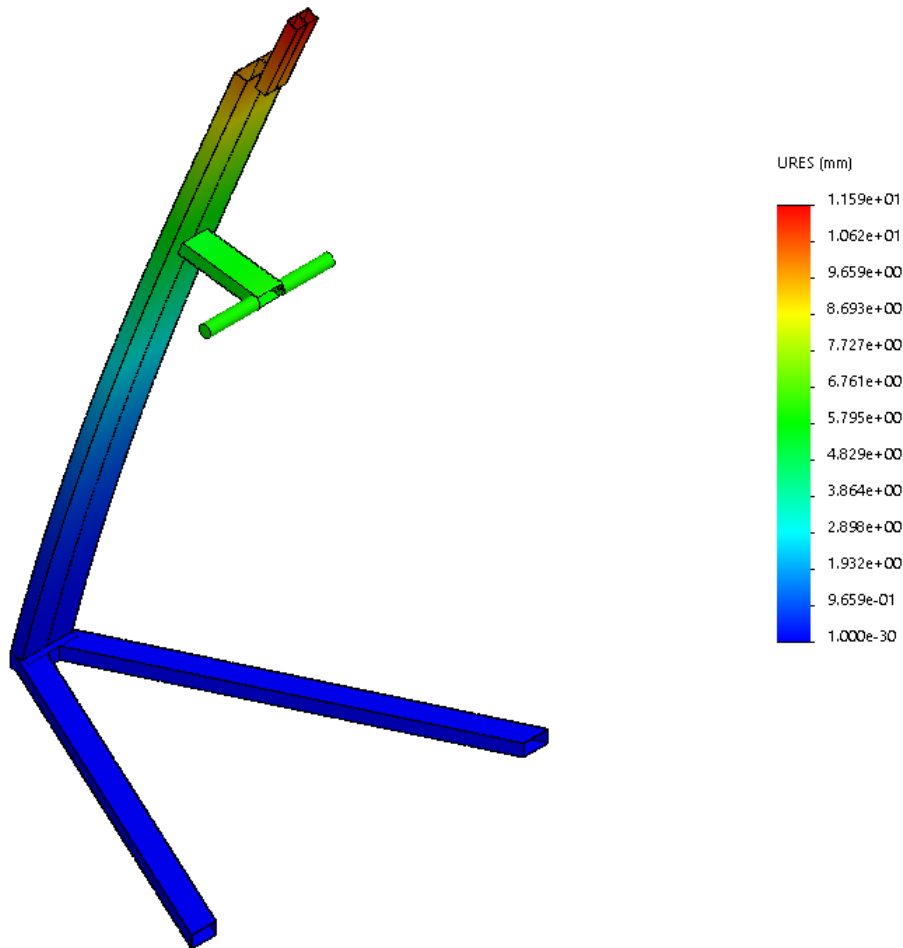


Figure 3-18 Displacement simulation during loading.

Arms

The arm components of the device are the movers of the leg. This component effectively translates the cranks' circular motion into the elliptical motion that the feet follow. The arms are 1200mm long, with a slot length of 360mm, to allow for the roller's translational movement. The distance from top dead centre to bottom dead centre is the same as the diameter of the crank circle path (300mm) however additional space is added to the slot to allow for the radius of the roller. The motion is achieved simply by doing this, without the need for precision manufactured sliders. The lack of complexity reduces the overall cost of the device.

To further increase this device's production efficiency, the bars used for the device's arms are made from standard sizes of mild steel tubing, namely 32x32x1.6mm square tube. The designed symmetrical arm is seen in Figure 3-19. As before with the frame body, the arm's steel can be cut to length and welded. There is no need for complex machining processes.

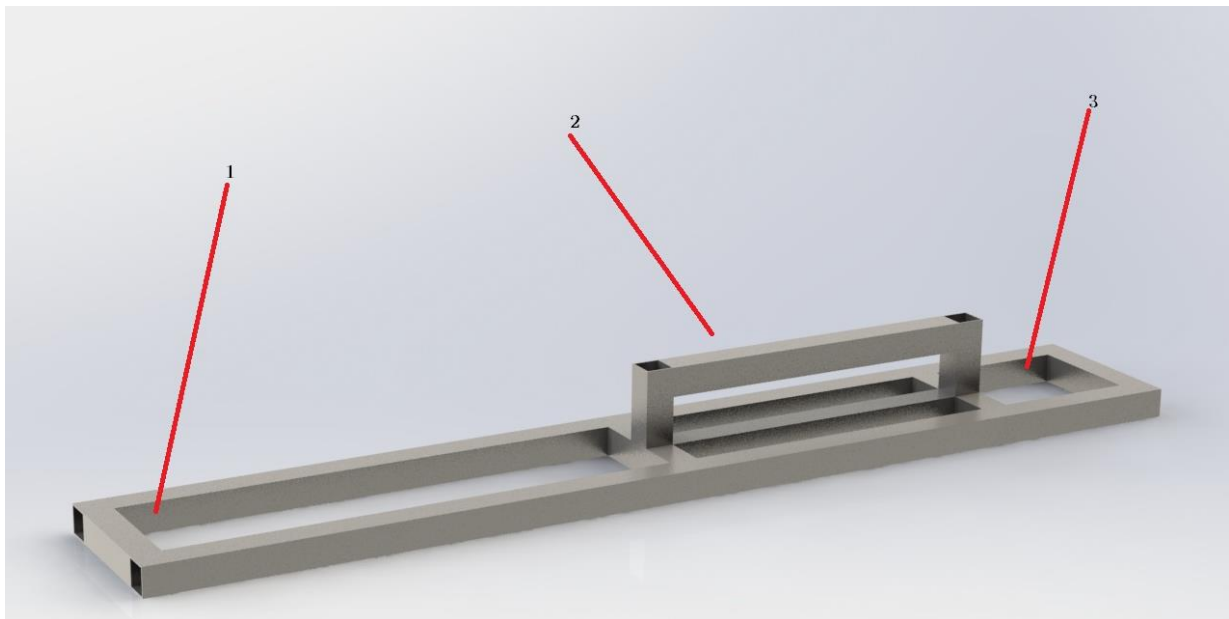


Figure 3-19 Symmetrical metal arms for the movement of the feet. 1) the proximal end to the cranks, 2) the slot within which the rollers are located, 3) the distal end for foot attachment

Power and Actuation Design

Actuator

A stepper motor is chosen as the actuator to allow for precise control and high torque for the motor and adaptation to future training schemes. The NEMA 23, 112mm stepper motor is used with a 30kg.cm torque. An image of the motor can be seen in Figure 3-20

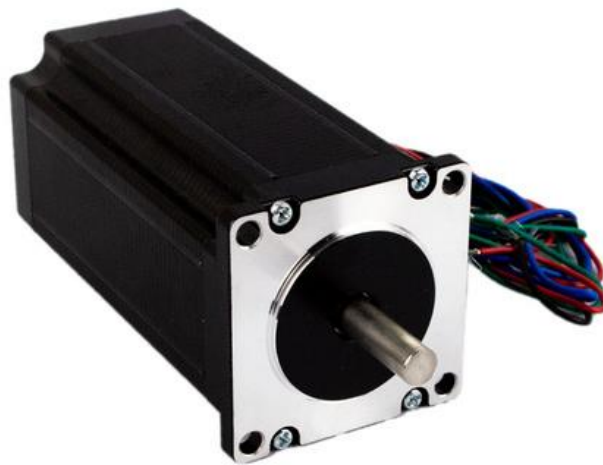


Figure 3-20 NEMA 23, 112mm stepper motor with 2.94Nm rated torque (3D-Printing-Store, 2020)

The specifications of the motor, found on 3D-Printing-Store (2020) are as follows:

- Size: NEMA 23 (57mm x 57mm)
- Length: 112mm
- Step angle: 1.8 Degrees
- Rated voltage: 6.3V
- Current/Phase: 3A
- Holding Torque: 30kg.cm

Gearbox

The motor does not meet the specifications of the project with the required torque, however, with the implementation of a gearbox (see Figure 3-21), can meet the torque

and speed requirements. Since the gear attached to the cranks of the bicycle we are using has 32 teeth, and the driving pinion has 8, we have a transmission of 4:1. The transmission ratio means that when the motor runs at the rated torque, the symmetrical arms have an applied torque force of 12Nm.

This 12 Nm is sufficient to cause rotation of the arms when attached to a 95 percentile 75kg human. A safety factor is then added to this to ensure that the motor functions even under higher loads.

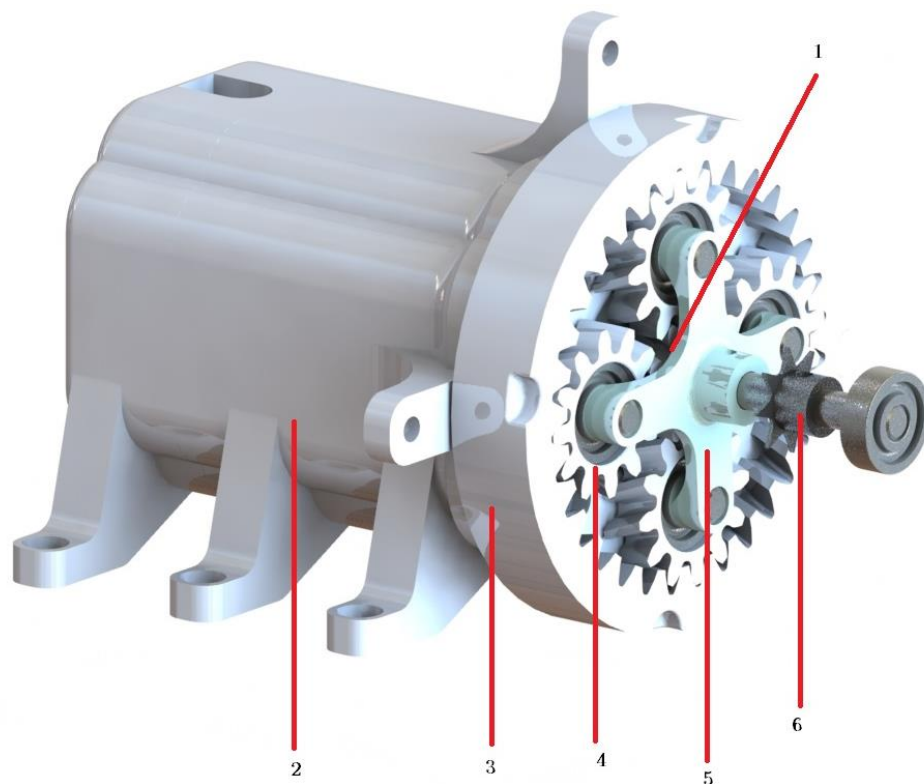


Figure 3-21 Designed gearbox and motor housing 1) Sun gear (8 teeth), 2) Motor housing, 3) Annulus (32 teeth), 4) Planet gear (12 teeth), 5) Carrier connection to the output shaft, 6) Pinion.

For this reason, a gearbox was designed. The gearbox is of helical epicyclic design and has a transmission ratio of 5:1. The gears had a module of 1 with a helix angle of 20 degrees to reduce the noise during operation. 4 planetary gears were

implemented to ensure the power transmission's further stability. The addition of the gearbox and pinion and gear creates a gear transmission ratio of 20:1. The transmission ratio creates a maximum running torque of nearly 60Nm, which allows for the movement of different weight legs.

The gearbox was 3-D printed so as to ensure that the mechanisms would work correctly. This also gave opportunity to test the functioning of the driving system. All of the components meshed correctly.

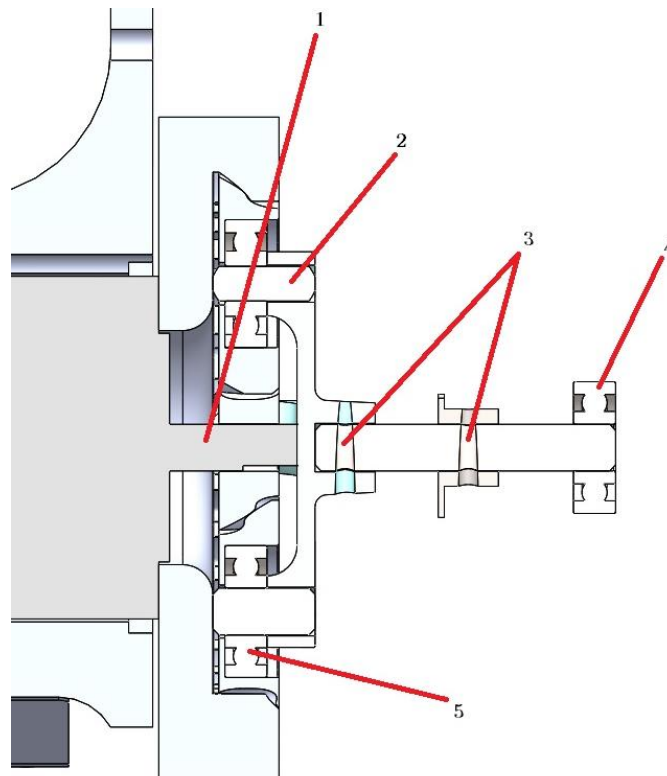


Figure 3-22 Cross-section of the gearbox, showing inner details. 1) The NEMA 23 motor and its shaft, 2) The pins that connect the planetary gears to the carrier, 3) Pins for torque transmission between shaft and attachments, 4) Locating bearing, 5) bearing for smooth rotation of the carrier.

Motor Housing

The gearbox and the motor require attachment to the frame of the device. For correct placement, the motor housing is used to locate this power transmission source variably. The housing allows for the correct placement and tensioning of the chain

system. The system is utilized to offset the issues faced by chains when too taught or too loose. The entire housing can be moved laterally to compensate for the chain's running direction. The housing can be moved further up or down the frame body to provide tensioning force to the device by altering where the clamps are tightened. The motor housing also includes a bearing housing for the location of the pinion shaft. The bearing and the housing reduces any axial bending of the pinion when under torsional load and allows the chain to run true.

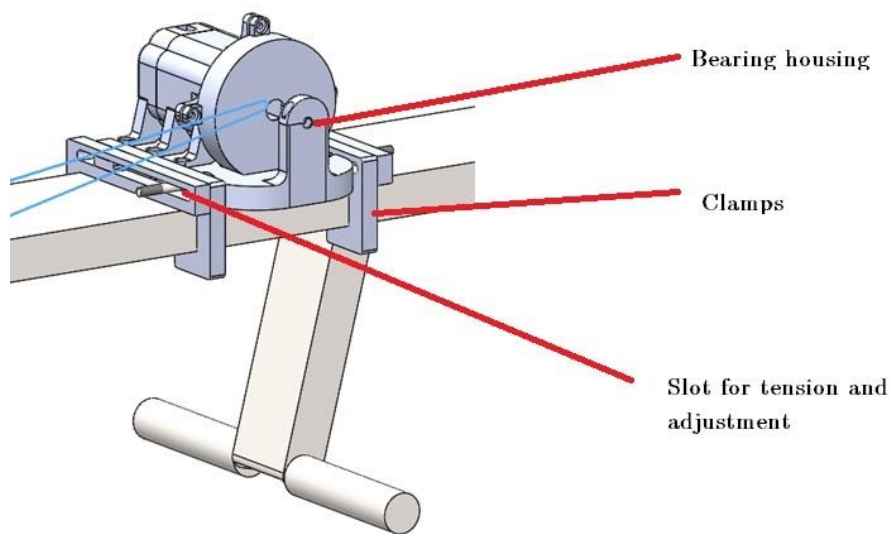


Figure 3-23 Motor housing and frame attachment system is shown interfacing with the frame body.

The motor housing can be moved laterally along the slots to correctly align the pinion with the driven gear. After that, the clamps can be positioned such that they grip onto the frame body. Once the positioning is correct, two bolts are tightened to keep the housing in place. A locating extrusion is developed to stop the slots from rotating around the bolt and restrict lateral translation movement. The basic principle of this is observed in Figure 3-24.

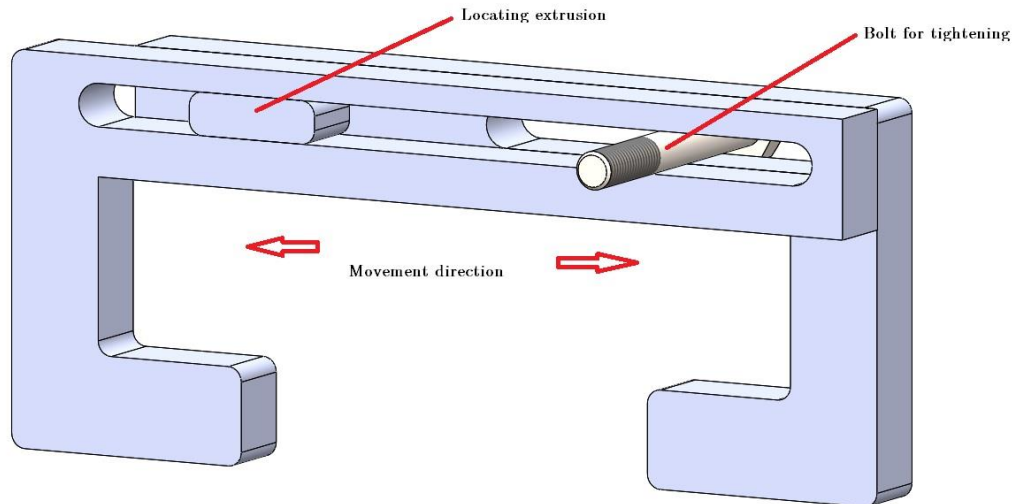


Figure 3-24 Isolated view of the clamps used to hold the motor housing to the frame body

3.2.4 Patient Attachment Design

An adjustable foot attachment is developed to allow a patient to be connected to the design. The attachment can be seen in Figure 3-25 and has a semi-rigid rubber body. The heel portion of the attachment reaches the mid-shank of the patient and, coupled with the semi-rigid material property, halts the flaccid limbs' rotational force. The rubber achieves this by resisting the torsional forces that would cause movement of the ankle. The support behind the ankle plays the most extensive role in this, while the forefoot attachment halts inversion and eversion of the foot, which would allow for a knock-on effect of joint movement. Resisting any of the joints' torsional movement does alter the leg movement profile to reside in the sagittal plane, leading to a lack of activation of smaller controlling muscles.

The heel portion is attached to a spring locked slot, whereby the lock can be compressed, and the size of the attachment changed. The rubber material within the foot attachment allows for a softer interaction with a patient's skin, and unlike completely rigid counterparts, the rubber material does not create a friction zone where a patient may blister or chafe. It would ultimately be recommended that the patient still utilise a sock to reduce skin friction further.

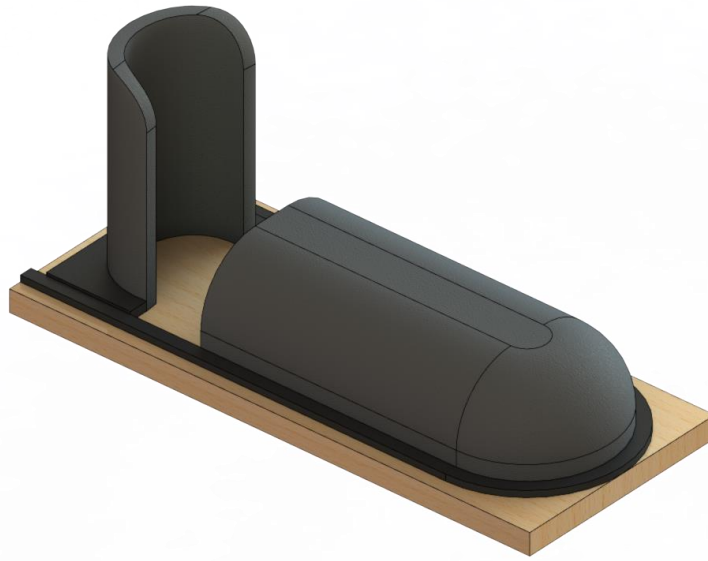


Figure 3-25 Foot attachment design with adjustable heel position

Further consideration of the design must be made with the placement of the patient on the bed. A minimum of 10cm clearance between the bed and the lowest point of the arms arc is implemented to allow for patient placement. The clearance, while necessary, does alter the starting hip angle of the patient. For the patient's safety, the device should also not cause the knee joints to 'lockout' or reach 0° . If the device were to reach this angle with a patient's knee, it becomes considerably more difficult to flex the knee due to the knees' natural tendency to maintain the legs' straightness in the screw home position. The patient's placement can be made such that the device has a minimal displacement effect on the patient through its range of movement. However, this is only for the described anthropomorphic case.

3.2.5 Clinician Interface Design

Components for the clinician interface are heavily influenced by the actuator and how that actuator must be controlled. The clinician interface must be able to control two main variables of the system for primary functionality; these are:

- Time of operation
- Speed of operation

Further development of the clinician interface would involve altering how much patient force can contribute to the system's movement. Altering the input methods

would allow for a tiered training approach and allow for variability and progressive training schemes.

Control Components

Stepper Motor Driver TB6600 V1.1

The NEMA 23 that is chosen requires 3A of current for optimal operation. Being a stepper motor, it also requires a motor driver. For the purposes described, the TB6600 motor driver was chosen, seen in Figure 3-26.

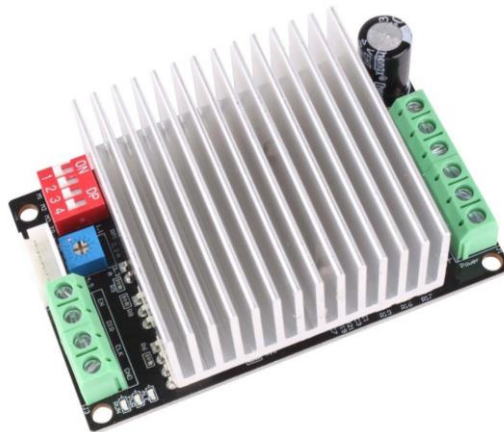


Figure 3-26 TB6600 V1.1 Motor driver (DIYElectronics.co.za, 2020)

The component is an inexpensive driver for stepper motors and offers a wide range of currents and excitation modes. The driver allows for controlling the direction of rotation of the motor and the frequency of stepping, allowing for speed control. The TB6600 offers the following specifications:

Table 3-2

Technical Specifications of TB6600 V1.1 as per DIYElectronics.co.za (2020)

Input Voltage	– 8V to 45V DC
Operating Voltage	– Up to 50V DC
Input Current	– 0.2A to 5.1A
Driving Current	– 4.5A Typical 5A Peak
Selectable Excitation Modes	– 1/1 ; 1/2 ; 1/4 ; 1/8 ; 1/16 Step
Safe Operating Temperatures	– -10° to +45°C
Dimensions	– 81 x 50mm

Thus, the driver can supply the necessary voltage and current to the stepper motor to operate at full power. The required torque outputs of the motor can then be achieved. The power supply, Arduino, and stepper motor are connected to the driver, as shown in Figure 3-27.



Figure 3-27 TB6600 Wiring scheme for connection to the power supply and the stepper motor.

Arduino Mega

For the motor's programming to allow for control, an Arduino Mega is chosen seen in Figure 3-28. The programming capabilities of the board allow it to provide the operational requirements of the device. The Arduino microcontroller can store a given program on it, making it ideal for the device's initial bench testing.



Figure 3-28 Arduino Mega Board (Arduino, 2020)

The other specifications that enable this device to be suitable for the device's development are listed in Table 3-3.

*Table 3-3
Technical Specifications of the Arduino Mega*

Operating Voltage	5V
Digital I/O Pins	54 (of which 15 provide PWM output)
Analog Input Pins	16
Flash Memory	256 KB of which 8 KB used by bootloader
Clock Speed	16 MHz
Length	101.52 mm
Width	53.3 mm
Weight	37 g

The Arduino could be programmed to achieve the clinicians desired training parameters. The Arduino is coded in Arduino language. The language makes use of several libraries. For this project, the AccelStepper library was utilised. The library allows for speeds to be set and for accelerations to be coded more simply. While utilising many other commands, the library allows for more precise control of the stepper motor. An example of some of the AccelStepper and Arduino code is shown below. This code snippet shows the necessary code to set the motor to accelerate at a specific rate up to a speed until it has moved a specified distance.

```
#include <AccelStepper.h>

// Define which stepper motor to use for the arduino
// Define the pins to be used on the arduino
// direction Digital 9 (CW), pulses Digital 8 (CLK)
AccelStepper stepper(1, 8, 9);
void setup()
{
  stepper.setMaxSpeed(1000);           //Set the running speed
  stepper.setAcceleration(100);        //Apply the acceleration
  stepper.moveTo(5000);                 //The number of steps to
move
}
```

The library’s simplicity and the coding process lends itself to a computer used to power the Arduino. A computer is also chosen to upload parameter changes to the speeds and distances used in the training programs.

Power Supply

A summary of the power requirements of the individual components can be seen in Table 3-4 and derive the requirements of the power supply unit (PSU)

*Table 3-4
Power consumptions of system components*

Component	Max Voltage (V)	Max Current (A)	Power Draw (W)
NEMA 23 Stepper Motor	6.3	3	Load Dependent
μC Arduino	20	0.8	2.2
TB6600 Driver	45	5.1	

The actuator is the largest source of power to draw for the system. The driver chosen allows for this range of currents and voltages needed for the different load cases. For the power supply, the Mean Well, 350W Embedded Switch Mode Power Supply was chosen pictured below in Figure 3-29. The power supply can supply 24V at 14.6A, which is sufficient for the device’s use cases.



Figure 3-29 Mean Well 24V Power Supply

The PSU converts the AC from a wall outlet into usable DC for the system. A switch between the wall plug and the PSU was added for more straightforward operation. Further, enclosures were designed to house the driver and the Arduino. This design can be seen in Figure 3-30

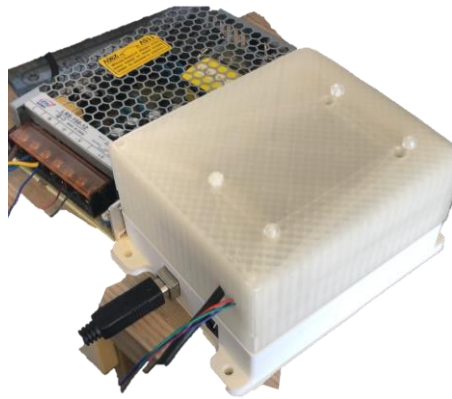


Figure 3-30 3D printed housing for the Arduino and Motor Driver with computer linking cable and PSU positioned to the side

3.2.6 Design Validation

The design validation process can be seen in Figure 3-31 and is broken up into three parts: the analysis of the subsystems individually, their integration, and the analysis of the completed assembly. The following sections detail the outcomes of this process and gives summaries of the findings.

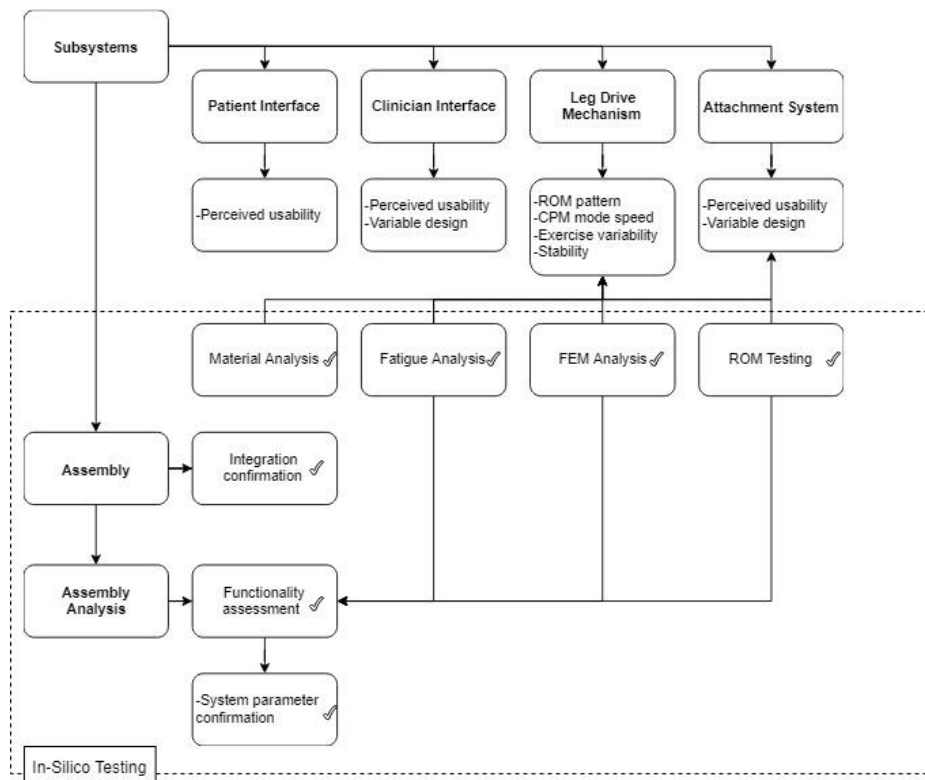


Figure 3-31 Design validation process methodology for each subsystem

Patient Interface and Attachment

The patient interface was shown to two physiotherapists. One was a sports physiotherapist, and the other a recently graduated physiotherapist. The range of experience of the physiotherapists proved beneficial to the validation of the device within its working environment. The physiotherapists were shown an animation of the device and its movement and then were shown the patient interface (Figure 3-32). They were then asked to rate the component's usability (not the device as a whole) based on its effectiveness, efficiency, and satisfaction. Each of these components is given a 1-5 rating, with 5 being the highest positive result.

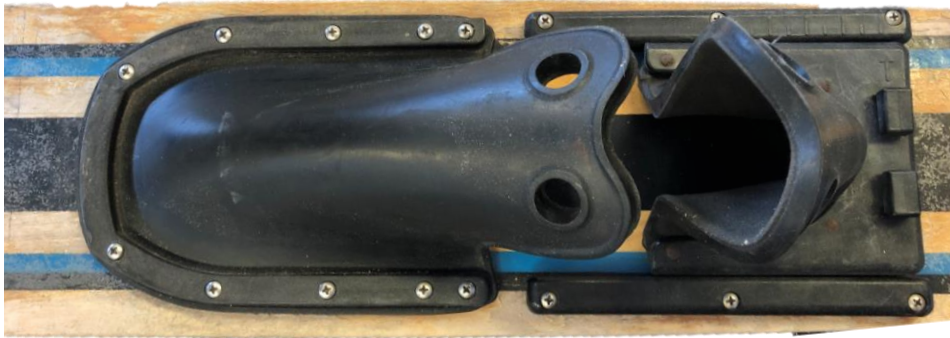


Figure 3-32 Prototyped patient interface made of rubber and a slot fixture mechanism to adapt to foot size.

The results of their assessment are tabulated below, with both scores being acceptable, and further comments noted below in the discussion and recommendations sections:

*Table 3-5
Usability assessment of patient interface system*

Component	Sports Physiotherapist	Graduate Physiotherapist
Effectiveness (1-5)	3	4
Efficiency (1-5)	4	4
Satisfaction (1-5)	3	4
Total	10	12

Both physiotherapist assessors thought that the component could fulfil the patient interface's role. The interface is sufficiently adaptable to the different patient's foot and shank sizes; however, they may not supply enough resistance to weighty patients' laxity. This lack of support could then lead to incorrect positioning of the patient during their movement. Ensuring that the ankle and knee joints can only move in a parasagittal plane, the hip joint does not go into external or internal rotation because the patient is lying in bed. Unsupported medial or lateral movement of the knee joints in SCI patients may result in injury to the knee ligaments, cartilage, stress on the interface and the patient's skin and alter the device's dynamics.

The placement of the finger holes in the rubber is noted as being an effective method of manipulating the rubber sheeting to the shape of the patient's foot during attachment. The spring-loaded locking system for the slot was also thought to be comfortable and practical to adjust the foot sizing

Clinician Interface

The same two physiotherapists were again consulted on their thoughts as to the usability of the clinician interface. While they understood how the code could be manipulated to input and adjust speeds, a more straightforward interface is required. It is noted that the current set up is sufficient for the prototyping stage and the assessment of the working mechanisms, but as a whole medical device does not supply a usable user interface.

Leg Drive Mechanism

The leg drive mechanism is validated through the design to achieve a successful ROM and sufficient speed testing. Here it is analysed concerning the materials used, the system's fatigue, and a finite element method (FEM) to determine any wayward deflections. Again, the system is assessed on its range of movement to ensure that the system's assembly was successful.

FEM Analysis

As discussed in Chapter 3.2.3, the device sees a maximum deflection of $\pm 10\text{mm}$, which is not of concern to the device's functioning. While steps could be made to decrease the deflection value, it would increase the costs of the manufacture of the frame of the device, and at this stage of design is unimportant.

Material Analysis

The materials used in the construction of both the frame and the arms are easily accessible and allow for the project's easy construction. The mild steel material is relatively inexpensive and easy to manipulate. A quote for a steel prototype came to R3179.00, which included labour and procurement costs.

ROM Analysis

The system's range of movement is assessed using SolidWorks simulation analysis, which confirms the device's successful movement pattern. The trace path of the movement of the device can be seen below in Figure 3-33. The traced path represents the line of motion that the lowest point of one of the arms follows through an entire cranks' rotation. With the cranks vertical as they are in the figure, the arms are at their lowest point to the bed. Further, Interference Detection was run on the SolidWorks assembly to ensure that no components were impacting one another and that the assembly could move freely.

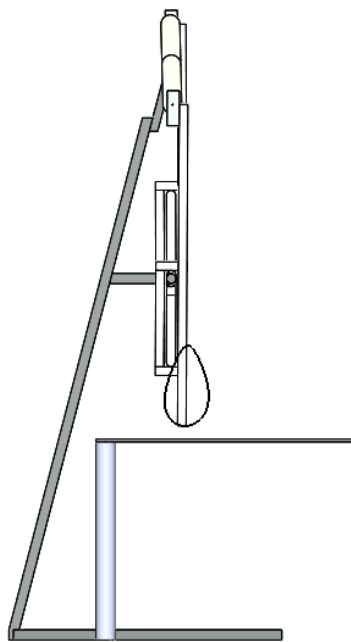


Figure 3-33 Traced path of the lowest point of the arms

Fatigue Analysis

The frame body was also run through a fatigue analysis, with the 45kg stresses measured previously. The study was set up to run for 200000 cycles in a fully reversed oscillating manner to approximate the cranks rotations. The SN curve for the material was derived from SolidWorks' elastic modulus properties of Carbon Steel.

The simulation results showed no damage placed onto the frame from the stresses sustained in the device's use. The life cycle of the various areas can be noted in Figure 3-34. It is seen that the life cycle of the product is all equal to or greater than 1,000,000 cycles and thus can be considered to have infinite life.

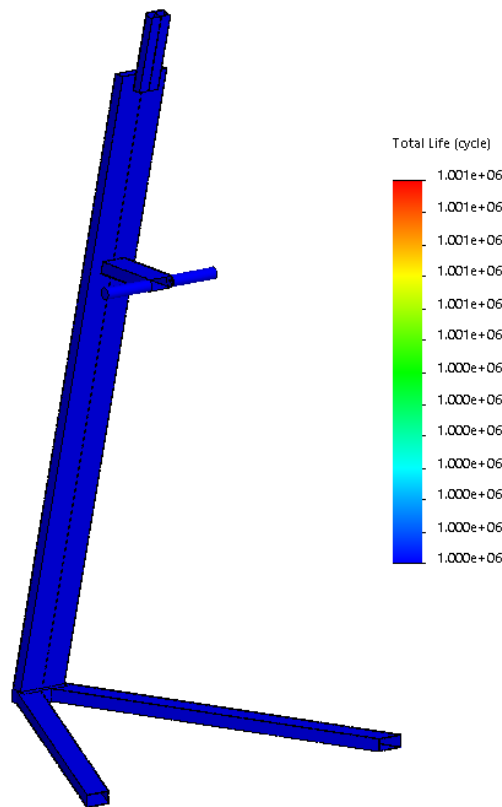


Figure 3-34 Life cycles under the stresses of operation of the frame body

While the life of the product could be considered an overdesign, the patient's safety is paramount. When looking at the device's use case, the device would likely be used across multiple hospital beds throughout the day. The cycle and exercise time would amount to a great deal of use, and thus the integrity of the device must remain.

3.2.7 Failure Modes and Effects Analysis

Risk is always present during device operation, regardless of the approaches taken during the design process to mitigate them. A Failure Modes and Effects Analysis (FMEA) systematically defines these risks and through this analysis, design controls can be put into place to further reduce the severities of these risks.

The process shown in Table 3-6 involves identifying risks involved, the consequences of said risks, rating the severities (SI), identifying causation of the risks, specifying probabilities of the occurrence (PO), identifying indicators of failure, and determining how detectable each cause is (DR). These results culminate in the risk priority number, which is calculated as the product of the other ratings ($RPN = SI \times PO \times DR$), and a can lead to recommendations for future design iterations.

The scales of severity and the rating scheme that can be applied to the FMEA can be seen below:

Score	Severity of Impact (SI)	Score	Probability for occurrence (PO)	Score	Ability to Detect Failure (DR)
1	None	1	None	1	Clear
2		2		2	
9		9		9	
10	Injure Patient	10	Inevitable	10	Imperceptible

The results of the FMEA indicate that importance should be placed on the support of the patients limbs and the safety of the patient during operation of the device. The scores of these risks are indicative of the fact that they hold the highest risk of failure of the exercise procedure.

The results indicate that any future design work should be focussed around developing mechanisms that reduce these risks. The FMEA process is to be implemented and analysed after each major iteration. Implementation of ISO 14971 for risk management should also be considered as an adjunct to the design process.

Table 3-6
FMEA model of device and subsystems

Subsystem	Possible Failure Mode	Potential Failure Effects	Potential Failure Cause	Current Controls	SI	PO	DR	RPN
Patient Interface and Attachment	Support structure material failure	Unable to move legs	Manufacturing flaw	Manufacturing inspection Designed from form fitting rubber and ABS plastics	10	3	3	90
	Patient does not fit on the device	Unable to perform procedure	Design flaws	Customizable foot size attachment Visual inspection	6	3	1	18
	Patients' feet come loose	Patient leg damage	Incorrect foot fit	High friction rubber contacts Adjustable foot size Low speed of use	10	2	1	20
	Foot slot adjuster breaks	Patient's leg comes loose	Spring loaded pins break Spring loaded pins not fully locked	ABS plastic for durability Spring loaded pin is visually out of place if not locked	7	1	2	14
	Patient lower limb discomfort	Friction rashes or lesions Disuse of device	Incorrect material finishing	Rubber interface design Manufacturing inspection	3	3	3	27
	Patients' limbs not supported fully	Patient tissue damage and injury	Incorrect Placement of Legs	Visual inspection Therapist inspection Implementation of lower leg support structures	10	4	7	280
Leg Drive Mechanism	Crank arm cannot apply sufficient load	Unable to create motion	Material failure	Visual inspection Lack of movement	10	2	1	20
	Gearbox failure	No motion	Material shearing Gears locking Overheating	Slow speed gearbox Correct gear tooth tolerancing	3	6	5	90
	Drive train failure	No motion Chain slippage	Chain breaking Sprocket teeth breaking Bearings locking Material Failure	Correct lubrication and maintenance Pre-manufacture part quality choice Correctly sized and chosen bearings ABS Plastic housings	3	6	5	90
	Speed too great for patients' abilities	Mass tissue damage to patient	Programming Control error	Visual inspection	10	2	2	40
	Inability to support patient weight	Procedure failure	Material failure/ Manufacturing flaw	Manufacturing inspection Visual inspection	4	5	1	20
	Locking up of device	Bearing/ Roller Failure	Rust	Visual inspection Applications of lubrication	5	7	5	175
Clinician Interface	Incorrect settings input	Incorrect speeds or time input	Programming error Control error	Visual inspection of speed	10	2	1	20
	Interface unresponsive	Incorrect protocols applied	Programming error	Emergency shutdown switch	10	2	3	60

4. Methodology and Results

This chapter provides an overview of the *in-silico* study and describes, in detail, all the testing methods and procedures that were used to achieve the results further shown. Resources used in testing and determining the correct recovery programmes are costly both in a monetary sense and in time resources of said specialists.

There is a need to find alternative options to save time and money when finding the best solution for individual patient pathologies. Software simulators can and have been implemented in the past, such as:

- Matlab,
- Ros,
- RoboDK,
- SimBody,
- OpenSim
- AnyBody

These tools and others play an essential role in modelling and simulating the physical body's system dynamics and musculoskeletal models, leading to better user-centred designs.

Another useful tool for motion analysis and studies is the simulation software built into SolidWorks, ADAMS. The ADAMS dynamic modelling software allows users to generate motion and force data from a given set of constraints surrounding the 3D modelled objects. In this way, a designed object's interaction with its environment may be studied.

4.1 Purpose of *In-silico* Study

The *in-silico* study aimed to investigate the effects that the rehabilitation device may have on the connected patient's movement patterns. The study is also used to investigate the potential ground reaction forces experienced by the patient. The study is performed *in silico* to attempt to reduce the resources used in human-centred design.

4.2 OpenSim to SolidWorks Cross-over

The device was simulated in the SolidWorks Motion Analysis environment to reduce the resources spent developing the project. Due to the lack of Musculoskeletal simulations in SolidWorks, OpenSim was considered a validated model information source. The models used within OpenSim are validated musculoskeletal models and can be used in various manners to compute variables that would be difficult to otherwise calculate on human subjects.

To utilise the ADAMS software models, the models would first have to be converted to SolidWorks assemblies and integrated with the designed components, before motion analysis could continue. The model's muscular components are represented as viscoelastic dampeners and could not be converted to SolidWorks components. The lack of muscular components was justified as acceptable, owing to the little force that a spinal cord patient would exert onto the device. The motion analysis would look purely at the developed kinematics of the patient's body. The exact model needed to be converted to a SolidWorks assembly to maintain the researched and validated parameters.

The process that would be followed would be to:

1. Create solid bone bodies
2. Apply correct inertial properties and material properties
3. Correctly recreate the joints of the model with SolidWorks equivalent mates.

4.2.1 Lower Limb Model 2010

The OpenSim model Lower Limb Model 2010 (E. M. Arnold, Ward, Lieber, & Delp, 2010) is used as the base for the model's properties to be converted to SolidWorks bodies. The model itself also includes an upper torso model, but this was not used for the described study.

Solid-Body Properties

The bone bodies found within the Lower Limb Model 2010 include those seen in Table 4-1. In the table is the information gathered from the OpenSim model and

properties given to the bones modelled in SolidWorks. The step of assigning properties is vital to uphold the relevance of the model and the validity of the import.

The segmental lengths described in the model are from previous studies by A. S. Arnold, Asakawa, and Delp (2000) and are used to create the base sizing for the geometry.

*Table 4-1.
Bones with their mass and inertial properties*

Bone	Mass (kg)	Moments of Inertia		
		XX	YY	ZZ
Right femur	9.3014	0.1339	0.0351	0.1412
Right tibia	3.7075	0.0504	0.0051	0.0511
Right patella	0.0862	0.00000287	0.00001311	0.00001311
Right talus	0.1000	0.0010	0.0010	0.0010
Right calcaneus	1.250	0.0014	0.0039	0.0041
Right toe	0.2166	0.0001	0.0002	0.0010
Left femur	9.3014	0.1339	0.0351	0.1412
Left tibia	3.7075	0.0504	0.0051	0.0511
Left patella	0.0862	0.00000287	0.00001311	0.00001311
Left talus	0.1000	0.0010	0.0010	0.0010
Left calcaneus	1.250	0.0014	0.0039	0.0041
Left toe	0.2166	0.0001	0.0002	0.0010

Joint Properties

The Lower Limb Model 2010 includes the metatarsophalangeal, subtalar, ankle, knee, hip, pelvis, and lumbar joints which are represented with the following relationships (E. M. Arnold et al., 2010):

- **Metatarsophalangeal Joint:** The metatarsophalangeal joints are modelled as revolute joints, and its range is -30° (extension) to 30° (flexion).
- **Subtalar Joint:** Subtalar joints are modelled as revolute joints, with a range of -20° (eversion) to 20° (inversion).

- **Ankle Joint:** Modelled as a revolute joint between tibia and talus and is defined by a range of -40° (plantarflexion) to 20° (dorsiflexion).
- **Knee Joint:** The knee joint is defined as a revolute joint. The knee angle ranges from 0° (full extension) to 100° (flexion)
- **Hip Joint:** Modeled as a ball and socket joint with three degrees of freedom: ranges are -20° (extension) to 90° (flexion), -40° (abduction) to 10° (adduction), and -40 (external rotation) to 40 (internal rotation).

Furthermore, the locations of the coordinate systems, seen in Figure 4-1, used to relate the joints are located on the bones as follows as per E. M. Arnold et al. (2010):

- **Femur:** Located at the centre of the femoral head,
- **Tibia:** From the midpoint of the femoral condyles with the knee in full extension,
- **Patella:** The distal pole of the patella,
- **Talus:** The midpoint of the line between the apices of the medial and lateral malleoli,
- **Calcaneus:** The lateral point on the posterior surface of the calcaneus,
- **Toe:** The distal end of the second metatarsal

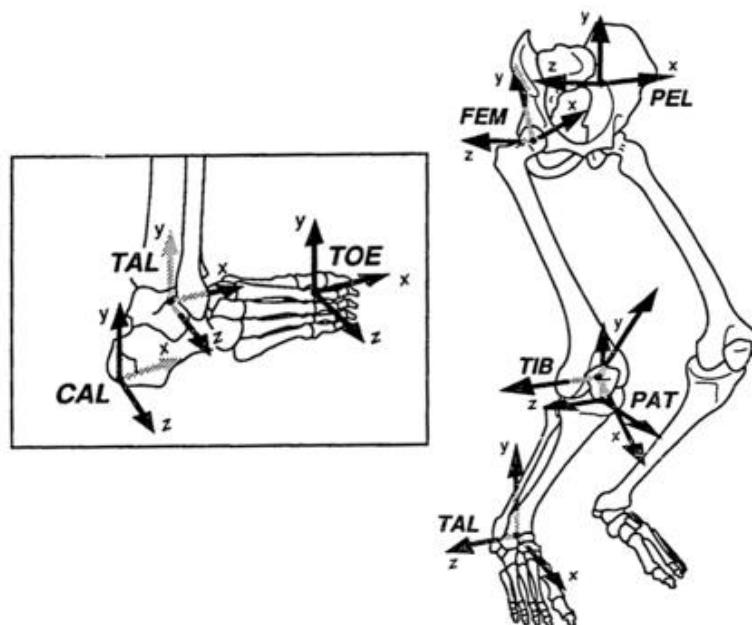


Figure 4-1 Visual representation of the location of the joints coordinate systems (Delp et al., 1990)

4.2.2 Solid-Body Modelling

The Visual Toolkit Polygonal Data (.vtp) geometry files of the OpenSim model were converted to Stereolithography (.STL) files, to import them as mesh bodies into SolidWorks. Using these files would give a visual representation to the body created that would otherwise be mass and inertial data on a coordinate system. The STL mesh files had to be cleaned and closed to avoid errors upon SolidWorks import using a program called Meshlab. The STL's are then imported into SolidWorks and scaled about their imported origin to represent the geometry best. The actual shape and the visual mesh size do not alter calculated results but play an essential role in identifying any erroneous mates or movements that the motion simulation may output.

Following the import of the mesh, the coordinate geometry was implemented. An example of the code read to implement the geometry and body data is shown below:

```
<Body name="femur_r">
  <mass>8.54926632</mass>
  <mass_center> 0 -0.199543 0</mass_center>
  <inertia_xx>0.16956431</inertia_xx>
  <inertia_yy>0.0444489</inertia_yy>
  <inertia_zz>0.17880867</inertia_zz>
  <inertia_xy>0</inertia_xy>
  <inertia_xz>0</inertia_xz>
  <inertia_yz>0</inertia_yz>
  <!--Joint that connects this body with the parent body.-->
  <Joint>
    <CustomJoint name="hip_r">
      <!--Name of the parent body to which this joint connects its
owner body.-->
      <parent_body>pelvis</parent_body>
      <!--Location of the joint in the parent body specified in
the parent reference frame. Default is (0,0,0).-->
      <location_in_parent>-0.0739512 -0.0691397
0.0873398</location_in_parent>
```

With all the bodies modelled, the Lower Limb Model 2010 is assembled by mating each body's coordinate systems according to the joint data noted previously and further coordinate location data noted in the code. The resulting lower leg imported into SolidWorks can be seen in the below figures:

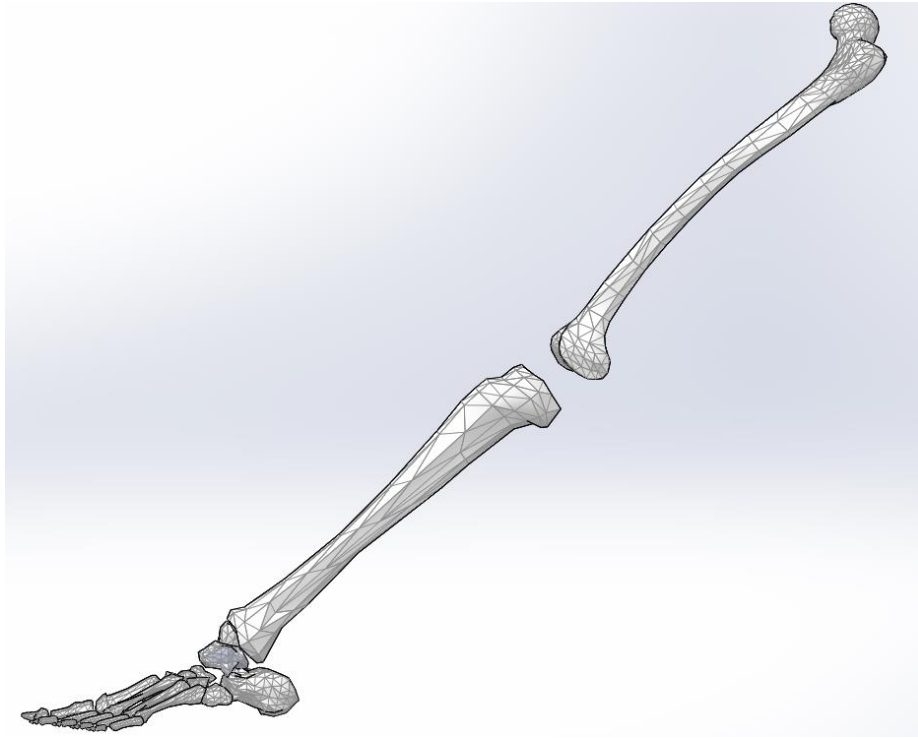


Figure 4-2 Fully Extended Lower Limb Model 2010 (E. M. Arnold et al., 2010) imported to SolidWorks

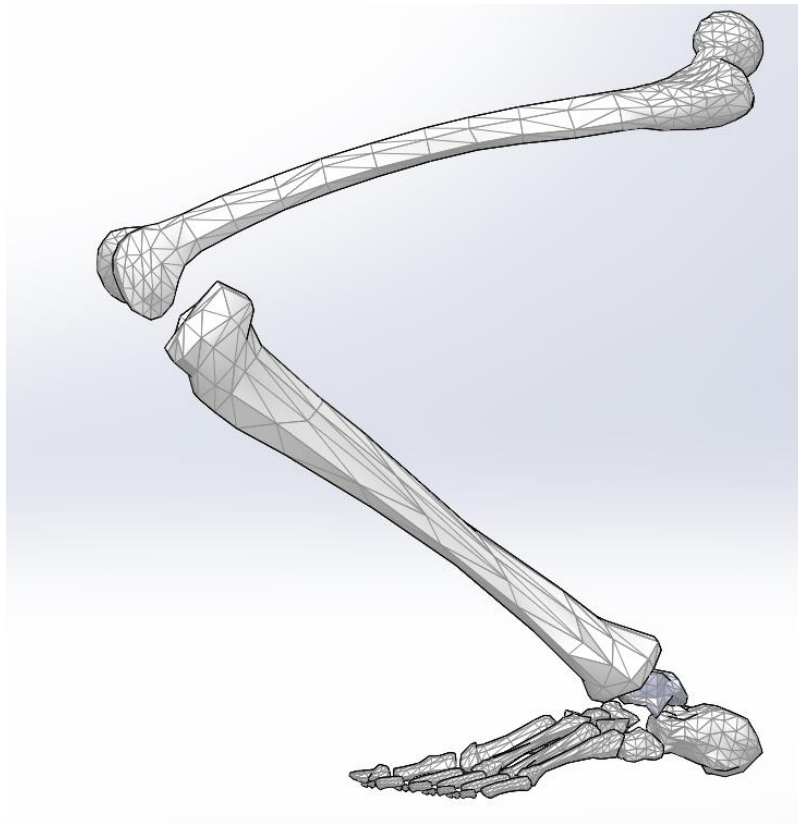


Figure 4-3 Fully Flexed Lower Limb Model 2010 (E. M. Arnold et al., 2010) imported to SolidWorks

4.2.3 *In-silico* Study Design

The 2010 Lower Limb Model is used as the patient in our *in-silico* study. Hereafter referred to as ‘the patient’, the 2010 Lower Limb Model is assembled onto a 3D modelled hospital bed.

The computing power used for the simulation utilised the following components:

- Intel® Core™ i7-7500U CPU @ 2.7GHz 2.90 GHz
- 16GB Installed RAM (15.9 GB Usable)

The steps for ensuring the successful simulation are thus:

1. Correct foot placement onto the arms of the device
2. Correct pelvic placement to stop the overextension of the joints
3. Setting the resolution, time and nature of the study
4. The implementation of the effects of gravity
5. The implementation of contact bodies into the device
6. Calculation of the study
7. Assessment of the areas of study, namely the foot, ankle, knee and hip

Following the steps’ order, the patient was placed onto the device and into the feet attachments. After that, the pelvic hinge points of the hips were placed. The placement was done in a trial and error method by moving the device through quarter rotations of the motor and ensuring that the knee did not reach a full lockout position. The result of which can be seen in Figure 4-4.

With the placement of the patient correct, the motion study could be set up. The Study was set up on SolidWorks in the category of Motion Analysis studies. The Motion Analysis study type is the most realistic type of motion simulated in SolidWorks and considers properties like friction forces, mass, gravity, materials, and is appropriate for a more accurate analysis of this patient-device system.

The study’s resolution was set to 30 frames per second so that a large number of individual calculations are made, and the resulting curves can be sufficiently smooth. The study did not utilise bushings for replacing redundant mates, as this would have

affected the mates' integrity set according to the 2010 Lower Limb Model. The study utilised a high 3D contact precision resolution and was set to maximum on the slider.



Figure 4-4 The foot placement of the patient onto the device, with the foot attachments hidden to show the foot and the arm

A rotary motor is enabled to initiate a cyclic movement for the study on the device's hub component, seen in Figure 4-5. This motor drives the system at a constant rate of 15RPM in a clockwise direction. The speed is chosen to match that of Huang et al. (2019) and Pohl et al. (2007).

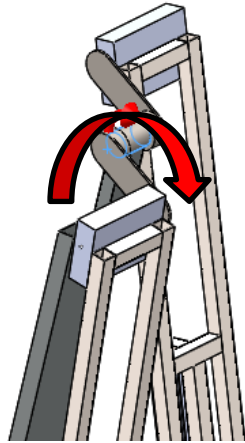


Figure 4-5 Motor direction and application zone, indicated by the red arrow

Solid-Body Contact interactions are made between either arm and the respective lower limb (right and left). The Solid-Body Contact interaction enables the measurement of simulated ground reaction forces between the foot and the device's arm. Solid-Works uses a gravity value of 9806.65mm/s^2 , which is also implemented in the simulation environment.

Calculation of the study is then run, and the motion of the device checked for flaws. The animation preview that occurs during the calculation allows for error checking in any system's constraints. Once completed, the system appeared as in Figure 4-6.

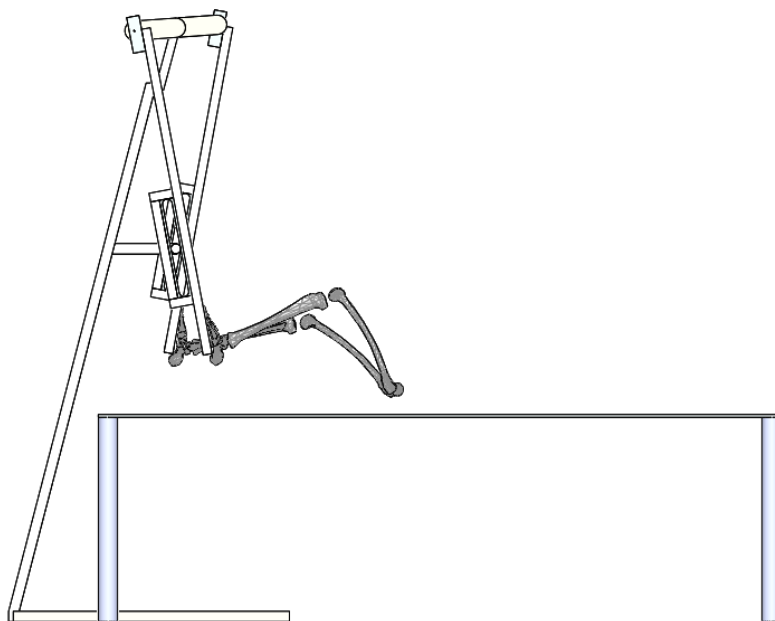


Figure 4-6 Simulation environment with constraints checked and the initial starting position of the legs.

Measurements of the joints are completed, with the assessment of the angles represented in Figure 4-7. These angles are measured by placing markers at each of the points respectively and then using the plotting software of SolidWorks Motion Analysis to create the relationships to be measured. Due to the joints not all starting at zero, the change of angle is measured.

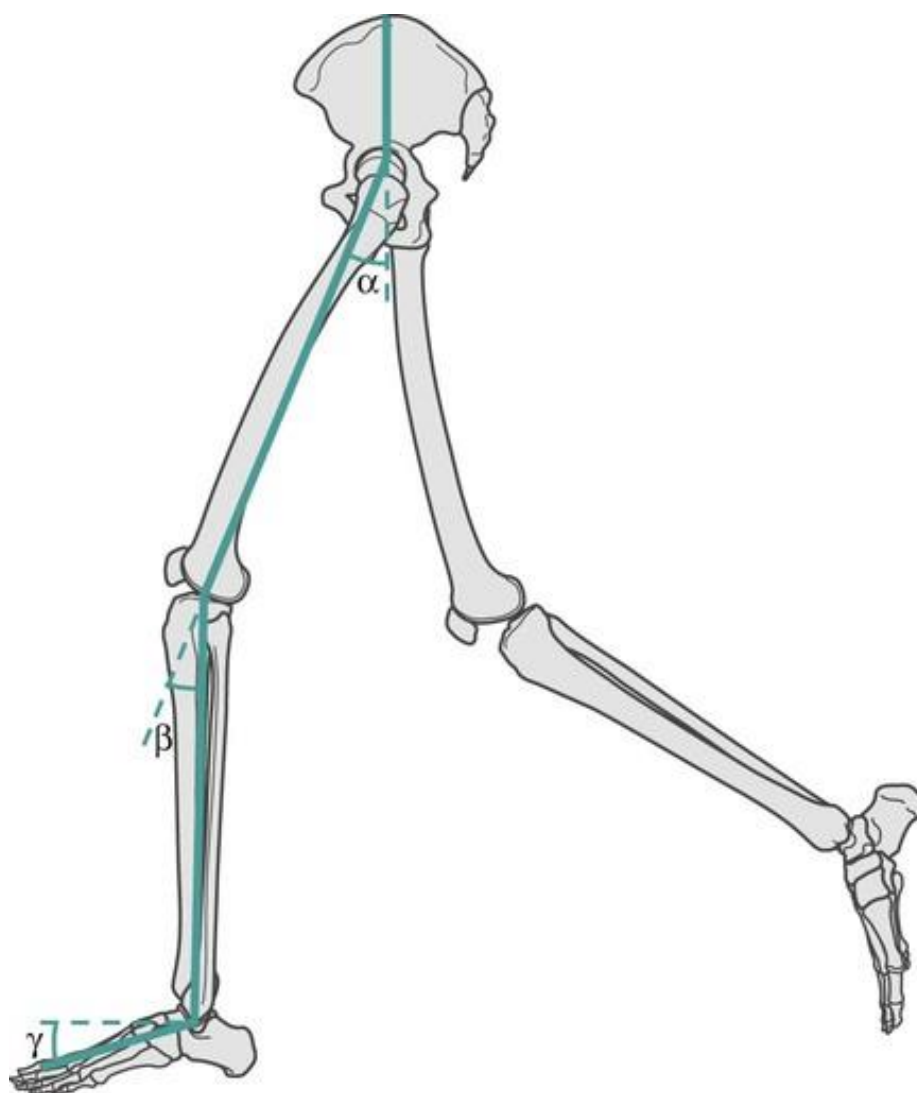


Figure 4-7 Angles measured during simulation results plotting (Richards, Chohan, & Erande, 2017)

4.3 Experimental Results

This section details the experimental outcomes of the *in-silico* study and looks at the results achieved. A successful *in-silico* test is calculated for a duration of 10 seconds, the movement of which can be seen in Figure 4-8, and joint angles for the hip, knee and ankle are measured. The joints are then assessed as to the angular velocity with which the segments move about one another. Trace paths of critical areas of the lower limb are assessed and then compared to that recorded in the literature of a normal gait. Also measured in the study are the magnitudes of forces experienced within the joints during the cycling period.

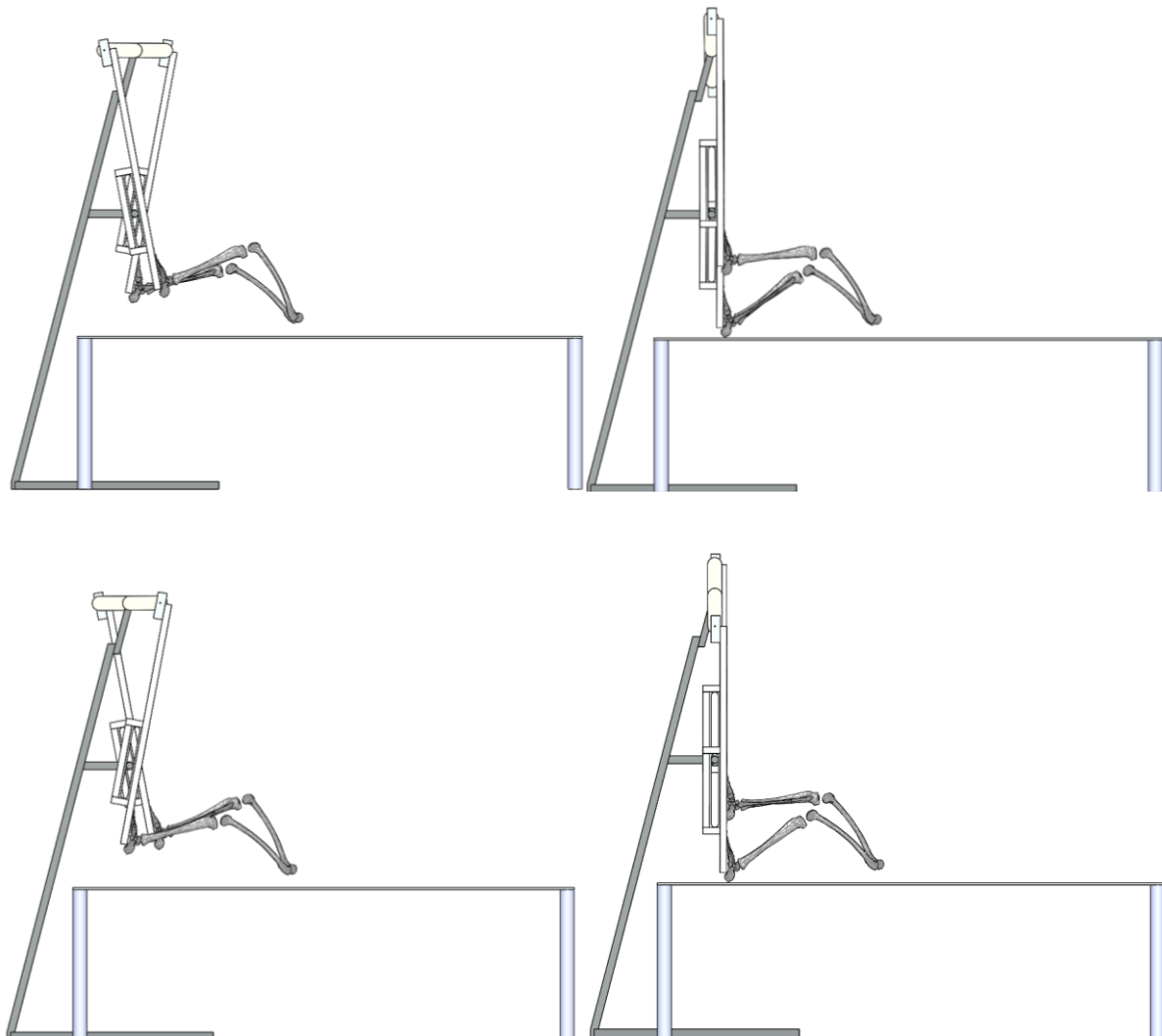


Figure 4-8 Snapshots of the movement of the simulated legs in quarterly rotations

4.3.1 Change of Angle

Ankle

The ankle joints movement and angular change are of great importance for the feet' functioning during walking. Not only does the change of angle allow for balance, but it also enables the shock absorption of the ground reaction forces. It is also essential that the ankle flexes at the appropriate phases of the gait cycle. In the simulation, the assessed gait cycle is from the point of 'heel strike' to 'heel strike' which correlates to the times of 0sec - 3.91sec. Richards et al. (2017) noted the four phases are 'heel strike', 'foot flat', 'toe-off', and 'swing', with the gait cycle after that being ended by another heel strike. The gait cycle and joint angles of the ankle can be seen in Figure 4-9.

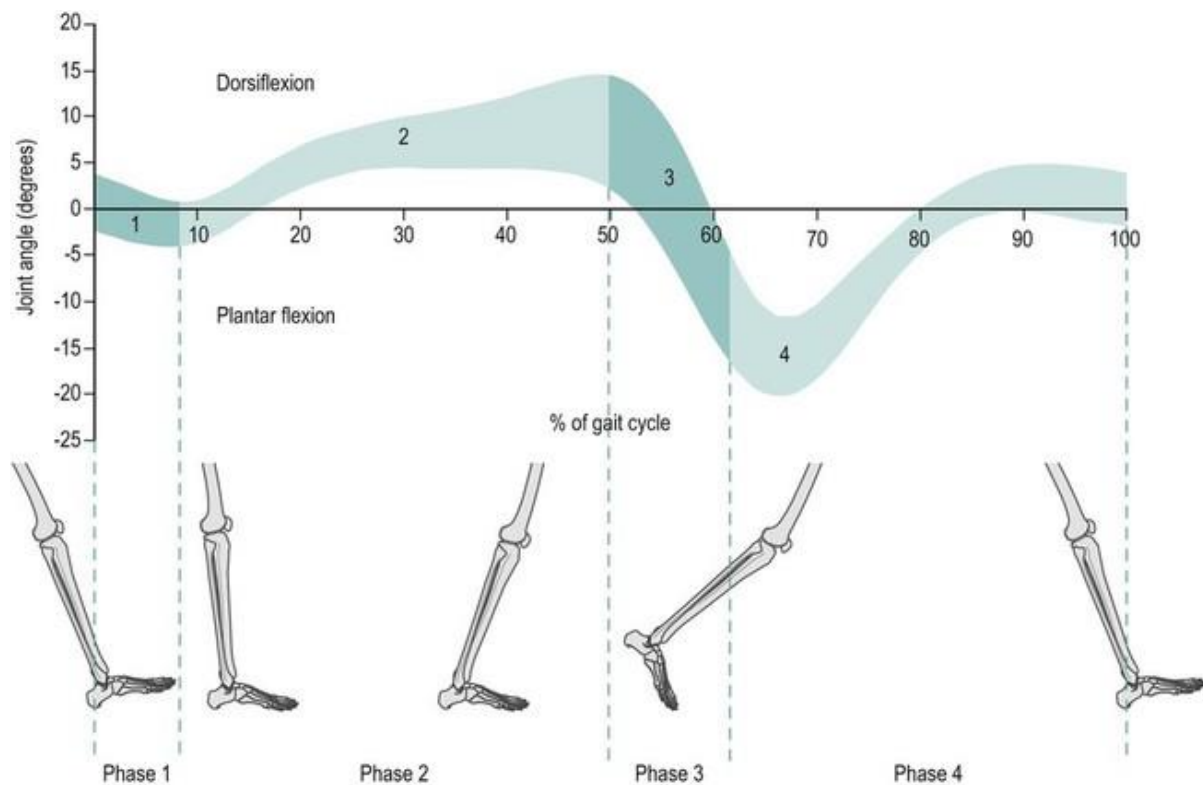


Figure 4-9 The joint angle changes of the ankle during the gait cycle (Richards et al., 2017)

In Figure 4-10, the results of the ankle's angular displacement are shown. This measurement is made about the tibia.

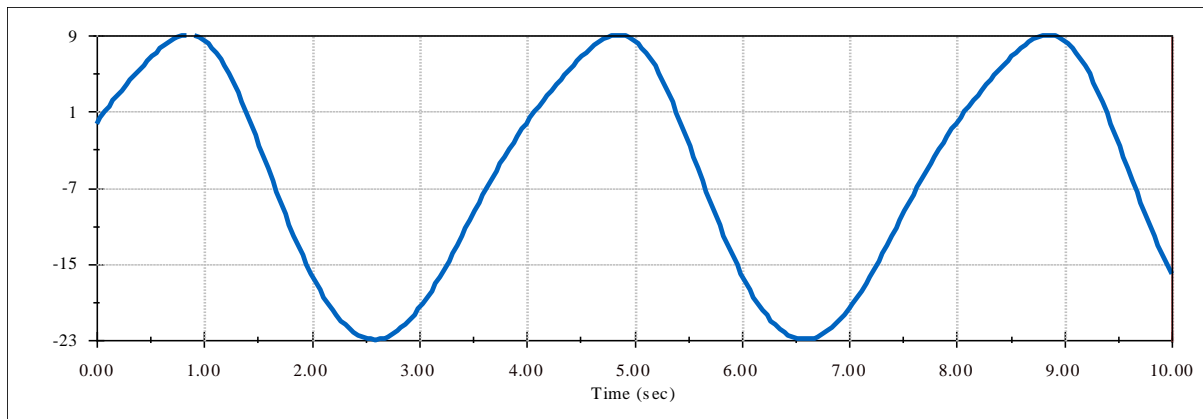


Figure 4-10 Angular displacement of the left foot with respect to the tibia

The angular displacement of the ankle shows a similar shape of displacement to that of the gate cycle. We see a rise and a point of inflection, just before 1 second of movement, which correlates to the respective rise seen at 50% of the gait cycle. While this rise does not match the timing of the normal gait cycle, it must be remembered that the device imparts less hip extension (being limited only to the area in front of the body and above the bed), and so the ankle and knee joints would require more angular displacement. After this, the graph's shape is similar to that of the gait cycle, with the angular displacement reaching its lowest point (- 23 degrees) at 2.54 seconds. The resultant angles can be likened to those experienced during the toe-off phase. Typically, the range of angular displacement falls between 20 and 40 degrees, according to Richards et al. (2017). The angular displacement shown in the graph has a range of 31 degrees of movement, which falls just above the documented average displacement.

Knee

The most considerable motion of the knee occurs in the sagittal plane of the body during walking. This motion imparted onto the knee often correlates with stride length, walking speed, and other pathological gait attributes. A typical range of knee movement during the gait cycle can be seen in Figure 4-11 and shall be used as a comparator for the results.

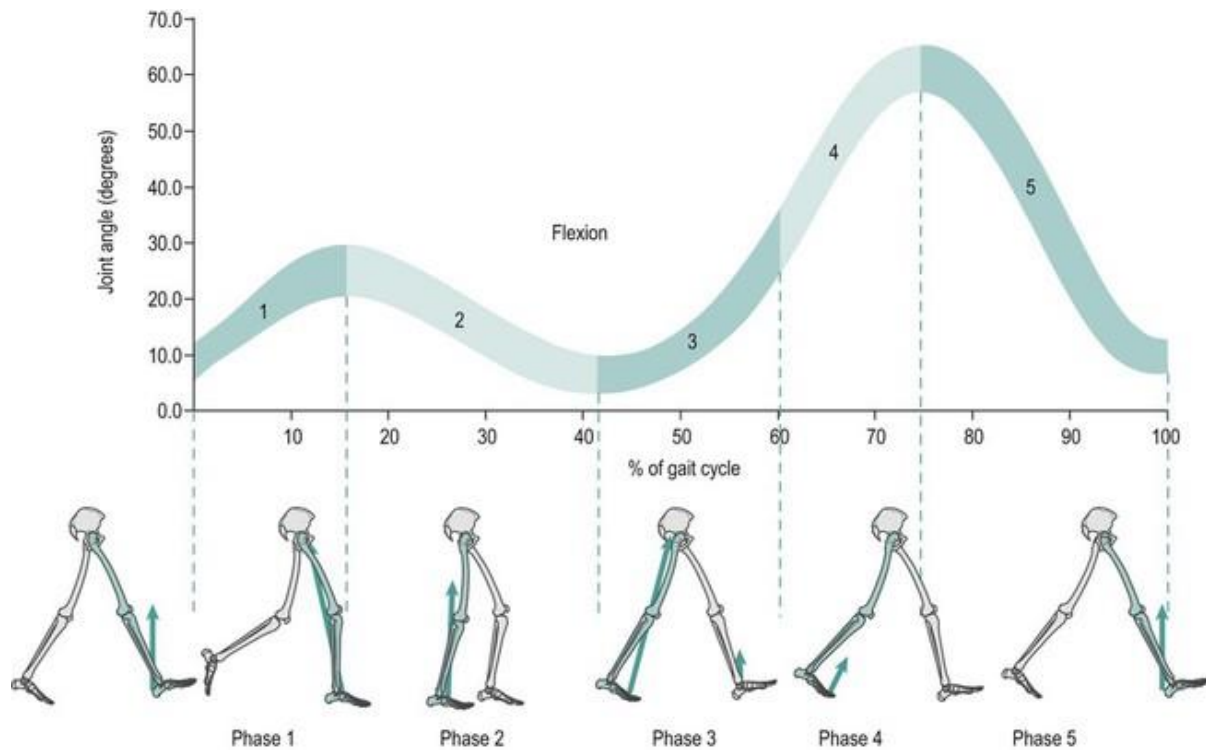


Figure 4-11 The knee joint angle during the gait cycle (Richards et al., 2017)

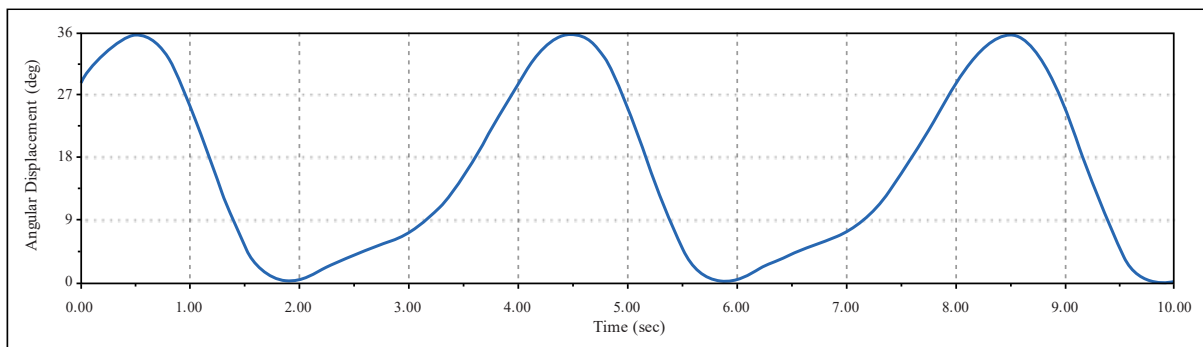


Figure 4-12 Angular displacement of the left knee joint during device movement

The angular displacement of the knee is considerably less than that noted in the literature. We note that the graph shows a range of movement of 36 degrees maximum, where the typical knee moves through a range of 70 degrees. The shape of the graph does, however, resemble that of the movement of the knee during gait. The graph shows two points of inflection. A small peak at 1.62 seconds and then a larger peak at 4.50 seconds. The timing of these peaks is indicative that the knee flexion is not synchronous with that of the ankle in terms of a regular gait pattern. The knee flexion

mimics the angle changes but does not do so at the correct points in the cycle. This disparity could suggest that a patient in constant hip flexion negatively influences the knees natural movement. Stimulating an angular displacement of the knee, regardless of amount or timing, leads to muscle stretch. This muscle stretch is beneficial to the patient's management (Joseph et al., 2013; O'Hea, 2003).

Hip

The motion of the hip, like the knee, occurs majorly in the sagittal plane. During initial contact with the ground, the hip extends as the body moves over the limb. Maximum hip extension occurs after foot strike of the opposite limb after which the weight is then transferred to the leading limb, and the opposite limb begins flexion at the hip (Richards et al., 2017). The motion can be seen in Figure 4-13 as the hip ranges between 40 degrees of flexion and 15 degrees of extension. This movement gives the hip a range of 55 degrees during normal walking.

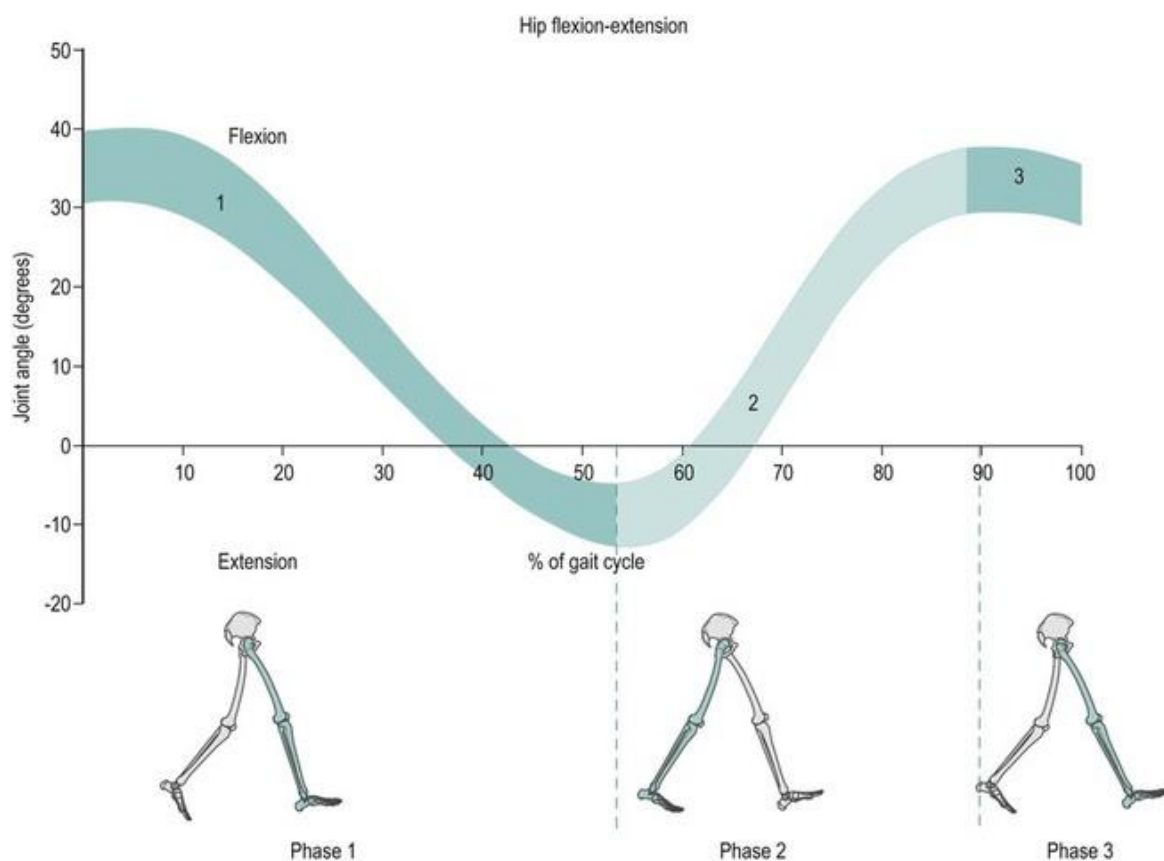


Figure 4-13 The extension and flexion of the hip during the gait cycle (Richards et al., 2017)

The results plotted below in Figure 4-14 show a total range of movement of 28 degrees. This low result is expected, as both of the patient's legs are initially flexed. This position occurs so that they might lay on the bed and be connected to the device. The range of movement then neglects any movement of the femur across the frontal plane.

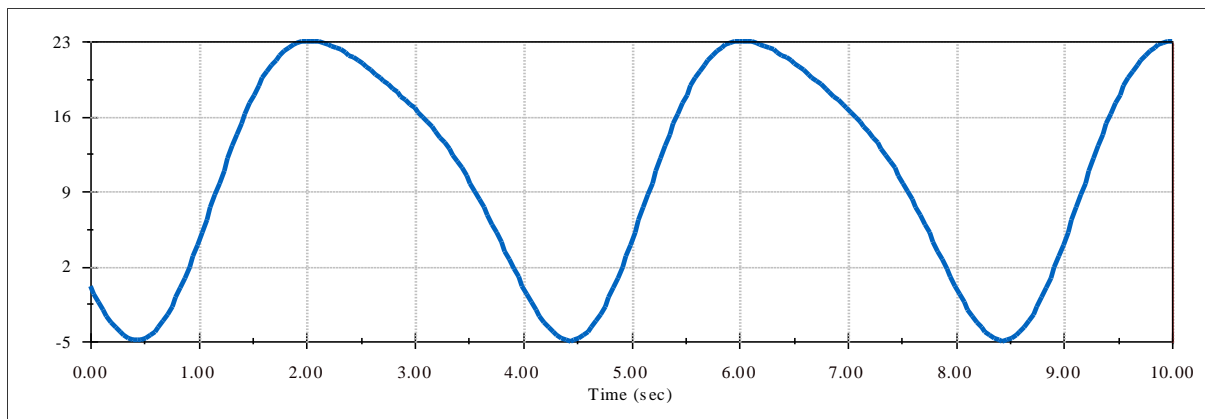


Figure 4-14 The angular displacement of the left hip during device movement from the initial position.

However, the shape of the graph indicates that the hip flexes and extends from its original position. The movement aligns with the flexion of the hip during normal walking, but similarly, with the knee, this movement's timing is not aligned with that of the gait cycle.

4.3.2 Rate of Change of Angle

From Mentiplay, Banky, Clark, Kahn, and Williams (2018) for measured joint angles and angular velocities, the shape is consistent regardless of the inputted walking speed. It is noted that as walking speed increased, so did the peak joint angles and angular velocities for the hip, knee and ankle. The most considerable angular velocity occurred when the knee joint extended towards the terminal swing phase of gait. For the ankle and hip joints, the most significant angular velocity occurred during push-off.

Ankle

The ankle's angular velocity profile is related to power production, which can be mostly seen in phase 3 and phase 4 of the ankle's movement. During this time the ankle rapidly plantar flexes and then dorsiflexes to generate push off from the ground.

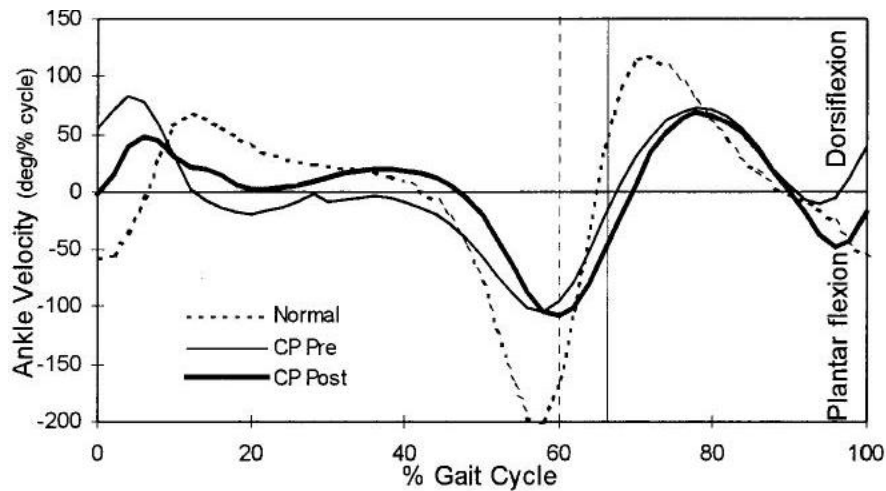


Figure 4-15 The ankle velocity profile of normal patients shown as the dotted line (Granata, Abel, & Damiano, 2000)

As might be expected with a cyclical movement pattern with constant angular velocity, the ankle's angular velocity (seen in Figure 4-16), is not as high as noted in the literature. The maximum angular velocity reached is 31 degrees per second, which is substantially lower than regular walking. However, the angular velocity being lower may lend itself to an aspect of safety for the patient, as the muscles that would usually guide and initiate this movement can no longer stabilise the joint.

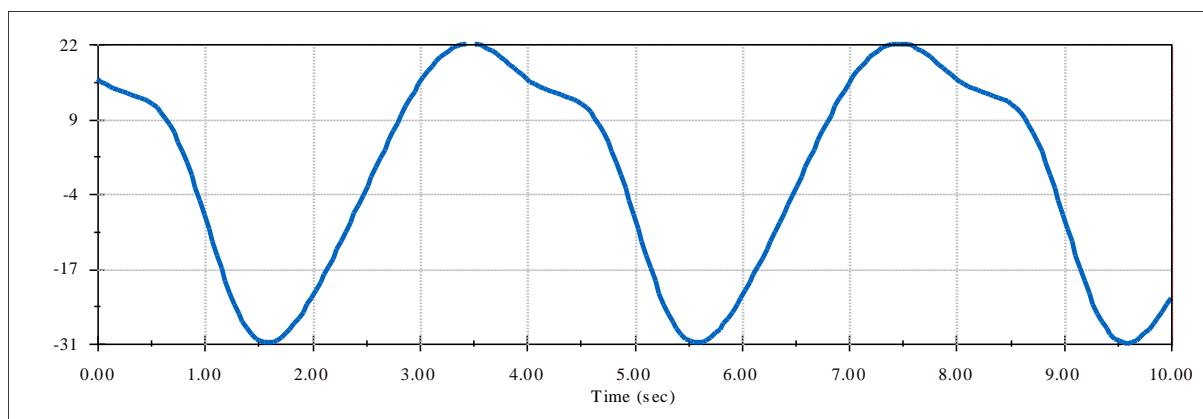


Figure 4-16 Velocity profile of the left simulated ankle during movement.

The shape of the velocity trace follows a similar rise and fall, as seen in Figure 4-17. The shape does have the correct placement of points of inflection at 1.63 seconds and 3.48 seconds, correlating to similar points in the gait cycle.

Knee

The angular velocity of the knee during its loaded condition of the gait cycle helps measure its eccentric control capabilities. The most crucial measure during movement of the knee is that the angular velocity curves remain smooth. The smooth trace shows control of the joint through its movement. The rate of knee flexion and extension is greater than that of the ankle, with the velocities reaching peaks of 300 degrees per second. The measured result can be seen in Figure 4-17. The shape that we have attained in Figure 4-18 points towards the knee velocities being higher than the ankle velocities. With maximum angular velocities of 28 and -45 degrees per second, this trace path shows a similar shape to that of the literature. The shape is again, as to be expected from the angular displacement graph, out of alignment with the timing of the gait cycle.

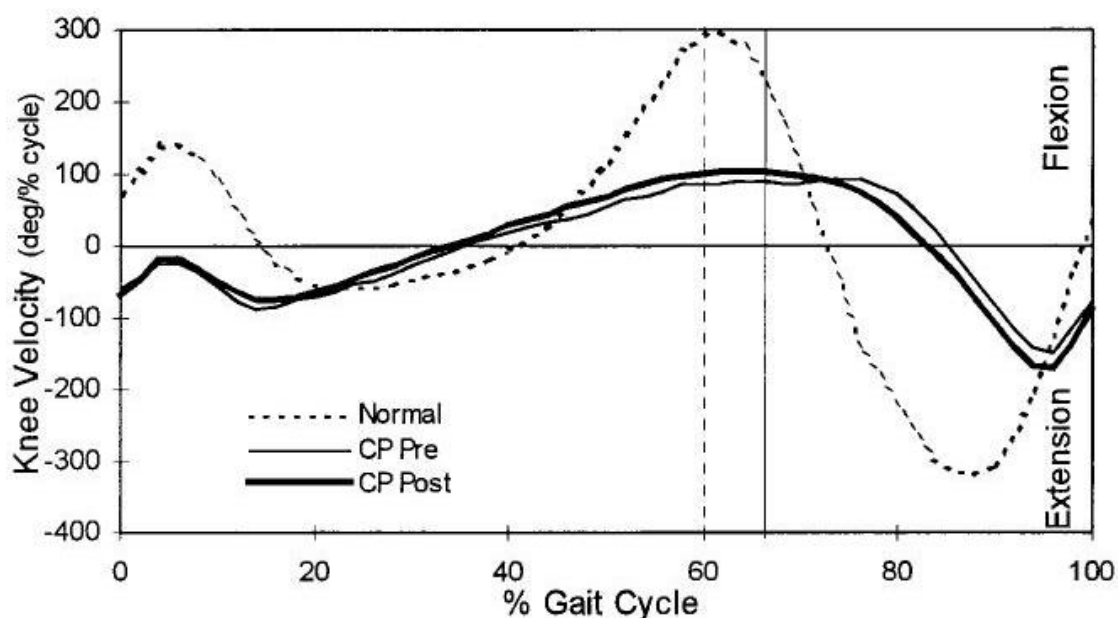


Figure 4-17 The knee velocity profile of normal patients shown as the dotted line (Granata et al., 2000)

The resultant graph also displays an additional inflection point before reaching its maximum negative angular velocity, which is not concurrent with the trace of the literature.

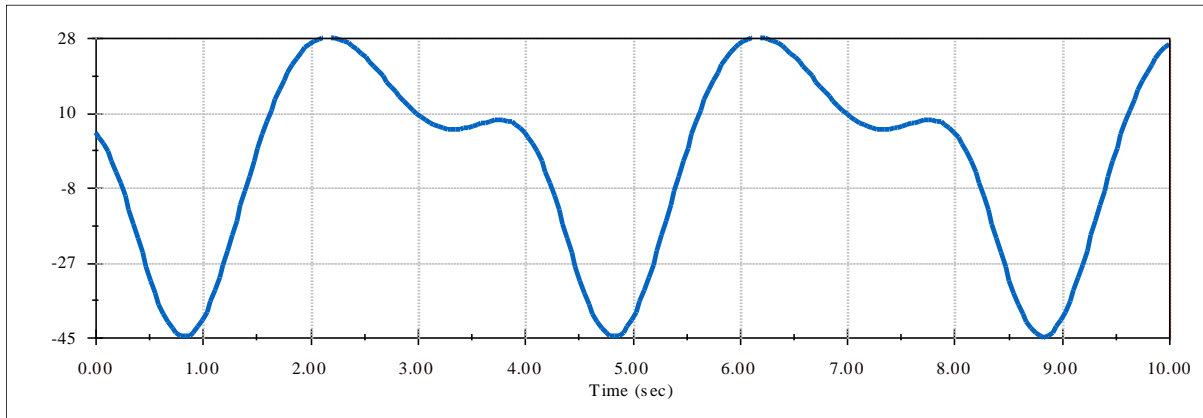


Figure 4-18 Angular velocity of the left knee during device movement.

The shape of the resultant curve shows a larger negative angular velocity than positive, which is in accord with the literature. While the velocities are not of the same magnitude, a lower angular velocity is preferred for an injured patient.

Hip

In comparing the shapes of the velocity trace of literature (Figure 4-19) and the measured result (Figure 4-20), we notice substantial differences in the shape and the timings of the velocity changes. As was noted in the angular displacement, the movement's timing is incorrect and not correlated to that of the gait cycle. It is out of phase. The shape of the resultant graph also shows a much faster change in velocities, which could indicate the initial flexed position of the hip attempting to catch up to the movement of the device.

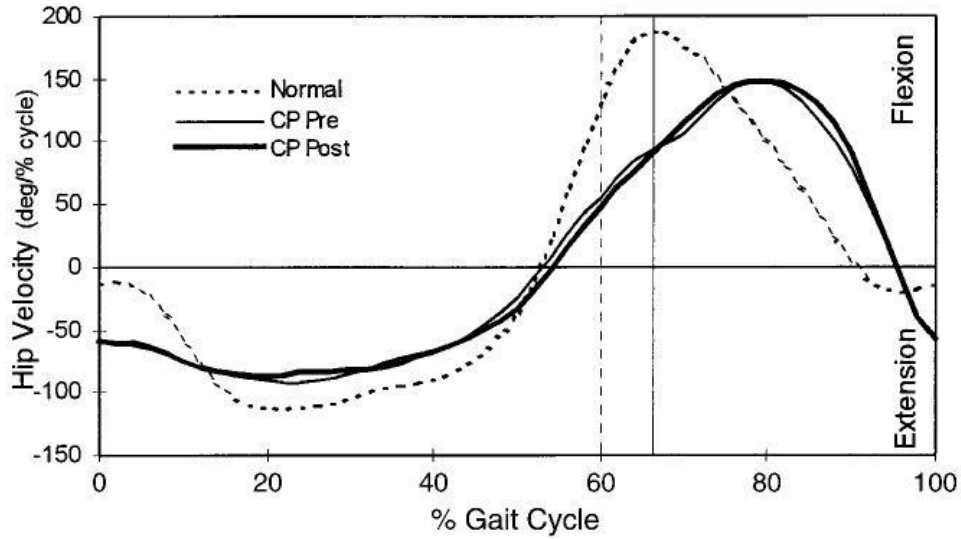


Figure 4-19 The hip velocity profile of normal patients shown as the dotted line (Granata et al., 2000)

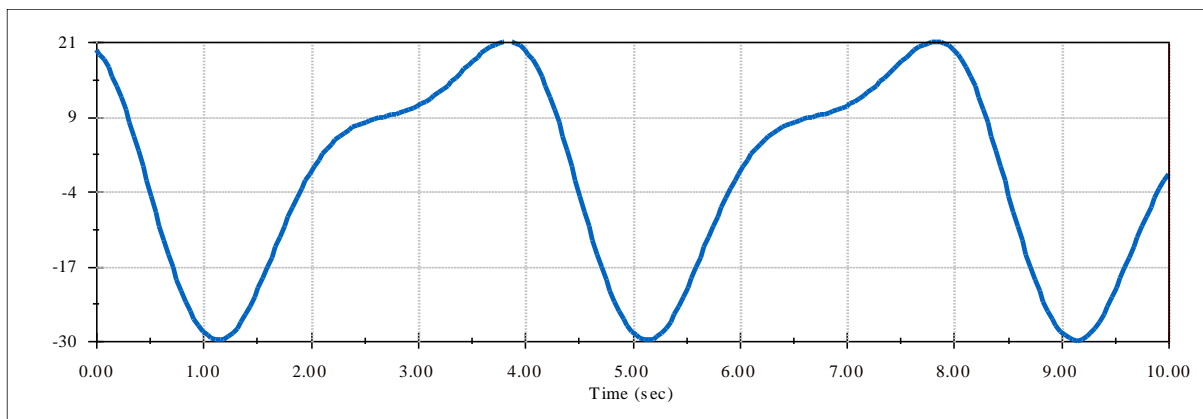


Figure 4-20 Angular velocity of the left hip during device movement.

4.3.3 Trace Paths

The resultant movement of the legs can be visualised with the trace markers and trace paths. The trace paths can be seen below in Figure 4-21. As the patient is mobilised and the device is used, the patient's ankle is moved in an elliptical pattern. The amount of vertical movement towards to front of the foot reduced. The vertical movement towards the rear of the foot is increased. This result is in line with that movement seen in the normal movement of a patient seen in Figure 4-22. It is also seen from the trace paths that the proximal end of the tibia experiences movement that isn't in a pure

arc. The distal end of the femur does, however, move in a small arc. The trace paths and measurements made within SolidWorks must also be noted because the stride length is equivalent to the diameter of the cranks utilised.

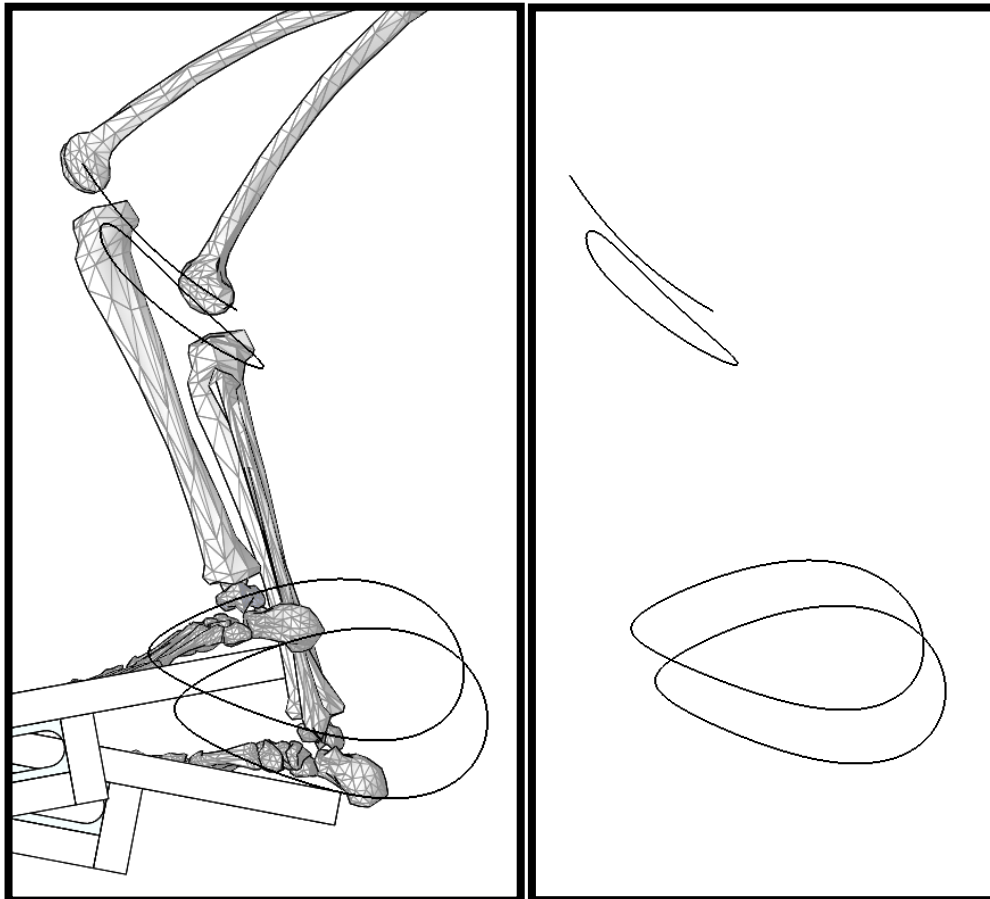


Figure 4-21 Trace paths, bottom to the top: the tip of the device's arms, the talus bone, the centre of the tibial plateau, and the centre of the femoral condyles. Displayed on the left with the reference bodies and on the right without solid bodies.

The shape of the talus path has a similar shape to that of regular walking. The shape does not, include a portion of trace where the talus temporarily traces back its path, a feature that can be seen in Figure 4-22 between the distances of 1.4 an 1.6

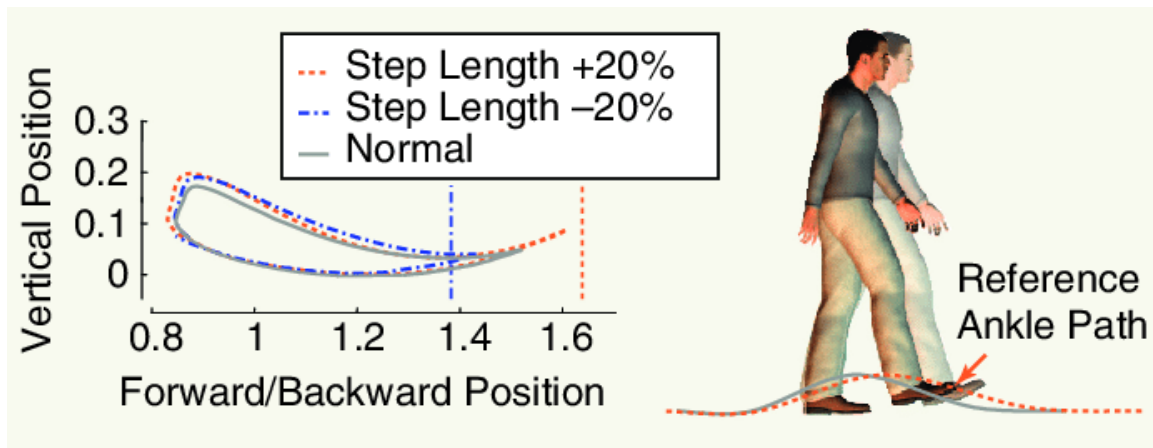


Figure 4-22 Normal step trajectory with reference person travelling left to right (Vallery et al., 2008)

4.3.4 Ground Reaction Forces

The ground reaction force (GRF) experienced during walking is a crucial part of rehabilitation as it creates a sensory stimulation to the foot, and as mentioned provides an environment for better rehabilitation (Dobkin et al., 2006). Figure 4-23 below represents the patient’s reaction force during the use of the device. The maximum force experienced is 148N, and the minimum is 58N. The lowest value does not go to zero, due to the leg’s weight resting upon the device at all times.

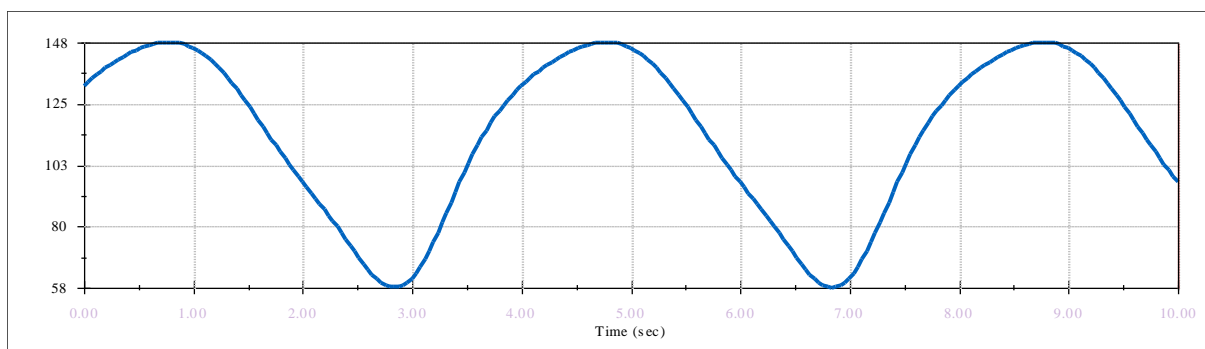


Figure 4-23 Ground reaction forces experienced by the foot during device use

The GRF that is shown occurs cyclically with the device’s movement and applies a more considerable force during the movement's stance phase. The comparable graph of the GRF measured in literature shown in Figure 4-24 also shows the peak of force

during the stance phase. However, the resultant graph shows no comparable reduction in force during the stance phase's peak during mid-stance.

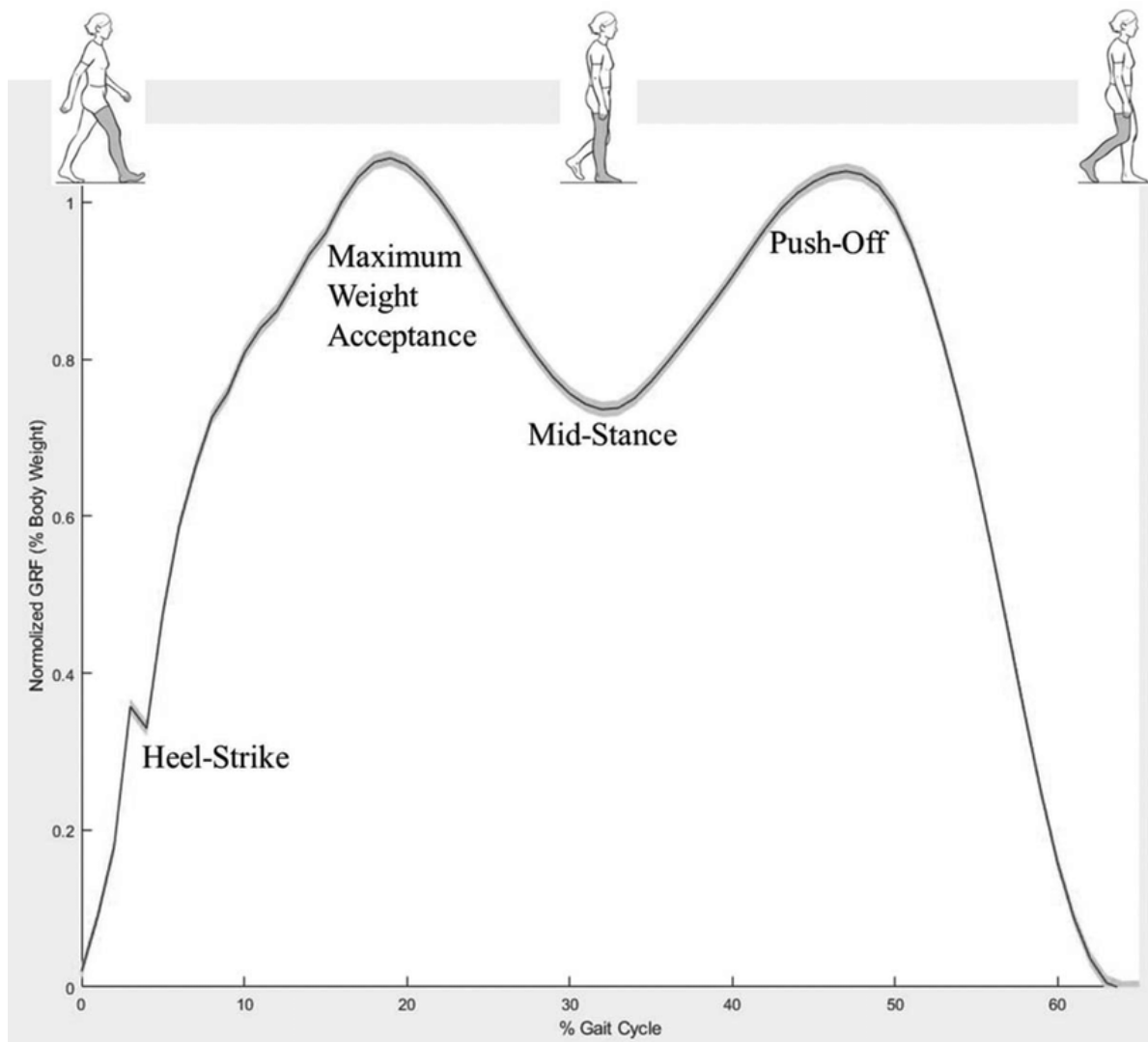


Figure 4-24 Typical vertical ground reaction forces during gait in healthy adults (Haddas & Ju, 2018).

The maximum amount of force stimulated by the device (148N) is equivalent to 20% of the patient's body weight. In literature during the peak of GRF, the force exceeds the patient's body weight.

4.3.5 Forces Experienced in the Joints

The joints while in motion experience forces from the other components acting on those joining features. While the computation was unable to provide accurate directions for these forces, the ankle hip and knee's total forces' magnitudes can be seen in the figures below.

As was expected, the forces experienced are cyclic and correspond to the gait pattern and angular displacements seen previously. It appears as though, in Figure 4-25, the hip is experiencing its force twice as regularly. However, the points of inflection of the velocity graph of the hip correlate correctly with this. The force does not alter largely within the hip, which can be attributed to the smaller range of motion of the hip and the joint's stability.

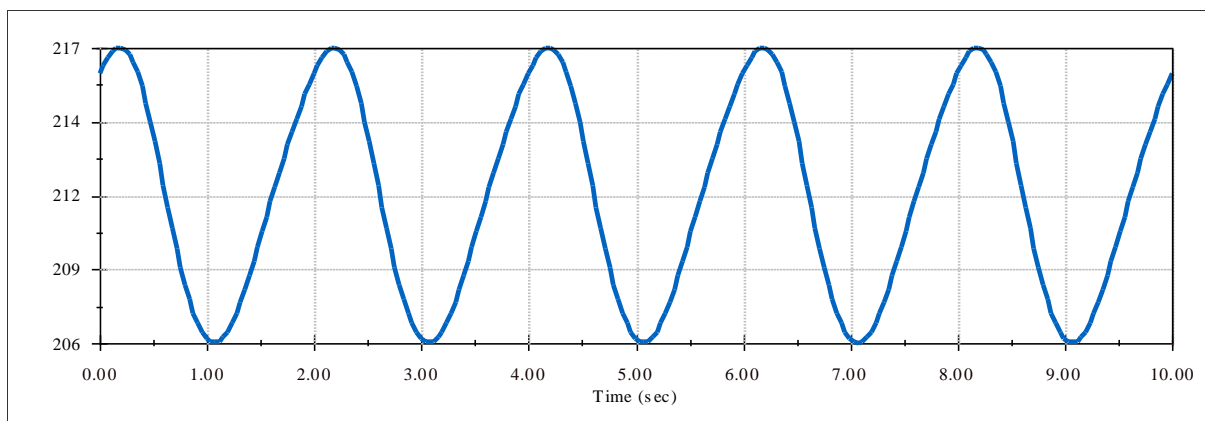


Figure 4-25 Magnitude of force experienced in the left hip during device use

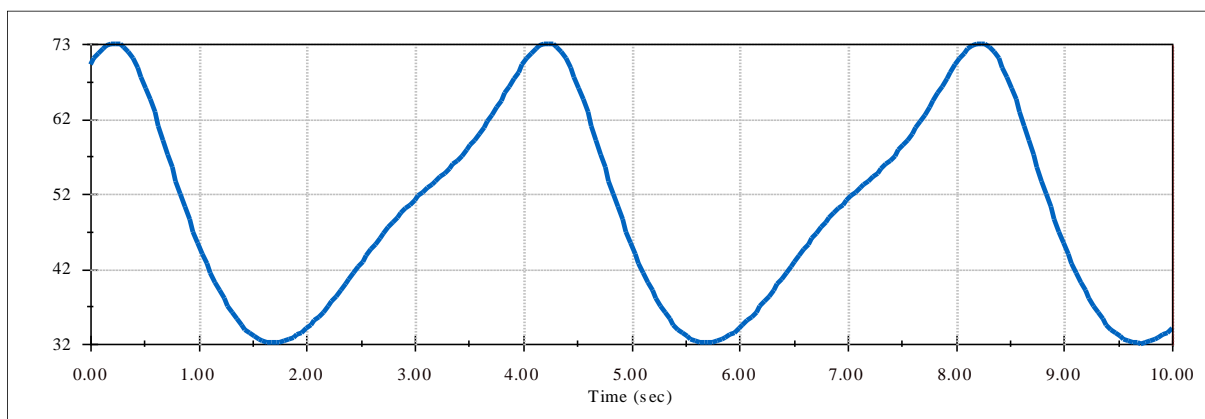


Figure 4-26 Magnitude of force experienced in the left knee during device use

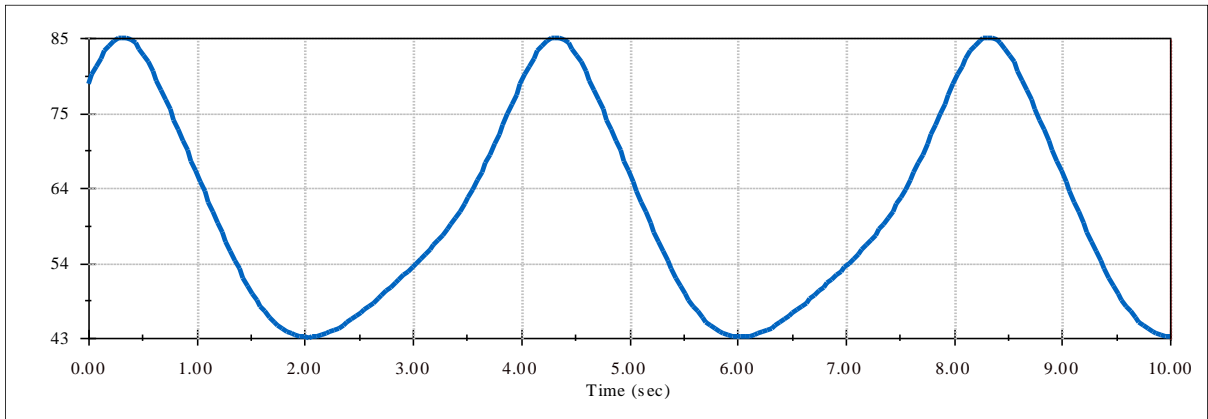


Figure 4-27 Magnitude of force experienced in the left ankle during use

4.3.1 Device Validation

An analysis was run on the device's motor, showing the torque requirements to move the body to validate the device's requirements. The results of this are shown in Figure 4-28. The peak torque shown in the graph is 7259N.mm, which is well within the motor and gearbox's output torque range.

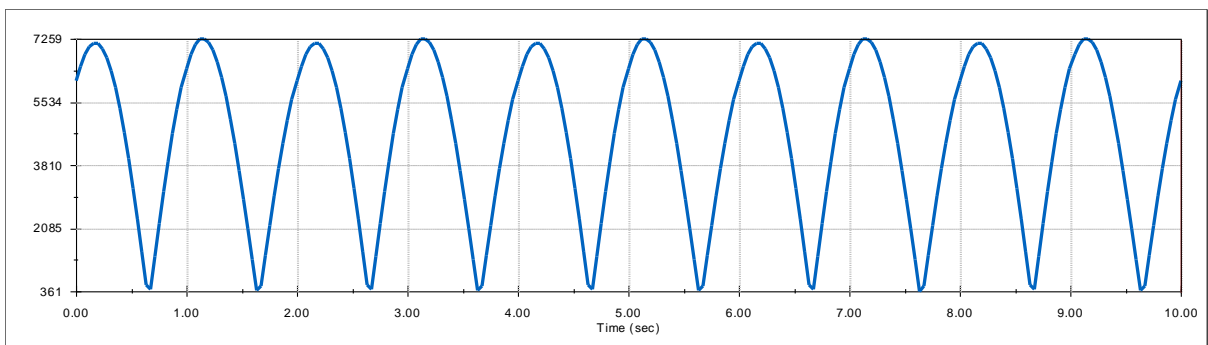


Figure 4-28 Torque requirement of the motor used to drive the device

5. Discussion

5.1 Design

The device was designed as per the requirements found through modelling, literature review and manufacturing requirements. It was designed to a point where it could be assessed *in-silico* as to whether it could proceed further into the physical development and advanced prototyping stage.

The device was specified to accommodate a 75kg, 1.7m male, and to allow for a gait similar movement pattern. Furthermore, it is designed to allow a clinician control of the training protocol. Physical patient interfacing was designed and assessed by two physiotherapists of different experience levels. It was found from this assessment that the patient interface would need to be physically assessed with a range of patient morphologies before conclusive decisions could be made about its suitability. The choices for a rubber design for the patient interface allow for a more comfortable fit for a patient and reduce friction between patient and device. The choice of rubber would also allow for a wider variety of patient morphologies. The structure of the device was designed in an economical manner, made out of mild steel components. Integrated into the design were components that could be salvaged from old bicycles. This design choice allows for the device's more complex componentry to be outsourced and readily available. SolidWorks simulations were run to verify the structural integrity of the frame and the critical components. The successful completion of these tasks allowed for certainty in the safety of the design.

In order to power and drive the system, an electronic subsystem was designed. These design considerations included the motor choice of a NEMA 23 stepper motor, Arduino Mega motor controlling and a gearbox to transmit the power. The gearbox was designed to allow for adjustability and maintenance in mind. When integrated with the electronic system, the physical system would mobilise the patients' legs through a gait similar pattern. A patient control scheme was suggested and related to other control schemes found in the literature. The concept of allowing a patient to

contribute a portion of power to the required motor output would allow continued training. Continual progression in training methods is seen to be a contributor to better patient outcomes.

Due to circumstances beyond the researcher's control, prototyping and manufacturing of the device could not be fully completed. Future work is required to build upon the fundamental areas of learning that this study provides.

5.2 Experimentation

In-silico testing was chosen as the preferential method of study in lieu of the lack of prototyping capabilities due to manufacturing delays. The study required the validated model of the Lower Limb 2010 Model to be imported into SolidWorks. The import would allow for SolidWorks Motion Analysis software to be utilised. Other, SolidWorks compatible modelling options were investigated but were not opted for either due to cost or integration complexity. The interaction of the imported model and the 3D modelled device could be made and assessed.

The device is able to mobilise the legs of the model successfully. The success of this is shown through the animations of SolidWorks and the interference check that can be performed within SolidWorks. Further assessment in SolidWorks showed how the device's movement provided a gait similar trajectory of the ankle with a stride length the length of the cranks circular diameter (300mm). The lower limb's motion was also assessed, and the ankle joint was found to assume the motion of the gait cycle best. It was able to move through a range of motion of 31 degrees of displacement. The timing of this was also gait similar and agreed with researched clinical gait analysis principles. When investigating the knee and hip joints, the gait similar results were less satisfactory but still promising. The joints could assume gait similar shapes, but their angular velocities and the timing at which motion occurred were not gait similar.

A crucial part of the investigation into the device's usefulness was assessed through its ability to provide a ground reaction force. The device was able to successfully provide 20% of the patient's body weight as GRF. While this stimulation is present, it is not comparable to full bodyweight walking, and its effectiveness as a stimulative effect should be analysed. The GRF did occur correctly concerning the gait cycle phasic timing, which further cements its possibility to be a targeted exercise device.

6. Conclusion and Recommendations

6.1 Conclusion

The following conclusions can be drawn from the study:

6.1.1 Rehabilitation Device Design

- The designed device can bear the weight of a range of patients safely in a stable manner when these weights were approximated *in-silico*. The device's stability means that it can be used in a spinal cord injury unit without fear of structural failure.
- The device designed proven *in-silico* to provide enough power to move a patient's legs through a gait similar pattern. The power capabilities would allow for patients of different weights and sizes to use the device.
- The device's *in-silico* gait pattern is comparable to the lower limbs' trajectories seen in the literature. The pattern of the device means that the device targets a specific function of living and provides physical therapists with the option of mobilisation.
- The joints' timings and ranges of motion that were discovered *in-silico* agree with that found in the literature for the ankle but differ for the hip and knee. However, each joint is moved through a range of motion from which the angular displacement and angular velocities resemble that of a typical gait pattern.
- The ground reaction force stimulated by the device's *in-silico testing* use makes it a useful adjunct to therapies currently in use by therapists. This feature significantly enhances gait training capabilities.

It is envisioned that this research is able to inform future prototypes and designs of this device so that it may be used as a rehabilitative tool for patients in hospital wards. Rehabilitation of the lower limbs to regain sensorimotor functions is a keenly researched topic worldwide, and this study provides the opportunity to add to the knowledge accumulated of late.

6.1.2 Device Usability

The device's usability must be further assessed in a different trial to make corrections to the design. This study provides critical information on the device's usefulness and critically reduces the cost and resources needed to validate its working principles. However, the study cannot provide insight into how a clinician may interact with the device or whether other factors may make the device unusable; for this to be adequately assessed, interaction with a prototype or minimum viable product must occur.

6.1.3 Recommendations, Inferences and Future Work

Designing and testing this device in an *in-silico* environment allowed for several recommendations to be drawn for future work discussed herein.

To begin further testing and dissection of the usefulness of the device, a prototype should be made. Prototyping will allow a range of further validation to occur and will begin the clinical validation stages of development.

Future work should be provisioned for the aesthetics of the device. Testing should be completed to understand the patient's thoughts surrounding the aesthetics of the device. It is foreseen that patients are more likely to respond in kind to the device if they believe it works and can provide them with a medical adjunct instead of a mechanical one.

Notable concern was made by clinicians as to future safety when SCI patients use the device. Future work must be made to investigate the current patient attachment design's suitability to deter rotation out of the parasagittal plane. It is envisioned that using a simple ROM knee brace attached to the arms of the device will have an effect on reducing the amount of rotation of the flaccid legs. The knee brace method does however introduce complexity in the design for different patient morphologies. A possible slot and pin attachment could be made by the ankle of the patient attachment system to accommodate for different shank lengths. However, future work must be done to assess the impact that this would have on the functioning of the device, and the effects of the extra weight of the attachment.

The design of the device only allows for a particular stride length. This restriction is due to the dependence of the slot dimensions on the crank length. In future work, the design should include a method of allowing the arms to slide about a fixed point without any restriction on sliding distance. From this adjustment, the crank length can be altered to increase the stride length. Bed placement should be considered here, however.



Figure 6-1 Possible implementation of a knee brace to reduce rotational movement of the legs.

A method of sensing the patient's force onto the device should be designed to allow for the control method described to be implemented. This addition will play a crucial role in transforming the device from a passive movement device into a targeted exercise device. In addition, a better user interface should be designed, and a screen added onto the controls device for a more accessible clinician interface.

7. References

- 3D-Printing-Store. (2020). STEPPER MOTOR, NEMA 23 X 112MM, 1.8 DEG/STEP. Retrieved December 11, 2020
http://www.3dprintingstore.co.za/stepper-motors/stepper-motor-nema-23-x-112mm-1-8-deg-step/?gclid=CjwKCAiA8ov_BRAoEiwAOZogwSJNSri1qQCZF2wiQ9TFS8QnsMJLBT1-iKi2e-KVZvPhUaABVtpPFRoCxq4QAvD_BwE
- Ahuja, C. S., Wilson, J. R., Nori, S., Kotter, M. R. N., Druschel, C., Curt, A., & Fehlings, M. G. (2017). Traumatic spinal cord injury. *Nature Reviews Disease Primers*, 3, 17018. doi:10.1038/nrdp.2017.18
- Arduino. (2020). ARDUINO MEGA 2560 REV3. Retrieved December 11, 2020
<https://store.arduino.cc/arduino-mega-2560-rev3>
- Arnold, A. S., Asakawa, D. J., & Delp, S. L. (2000). Do the hamstrings and adductors contribute to excessive internal rotation of the hip in persons with cerebral palsy? *Gait Posture*, 11(3), 181-190. doi:10.1016/s0966-6362(00)00046-1
- Arnold, E. M., Ward, S. R., Lieber, R. L., & Delp, S. L. (2010). A Model of the Lower Limb for Analysis of Human Movement. *Annals of Biomedical Engineering*, 38(2), 269-279. doi:10.1007/s10439-009-9852-5
- Ashrafiun, H., Grosh, K., Burke, K. J., & Bommer, K. (2010). An Intelligent Exoskeleton for Lower Limb Rehabilitation. Paper presented at the ASME 2010 International Design Engineering Technical Conferences & Computers and Information in Engineering Conference, Montreal, Quebec, Canada.
- Backus, D. (2010). Exploring the potential for neural recovery after incomplete tetraplegia through nonsurgical interventions. *2(12 Suppl 2)*, S279-285. doi:10.1016/j.pmrj.2010.10.004
- Beekhuizen, K. S., & Field-Fote, E. C. (2005). Massed practice versus massed practice with stimulation: effects on upper extremity function and cortical plasticity in individuals with incomplete cervical spinal cord injury. *Neurorehabil Neural Repair*, 19(1), 33-45. doi:10.1177/1545968305274517
- Behrman, A. L., Bowden, M. G., & Nair, P. M. (2006). Neuroplasticity after spinal cord injury and training: an emerging paradigm shift in rehabilitation and walking recovery. *Phys Ther*, 86.
- Behrman, A. L., & Harkema, S. J. (2000). Locomotor Training After Human Spinal Cord Injury: A Series of Case Studies. *Physical Therapy*, 80, 688-700.
- Bloch, R. F., & Basbaum, M. (1986). Management of spinal cord injuries (R. F. Bloch & M. Basbaum Eds. Vol. 2). University of Michigan: Williams & Wilkins.
- Chaparro-Cárdenas, S. L., Lozano-Guzmán, A. A., Ramirez-Bautista, J. A., & Hernández-Zavala, A. (2018). A review in gait rehabilitation devices and

- applied control techniques. *Disabil Rehabil Assist Technol*, 13(8), 819-834. doi:10.1080/17483107.2018.1447611
- Cheung, A., Gray, H., Schache, A., Hoermann, R., Lim Joon, D., Zajac, J., . . . Grossmann, M. (2016). Androgen deprivation causes selective deficits in the biomechanical leg muscle function of men during walking: a prospective case-control study: Biomechanical leg muscle function deficits with ADT. *Journal of Cachexia, Sarcopenia and Muscle*, 8. doi:10.1002/jcsm.12133
- Colombo, G., Schreier, R., Mayr, A., Plewa, H., & Rupp, R. (2005, 28 June-1 July 2005). Novel tilt table with integrated robotic stepping mechanism: design principles and clinical application. Paper presented at the 9th International Conference on Rehabilitation Robotics, 2005. ICORR 2005.
- Colombo, G., Wirz, M., & Dietz, V. (2001). Driven gait orthosis for improvement of locomotor training in paraplegic patients. *Spinal Cord*, 39(5), 252-255. doi:10.1038/sj.sc.3101154
- Cote, M. P., Murray, M., & Lemay, M. A. (2017). Rehabilitation Strategies after Spinal Cord Injury: Inquiry into the Mechanisms of Success and Failure. *J Neurotrauma*, 34(10), 1841-1857. doi:10.1089/neu.2016.4577
- Cramer, S. C., Lastra, L., Lacourse, M. G., & Cohen, M. J. (2005). Brain motor system function after chronic, complete spinal cord injury. *Brain*, 128(Pt 12), 2941-2950. doi:10.1093/brain/awh648
- Curt, A., Keck, M. E., & Dietz, V. (1998). Functional outcome following spinal cord injury: significance of motor-evoked potentials and ASIA scores. *Arch Phys Med Rehabil*, 79(1), 81-86. doi:10.1016/s0003-9993(98)90213-1
- Curt, A., Van Hedel, H. J., Klaus, D., & Dietz, V. (2008). Recovery from a spinal cord injury: significance of compensation, neural plasticity, and repair. *J Neurotrauma*, 25(6), 677-685. doi:10.1089/neu.2007.0468
- DeJong, B. P. (2007). On Cyclic Robots for the Lower Limb. (Doctor of Philosophy). Northwestern University, ProQuest. (3278033)
- Delp, S. L., Loan, J. P., Hoy, M. G., Zajac, F. E., Topp, E. L., & Rosen, J. M. (1990). An interactive graphics-based model of the lower extremity to study orthopaedic surgical procedures. *IEEE Trans Biomed Eng*, 37(8), 757-767. doi:10.1109/10.102791
- Díaz, I., Gil, J. J., & Sánchez, E. (2011). Lower-Limb Robotic Rehabilitation: Literature Review and Challenges. *Journal of Robotics*, 2011, 759764. doi:10.1155/2011/759764
- Dietz, V., & Fouad, K. (2013). Restoration of sensorimotor functions after spinal cord injury. *Brain*, 137(3), 654-667. doi:10.1093/brain/awt262
- Dijkers, M. P., & Zanca, J. M. (2013). Factors complicating treatment sessions in spinal cord injury rehabilitation: nature, frequency, and consequences. *Arch Phys Med Rehabil*, 94(4 Suppl), S115-124. doi:10.1016/j.apmr.2012.11.047
- DIYElectronics.co.za. (2020). MKS TB6600 EXTERNAL STEPPER MOTOR DRIVER. Retrieved December 14, 2020


- https://www.diyelectronics.co.za/store/drivers/2796-mks-tb6600-external-stepper-motor-driver.html?gclid=CjwKCAiAudD_BRBXEiwAudakX6Riar3R3uMHuv2QU9KwhKQ_dCwomznCUrW576kqf87Up3jnzVihRhoC26UQAvD_BwE
- Dobkin, B., Apple, D., Barbeau, H., Basso, M., Behrman, A., Deforge, D., . . . Scott, M. (2006). Weight-supported treadmill vs over-ground training for walking after acute incomplete SCI. *Neurology*, 66(4), 484-493. doi:10.1212/01.wnl.0000202600.72018.39
- Edgerton, V. R., de Leon, R. D., Tillakaratne, N., Recktenwald, M. R., Hodgson, J. A., & Roy, R. R. (1997). Use-dependent plasticity in spinal stepping and standing. *Adv Neurol*, 72, 233-247.
- Edgerton, V. R., & Roy, R. R. (2009). Robotic training and spinal cord plasticity. *Brain Research Bulletin*, 78(1), 4-12. doi:10.1016/j.brainresbull.2008.09.018
- Granata, K. P., Abel, M. F., & Damiano, D. L. (2000). Joint angular velocity in spastic gait and the influence of muscle-tendon lengthening. *The Journal of bone and joint surgery. American volume*, 82(2), 174-186. doi:10.2106/00004623-200002000-00003
- Green, J. B., Sora, E., Bialy, Y., Ricamato, A., & Thatcher, R. W. (1998). Cortical sensorimotor reorganization after spinal cord injury: an electroencephalographic study. *Neurology*, 50(4), 1115-1121. doi:10.1212/wnl.50.4.1115
- Haddas, R., & Ju, K. (2018). Gait Alteration in Cervical Spondylotic Myelopathy Elucidated By Ground Reaction Forces. *SPINE*, 44, 1. doi:10.1097/BRS.0000000000002732
- Harkema, S. J. (2008). Plasticity of interneuronal networks of the functionally isolated human spinal cord. *Brain Res Rev*, 57(1), 255-264. doi:10.1016/j.brainresrev.2007.07.012
- Huang, G., Ceccarelli, M., Huang, Q., Zhang, W., Yu, Z., Chen, X., & Mai, J. (2019). Design and Feasibility Study of a Leg-exoskeleton Assistive Wheelchair Robot with Tests on Gluteus Medius Muscles. *Sensors*, 19(3), 548. doi:10.3390/s19030548
- Interroll. (2020). Retrieved December 18,2020 <https://in.rsdelivers.com/product/interroll/2910/interroll-polyamide-round-flanged-conveyor-roller/2350896>
- Israel, J. F., Campbell, D. D., Kahn, J. H., & Hornby, T. G. (2006). Metabolic costs and muscle activity patterns during robotic- and therapist-assisted treadmill walking in individuals with incomplete spinal cord injury. *Phys Ther*, 86(11), 1466-1478. doi:10.2522/ptj.20050266
- Jakob, W., Wirz, M., van Hedel, H. J., & Dietz, V. (2009). Difficulty of elderly SCI subjects to translate motor recovery--"body function"--into daily living activities. *J Neurotrauma*, 26(11), 2037-2044. doi:10.1089/neu.2008.0824

- Joseph, C. (2016). Traumatic Spinal Cord Injury in South Africa and Sweden: Epidemiologic Features and Functioning. (Ph.D.). Karolinska Institutet,
- Joseph, C., Delcarme, A., Vlok, I., Wahman, K., Phillips, J., & Nilsson Wikmar, L. (2015). Incidence and aetiology of traumatic spinal cord injury in Cape Town, South Africa: a prospective, population-based study. *Spinal Cord*, 53(9), 692-696. doi:10.1038/sc.2015.51
- Joseph, C., Mji, G., Statham, S., Mlenzana, N., de Wet, C., & Rhoda, A. (2013). Changes in activity limitations and predictors of functional outcome of patients with spinal cord injury following in patient rehabilitation. 2013, 69(1), 9. doi:10.4102/sajp.v69i1.371
- Joseph, C., Scriba, E., Wilson, V., Mothabeng, J., & Theron, F. (2017). People with Spinal Cord Injury in Republic of South Africa. *Am J Phys Med Rehabil*, 96(2 Suppl 1), S109-s111. doi:10.1097/phm.0000000000000594
- Key, A. G., & Hurford, S. M. (1982). Social reintegration of paraplegics and tetraplegics in the Cape Province of the Republic of South Africa. *Paraplegia*, 20(2), 103-107. doi:10.1038/sc.1982.18
- Khorasanizadeh, M., Yousefifard, M., Eskian, M., Lu, Y., Chalangari, M., Harrop, J. S., . . . Rahimi-Movaghar, V. (2019). Neurological recovery following traumatic spinal cord injury: a systematic review and meta-analysis. *Journal of neurosurgery. Spine*, 1-17.
- Krueger, H., Noonan, V. K., Trenaman, L. M., Joshi, P., & Rivers, C. S. (2013). The economic burden of traumatic spinal cord injury in Canada. *Chronic Dis Inj Can*, 33(3), 113-122.
- Lederman, E. (2010). *Motor Adaptations (Vol. 1)*: Elsevier.
- Luft, A., Bastian, A., & Dietz, V. (2012). Learning in the Damaged Brain/Spinal Cord: Neuroplasticity. doi:10.5167/uzh-73417
- Maart, S., & Jelsma, J. (2014). Disability and access to health care - a community based descriptive study. *Disabil Rehabil*, 36(18), 1489-1493. doi:10.3109/09638288.2013.807883
- Matthew, H. (2018). Nervous System. Retrieved October 11, 2020, from Chegg <https://www.studyblue.com/notes/note/n/lab--%C2%A0nervous-system-deck/deck/21326926>
- McGlinchey, M. P., James, J., McKeivitt, C., Douiri, A., & Sackley, C. (2020). The effect of rehabilitation interventions on physical function and immobility-related complications in severe stroke: a systematic review. *BMJ Open*, 10(2), e033642. doi:10.1136/bmjopen-2019-033642
- Mehrholz, J., Thomas, S., Werner, C., Kugler, J., Pohl, M., & Elsner, B. (2017). Electromechanical-assisted training for walking after stroke. *Cochrane Database Syst Rev*, 5(5), Cd006185. doi:10.1002/14651858.CD006185.pub4
- Mendoza-Crespo, R., Torricelli, D., Huegel, J. C., Gordillo, J. L., Pons, J. L., & Soto, R. (2019). An Adaptable Human-Like Gait Pattern Generator Derived From a Lower Limb Exoskeleton. *Frontiers in Robotics and AI*, 6(36). doi:10.3389/frobt.2019.00036


- Mentiplay, B. F., Banky, M., Clark, R. A., Kahn, M. B., & Williams, G. (2018). Lower limb angular velocity during walking at various speeds. *Gait Posture*, 65, 190-196. doi:10.1016/j.gaitpost.2018.06.162
- Meriam, J. L., & Kraige, L. G. (2011). *Engineering Mechanics: Statics*: Wiley.
- Nas, K., Yazmalar, L., Sah, V., Aydin, A., & Ones, K. (2015). Rehabilitation of spinal cord injuries. *World J Orthop*, 6(1), 8-16. doi:10.5312/wjo.v6.i1.8
- O’Hea, J. (2003). Physiotherapy management of ankylosingspondylitis. In: Porter S editor(s). *Tidy’s Physiotherapy.*, 1, 274-290.
- P. McGurrin. (2016). Making Sense of Touch. ASU - Ask A Biologist Retrieved February 22, 2020, from Arizona State University School of Life Sciences <https://askabiologist.asu.edu/fr/understanding-touch>
- Pearson, K. G., & Misiaszek, J. E. (2000). Use-dependent gain change in the reflex contribution to extensor activity in walking cats. *Brain Res*, 883(1), 131-134. doi:10.1016/s0006-8993(00)02880-8
- Physio.co.uk. (2020). Contracture Management. Retrieved November 16, 2020, from physio.co.uk <https://www.physio.co.uk/treatments/neurological-rehabilitation/contracture-management.php>
- Pohl, M., Werner, C., Holzgraefe, M., Kroczeck, G., Mehrholz, J., Wingendorf, I., . . . Hesse, S. (2007). Repetitive locomotor training and physiotherapy improve walking and basic activities of daily living after stroke: a single-blind, randomized multicentre trial (DEutsche GAngtrainerStudie, DEGAS). *Clin Rehabil*, 21(1), 17-27. doi:10.1177/0269215506071281
- Prabhu, R. K. R., Swaminathan, N., & Harvey, L. A. (2013). Passive movements for the treatment and prevention of contractures. *Cochrane Database of Systematic Reviews*(12). doi:10.1002/14651858.CD009331.pub2
- Richards, J., Chohan, A., & Erande, R. (2017). *Clinical Gait Analysis*. Retrieved May 1, 2020, from Musculoskeletal Key <https://musculoskeletalkey.com/biomechanics-2/>
- Ruff, R. L., McKerracher, L., & Selzer, M. E. (2008). Repair and Neurorehabilitation Strategies for Spinal Cord Injury. *Annals of the New York Academy of Sciences*. doi:10.1196/annals.1444.004
- Santos, M., Zahner, L. H., & McKiernan, B. J. (2006). Neuromuscular electrical stimulation improves severe hand dysfunction for individuals with chronic stroke: a pilot study. *Neurol Phys Ther*, 30.
- Sargsyan, S., Arakelian, V., & Briot, S. (2012). *Robotic Rehabilitation Devices of Human Extremities: Design Concepts and Functional Particularities*. Paper presented at the ASME 2012 11th Biennial Conference on Engineering Systems Design and Analysis, Nantes, France.
- Smith, A. (2019). Build a Bike. Retrieved December 18, 2020 <http://westtownbikes.org/event/build-a-bike-2-of-8-2/>
- Somers, M. F. (2001). Spinal Cord Injury. In *Functional Rehabilitation* (3rd ed., pp. 64-68): Pearson.

- Sothmann, J., Stander, J., Kruger, N., & Dunn, R. (2015). Epidemiology of acute spinal cord injuries in the Groote Schuur Hospital Acute Spinal Cord Injury (GSH ASCI) Unit, Cape Town, South Africa, over the past 11 years. *South African Medical Journal*, 105, 835-839.
doi:10.7196/SAMJnew.8072
- Spiess, M. R., Müller, R. M., Rupp, R., Schuld, C., & van Hedel, H. J. (2009). Conversion in ASIA impairment scale during the first year after traumatic spinal cord injury. *J Neurotrauma*, 26(11), 2027-2036.
doi:10.1089/neu.2008.0760
- Swinnen, E., Duerinck, S., Baeyens, J. P., Meeusen, R., & Kerckhofs, E. (2010). Effectiveness of robot-assisted gait training in persons with spinal cord injury: a systematic review. *Rehabilitation Medicine*, 42.
doi:10.2340/16501977-0538
- Vallery, H., Veneman, J., van Asseldonk, E., Ekkelenkamp, R., Buss, M., & Kooij, H. (2008). Compliant actuation of rehabilitation robots. *Robotics & Automation Magazine, IEEE*, 15, 60-69. doi:10.1109/MRA.2008.927689
- Ward, N. S., Brown, M. M., Thompson, A. J., & Frackowiak, R. S. (2003). Neural correlates of outcome after stroke: a cross-sectional fMRI study. *Brain*, 126(Pt 6), 1430-1448. doi:10.1093/brain/awg145
- WHO. (2001). *International classification of functioning, disability, and health : ICF: Version 1.0*. Geneva : World Health Organization, [2001] ©2001.
Retrieved from <https://search.library.wisc.edu/catalog/999977181002121>
- Williams, R., & Murray, A. (2015). Prevalence of depression after spinal cord injury: a meta-analysis. *Arch Phys Med Rehabil*, 96(1), 133-140.
doi:10.1016/j.apmr.2014.08.016

Appendix A ISNCSCI Impairment Exam



INTERNATIONAL STANDARDS FOR NEUROLOGICAL CLASSIFICATION OF SPINAL CORD INJURY (ISNCSCI)



INTERNATIONAL SPINAL CORD SOCIETY

Patient Name _____ Date/Time of Exam _____

Examiner Name _____ Signature _____

RIGHT

MOTOR KEY MUSCLES

UER (Upper Extremity Right)

Elbow flexors C5

Wrist extensors C6

Elbow extensors C7

Finger flexors C8

Finger abductors (little finger) T1

LER (Lower Extremity Right)

Hip flexors L2

Knee extensors L3

Ankle dorsiflexors L4

Long toe extensors L5

Ankle plantar flexors S1

(VAC) Voluntary Anal Contraction (Yes/No)

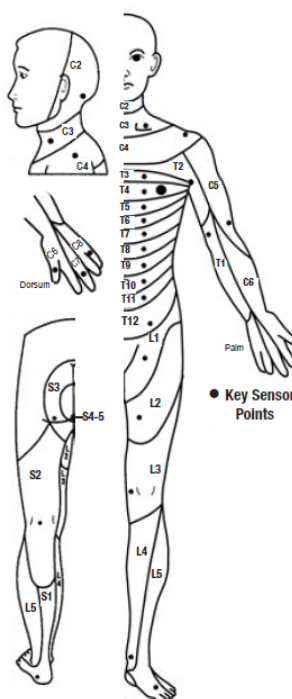
RIGHT TOTALS (MAXIMUM)

(50) (56) (56)

MOTOR SUBSCORES

UER + UEL = **UEMS TOTAL**
MAX (25) (25) (50)

LER + LEL = **LEMS TOTAL**
MAX (25) (25) (50)



● Key Sensory Points

SENSORY KEY SENSORY POINTS

Light Touch (LTR) Pin Prick (PPR)

C2

C3

C4

C5

C6

C7

C8

T1

T2

T3

T4

T5

T6

T7

T8

T9

T10

T11

T12

L1

L2

L3

L4

L5

S1

S2

S3

S4-5

SENSORY SUBSCORES

LTR + LTL = **LT TOTAL**
MAX (56) (56) (112)

PPR + PPL = **PP TOTAL**
MAX (56) (56) (112)

LEFT

MOTOR KEY MUSCLES

UEL (Upper Extremity Left)

Elbow flexors C5

Wrist extensors C6

Elbow extensors C7

Finger flexors C8

Finger abductors (little finger) T1

LEL (Lower Extremity Left)

Hip flexors L2

Knee extensors L3

Ankle dorsiflexors L4

Long toe extensors L5

Ankle plantar flexors S1

(DAP) Deep Anal Pressure (Yes/No)

LEFT TOTALS (MAXIMUM)

(50) (56) (56)

MOTOR SUBSCORES

UER + UEL = **UEMS TOTAL**
MAX (25) (25) (50)

LER + LEL = **LEMS TOTAL**
MAX (25) (25) (50)

Comments (Non-key Muscle? Reason for NT? Pain?):

NEUROLOGICAL LEVELS

Steps 1-5 for classification as on reverse

	R	L			R	L	
1. SENSORY	<input type="checkbox"/>	<input type="checkbox"/>	3. NEUROLOGICAL LEVEL OF INJURY (NLI)	<input type="checkbox"/>	ZONE OF PARTIAL PRESERVATION <small>(In complete injuries only) Most caudal level with any innervation</small>	<input type="checkbox"/>	<input type="checkbox"/>
2. MOTOR	<input type="checkbox"/>	<input type="checkbox"/>	4. COMPLETE OR INCOMPLETE?	<input type="checkbox"/>		<input type="checkbox"/>	<input type="checkbox"/>
			5. ASIA IMPAIRMENT SCALE (AIS)	<input type="checkbox"/>		<input type="checkbox"/>	<input type="checkbox"/>

Muscle Function Grading

- 0** = total paralysis
- 1** = palpable or visible contraction
- 2** = active movement, full range of motion (ROM) with gravity eliminated
- 3** = active movement, full ROM against gravity
- 4** = active movement, full ROM against gravity and moderate resistance in a muscle specific position
- 5** = (normal) active movement, full ROM against gravity and full resistance in a functional muscle position expected from an otherwise unimpaired person
- 5*** = (normal) active movement, full ROM against gravity and sufficient resistance to be considered normal if identified inhibiting factors (i.e. pain, disuse) were not present
- NT** = not testable (i.e. due to immobilization, severe pain such that the patient cannot be graded, amputation of limb, or contracture of > 50% of the normal ROM)

Sensory Grading

- 0** = Absent
- 1** = Altered, either decreased/impaired sensation or hypersensitivity
- 2** = Normal
- NT** = Not testable

When to Test Non-Key Muscles:

In a patient with an apparent AIS B classification, non-key muscle functions more than 3 levels below the motor level on each side should be tested to most accurately classify the injury (differentiate between AIS B and C).

Movement	Root level
Shoulder: Flexion, extension, abduction, adduction, internal and external rotation Elbow: Supination	C5
Elbow: Pronation Wrist: Flexion	C6
Finger: Flexion at proximal joint, extension. Thumb: Flexion, extension and abduction in plane of thumb	C7
Finger: Flexion at MCP joint Thumb: Opposition, adduction and abduction perpendicular to palm	C8
Finger: Abduction of the index finger	T1
Hip: Adduction	L2
Hip: External rotation	L3
Hip: Extension, abduction, internal rotation Knee: Flexion Ankle: Inversion and eversion Toe: MP and IP extension	L4
Hallux and Toe: DIP and PIP flexion and abduction	L5
Hallux: Adduction	S1

ASIA Impairment Scale (AIS)

A = Complete. No sensory or motor function is preserved in the sacral segments S4-5.

B = Sensory Incomplete. Sensory but not motor function is preserved below the neurological level and includes the sacral segments S4-5 (light touch or pin prick at S4-5 or deep anal pressure) AND no motor function is preserved more than three levels below the motor level on either side of the body.

C = Motor Incomplete. Motor function is preserved at the most caudal sacral segments for voluntary anal contraction (VAC) OR the patient meets the criteria for sensory incomplete status (sensory function preserved at the most caudal sacral segments (S4-S5) by LT, PP or DAP), and has some sparing of motor function more than three levels below the ipsilateral motor level on either side of the body.
(This includes key or non-key muscle functions to determine motor incomplete status.) For AIS C – less than half of key muscle functions below the single NLI have a muscle grade ≥ 3 .

D = Motor Incomplete. Motor incomplete status as defined above, with at least half (half or more) of key muscle functions below the single NLI having a muscle grade ≥ 3 .

E = Normal. If sensation and motor function as tested with the ISNCSCI are graded as normal in all segments, and the patient had prior deficits, then the AIS grade is E. Someone without an initial SCI does not receive an AIS grade.

Using ND: To document the sensory, motor and NLI levels, the ASIA Impairment Scale grade, and/or the zone of partial preservation (ZPP) when they are unable to be determined based on the examination results.



Steps in Classification

The following order is recommended for determining the classification of individuals with SCI.

1. Determine sensory levels for right and left sides.

The sensory level is the most caudal, intact dermatome for both pin prick and light touch sensation.

2. Determine motor levels for right and left sides.

Defined by the lowest key muscle function that has a grade of at least 3 (on supine testing), providing the key muscle functions represented by segments above that level are judged to be intact (graded as a 5).

Note: In regions where there is no myotome to test, the motor level is presumed to be the same as the sensory level, if testable motor function above that level is also normal.

3. Determine the neurological level of injury (NLI)

This refers to the most caudal segment of the cord with intact sensation and antigravity (3 or more) muscle function strength, provided that there is normal (intact) sensory and motor function rostrally respectively.

The NLI is the most cephalad of the sensory and motor levels determined in steps 1 and 2.

4. Determine whether the injury is Complete or Incomplete.

(i.e. absence or presence of sacral sparing)

If voluntary anal contraction = **No** AND all S4-5 sensory scores = **0** AND deep anal pressure = **No**, then injury is **Complete**.

Otherwise, injury is **Incomplete**.

5. Determine ASIA Impairment Scale (AIS) Grade:

Is injury **Complete**? If **YES**, AIS=**A** and can record ZPP (lowest dermatome or myotome on each side with some preservation)

NO ↓

Is injury **Motor Complete**? If **YES**, AIS=**B**

NO ↓

(No=voluntary anal contraction OR motor function more than three levels below the motor level on a given side, if the patient has sensory incomplete classification)

Are **at least half** (half or more) of the key muscles below the neurological level of injury graded 3 or better?

NO ↓

AIS=**C**

YES ↓

AIS=**D**

If sensation and motor function is normal in all segments, AIS=**E**

Note: AIS E is used in follow-up testing when an individual with a documented SCI has recovered normal function. If at initial testing no deficits are found, the individual is neurologically intact; the ASIA Impairment Scale does not apply.

Appendix B Dempster's Parameters

Segment Name	Endpoints (proximal to digital)	Seg. Mass /total mass	Centre of mass /segment length		Radius of gyration /segment length		
			R_{proximal}	R_{Distal}	K_{cg}	K_{Proximal}	K_{Distal}
Hand	Wrist axis to knuckle II third finger	0.0060	0.506	0.494	0.279	0.587	0.577
Forearm	Elbow axis to ulnar styloid	0.0160	0.430	0.570	0.303	0.526	0.647
Upper arm	Glenohumeral joint to elbow axis	0.0280	0.436	0.564	0.322	0.542	0.645
Forearm & hand	Elbow axis to ulnar styloid	0.0220	0.682	0.318	0.468	0.827	0.565
Upper extremity	Glenohumeral joint to elbow axis	0.0500	0.530	0.470	0.368	0.645	0.596
Foot	Lateral malleolus to head metatarsal II	0.0145	0.500	0.500	0.475	0.690	0.690
Leg	Femoral condyles to medial malleolus	0.0465	0.433	0.567	0.302	0.528	0.643
Thigh	Greater trochanter to femoral condyles	0.1000	0.433	0.567	0.323	0.540	0.653
Leg & foot	Femoral condyles to medial malleolus	0.0610	0.606	0.394	0.416	0.735	0.572
Lower extremity	Greater trochanter to medial malleolus	0.1610	0.448	0.553	0.326	0.560	0.650
Head	C7-T1 to ear canal	0.0810	1.000	0.000	0.495	1.116	0.495
Shoulder	Sternoclavicular joint to glenohumeral joint	0.0158	0.7015	0.288			
Thorax	C7-T1 to T12-L1	0.2160	0.820	0.180			
Abdomen	T12-L1 to L4-L5	0.1390	0.440	0.560			
Pelvis	L4-L5 to trochanter	0.120	0.105	0.895			
Thorax & abdomen	C7-T1 to L4-L5	0.3550	0.630	0.370			
Abdomen & pelvis	T12-L1 to greater trochanter	0.2810	0.270	0.730			
Trunk	Greater trochanter to glenohumeral joint	0.4970	0.495	0.505	0.406	0.640	0.648
Trunk & head	Greater trochanter to glenohumeral joint	0.5780	0.660	0.340	0.503	0.830	0.607
Head, arms & trunk	Greater trochanter to glenohumeral joint	0.6780	0.626	0.374	0.496	0.798	0.621
Head, arms & trunk	Greater trochanter to midrib	0.6780	1.142	-0.142	0.903	1.456	0.914

Equations

$$\sum_{i=1}^n P_i = 1.00$$

$$m_{total\ body} = \sum_{i=1}^n m_i$$

$$R_{proximal} + R_{distal} = 1.000$$

$$r_{proximal} = R_{proximal} \cdot length$$

$$S_{cg} = S_{proximal} + R_{proximal} (S_{distal} - S_{proximal})$$

$$s_{limb} = \frac{\sum_{i=1}^L P_i s_{cg_i}}{\sum_{i=1}^L P_i}$$

$$s_{totalbody} = \sum_{i=1}^n P_i s_{cg_i}$$

$$k_{proximal} = K_{proximal} \times length$$

$$K_{cg} = \sqrt{K_{proximal}^2 - R_{proximal}^2}$$

$$K_{proximal} = \sqrt{K_{cg}^2 + R_{proximal}^2}$$

$$I_{cg} = m(K_{cg} \cdot length)^2$$

$$I_{proximal} = mK_{cg}^2 + mr_{proximal}^2$$

$$I_{proximal} = m(K_{cg} \times length)^2 + m(R_{proximal} \times length)^2$$

$$I_{totalbody} = \sum_{i=1}^n I_{cg_i} + \sum_{i=1}^n m_i r_i^2$$

Where n is the number of body segments and i is the segment number and P_i is the segment mass proportion
 m_i is mass of a segment

R is distance to centre of gravity as proportion of segment length
 $R_{proximal}$ is distance from centre of gravity to proximal end

s represents position in x, y or z directions

where L is the number of segments in the limb

$k_{proximal}$ is radius of gyration for axes through the proximal end and $K_{proximal}$ is the radius of gyration as a proportion of the segment length I

I_{cg} is moment of inertia about an axis through the centre of gravity

where r_i is the distance between the total body centre of gravity and each segment's centre of gravity

Appendix C ICF Components

Definitions: Functioning, disability and the components of the ICF

Body functions - The physiological functions of body systems (including psychological functions).

Body structures - Anatomical parts of the body such as organs, limbs and their components.

Impairments - Problems in body function and structure such as significant deviation or loss.

Activity - The execution of a task or action by an individual.

Participation - Involvement in a life situation.

Activity limitations - Difficulties an individual may have in executing activities.

Participation restrictions - Problems an individual may experience in involvement in life situations.

Environmental factors - The physical, social and attitudinal environment in which people live and conduct their

lives. These are either barriers to or facilitators of the person's functioning.

Functioning is an umbrella term for body function, body structures, activities and participation. It denotes the

positive or neutral aspects of the interaction between a person's health condition(s) and that individual's

contextual factors (environmental and personal factors).

Disability is an umbrella term for impairments, activity limitations and participation restrictions. It denotes the

negative aspects of the interaction between a person's health condition(s) and that individual's contextual factors

(environmental and personal factors).

ICF components and domains/chapters

Body Function:

- Mental functions
- Sensory functions and pain
- Voice and speech functions
- Functions of the cardiovascular, haematological, immunological and respiratory systems
- Functions of the digestive, metabolic, endocrine systems
- Genitourinary and reproductive functions
- Neuromusculoskeletal and movement-related functions
- Functions of the skin and related structures

Activities and Participation:

- Learning and applying knowledge
- General tasks and demands
- Communication
- Mobility
- Self care
- Domestic life
- Interpersonal interactions and relationships
- Major life areas
- Community, social and civic life

Body Structure:

- Structure of the nervous system
- The eye, ear and related structures
- Structures involved in voice and speech
- Structure of the cardiovascular, immunological and respiratory Systems

- Structures related to the digestive, metabolic and
- endocrine systems
- Structure related to genitourinary and reproductive systems
- Structures related to movement
- Skin and related structures

Environmental Factors:

- Products and technology
- Natural environment and human-made changes to
- environment
- Support and relationships
- Attitudes
- Services, systems and policies

ICF Qualifier scales

Generic qualifier:

- 0 No problem
- 1 Mild problem
- 2 Moderate problem
- 3 Severe problem
- 4 Complete problem
- 8 Not specified
- 9 Not applicable

Qualifier for Environmental factors:

- .0 No barrier +0 No facilitator
- .1 Mild barrier +1 Mild facilitator
- .2 Moderate barrier +2 Moderate facilitator
- .3 Severe barrier +3 Substantial facilitator

- .4 Complete barrier +4 Complete facilitator
- .8 Barrier, not specified +8 Facilitator, not specified
- .9 Not applicable +9 Not applicable